2014

Developing a facies model and sequence stratigraphic framework for the Devonian-Mississippian Sappington Formation in southwestern-central Montana

Tetsuro Nagase
The University of Montana

DEVELOPING A FACIES MODEL AND SEQUENCE STRATIGRAPHIC FRAMEWORK FOR THE DEVONIAN-MISSISSIPPIAN SAPPINGTON FORMATION IN SOUTHWESTERN-CENTRAL MONTANA

By

TETSURO NAGASE

Bachelor of Science, Southwest Minnesota State University, Marshall, Minnesota, 2011
Associate of Arts, Lakeland College Japan, Tokyo, Tokyo, 2008

Thesis

presented in partial fulfillment of the requirements
for the degree of

Master of Science
in Geosciences

The University of Montana
Missoula, MT

March 2014

Approved by:

Sandy Ross, Associate Dean of The Graduate School
Graduate School

Marc S. Hendrix, Committee Chair
Department of Geosciences

Michael H. Hofmann
Department of Geosciences

Christopher P. Palmer
Department of Chemistry and Biochemistry

Tetsuro, Nagase, M.S., Spring, 2014 Geosciences

Developing a facies model and sequence stratigraphic framework for the Devonian-Mississippian Sappington Formation in southwestern-central Montana

Chairperson: Marc S. Hendrix

Over the past decade, exploration and development of the Devonian Bakken petroleum system in North Dakota and Montana has grown to become the top producing petroleum play in the United States. Despite this remarkable economic boom, relatively little is known about the stratigraphy and sedimentology of equivalent Devonian strata exposed at the surface to the west in the Bridger and Tobacco Root Ranges of southwestern-central Montana. There, the Bakken-equivalent Sappington Formation has not been stratigraphically evaluated since the 1950's and 1960's, long before the widespread application of sequence stratigraphy. This thesis provides an outcrop-based sequence stratigraphic analysis of the Sappington Formation in order to better understand the depositional history of these strata, while offering a set of predictive tools for evaluation of time-equivalent rocks more regionally.

The main objectives of this study are the following: 1) to develop a facies model for the Sappington Formation in southwestern-central Montana; 2) to establish a sequence stratigraphic framework for the Sappington Formation in the same area; and 3) to extend this interpretation into the subsurface more regionally, beyond the 'Sappington depositional basin'. To meet these objectives, an outcrop investigation was conducted including sedimentologic, petrographic, petrophysical, and geochemical analyses. These results were used to inform a more regional well log investigation of time-equivalent strata in Montana.

The following eight lithofacies characterize the Sappington Formation in southwestern-central Montana: 3) 1) organic-rich mudstone; 2) bioturbated, calcareous/dolomitic muddy siltstone; bioturbated, wavy-laminated/lenticular silty dolostone with interbedded/interlaminated mudstone; 4) hummocky cross-stratified silty dolostone; 5) bioturbated, ripple-laminated, calcareous/dolomitic siltstone-silty dolostone; 6) ripple-laminated silty dolostone; 7) planar-bedded silty dolostone; and 8) oncolitic, fossil-bearing floatstone. From these facies, the following four sedimentary environments are interpreted based on facies associations: 1) partly restricted offshore marine environment; 2) open marine carbonate build-up environment; 3) open marine offshore to offshore transition environment; and 4) open marine storm-dominated shoreface environment.

Based on a depositional sequence stratigraphic approach, the Sappington Formation is interpreted to include two higher order sequences with an additional sequence continuing into the overlying Lodgepole limestone. Log-based analysis of depositional patterns for the Sappington Formation and its equivalents in southwestern-central Montana are consistent with sedimentary environments interpreted from outcrop work in suggesting that the lower and upper Sappington mudstone units were deposited in semi-isolated, restricted marine basins, whereas the middle Sappington member carbonate units were deposited in an open marine basin.

ACKNOWLEDGEMENTS

I would like to give special thanks to my thesis advisers, Dr. Marc Hendrix, and Dr. Michael Hofmann for leading me to a completion of my master's thesis, while providing me excellent opportunities to study sedimentary geology in and around Montana. I also would like to give special thanks to Mr. Thomas Neely from ConocoPhillips for funding my research project and participating in summer field work in 2012. I appreciate the generosity of Mr. James M. Griffin, who allowed us to investigate the Sappington Formation on his property in 2012. I also appreciate Mr. Dale Ployner from Zortman, MT, who kindly permitted us to investigate potential outcrops of the Sappington Formation on his land as well as providing me a precious experience in a beautiful part of Montana. Additionally, I would like to thank Matt Young for all his help with the geochemical analysis of my rock samples. I also thank all the faculty members, staff, and geology students at the Geosciences Department as well as all the people I met while in Montana who helped make my oversea experience there more valuable.

Finally, I would like to give special thanks to my parents, Toshio Nagase and Naomi Nagase, for all their support which make it possible for me to pursue my master's degree in geology and to gain all the experiences I have had in Montana.

TABLE OF CONTENTS

1. INTRODUCTION

1.1. Sequence Stratigraphy

Sequence stratigraphy involves the subdivision of sedimentary rock units into time equivalent packages separated by unconformities or their correlative conformities (e.g., Van Wagoner *et al*., 1988; Catuneanu, 2006, Catuneanu *et al*., 2009). Historically, sequence stratigraphic analysis has been applied to coarse-grained sedimentary rocks primarily associated with passive continental margin settings (e.g. Van Wagoner *et al*., 1988; Hunt and Tucker, 1994). More recently, variations of the same concept have also been applied to other sedimentary environments, including fluvial environments (e.g. Blum *et al*., 1994; Fanti and Catuneanu, 2010; Hofmann *et al*., 2011), lacustrine basins (Oviatt, *et al*., 1994, Keighley, *et al*., 2003), and deep water systems (Prather *et al*., 1998). Despite the volumetric importance of mudstone in the rock record, until recently application of sequence stratigraphic principles to fine-grained sedimentary systems has lagged behind that of coarser-grained strata (e.g. MacQuaker *et al*., 2007; Straeten *et al.*, 2011). This lag is mainly attributed to the difficulty of analyzing fine-grained sedimentary rocks on a macroscopic scale in outcrop and core and the historic perception that mudstone has less economic value than other lithologies such as sandstone or limestone (e.g. Potter *et al.*, 1980; Schieber, 2011; Straeten *et al.*, 2011). Because of technological advances associated with horizontal drilling and hydraulic fracturing, organic-rich mudstone sequences have recently received more attention as important unconventional petroleum resources (e.g. Jiang and Li, 2002; Rahm, 2011: Soliman, *et al*., 2012), prompting the application of sequence stratigraphic analysis to these lithologies.

In the Williston Basin, located in western North Dakota, southern Saskatchewan and northeastern Montana, the Devonian-Mississippian Bakken Formation contains organic-rich mudstone that is the main source of hydrocarbons within adjacent strata (e.g., Jiang and Li, 2002; Obermajer *et al*., 2000, 2002; Sonnenberg *et al.*, 2011). Deposition of the lower and upper members of the formation occurred in a restricted marine basin, where anoxic, and likely euxinic, bottom water conditions in the deeper basin and upwelling of nutrient-rich flows in the upper basin had been established during late Devonian and early

Mississippian transgression (e.g. Smith and Bustin, 1998, 2000; Obermajer *et al*., 2000; Jiang and Li, 2002).

1.2. Petroleum Resources

According to the latest assessment of the Bakken Total Petroleum System (TPS) – which includes the Devonian Three Forks Formation, the Devonian-Mississippian Bakken Formation, and the lower part of the Mississippian Lodgepole Formation - in the Williston Basin alone, the mean undiscovered volume of producible Bakken-sourced oil is estimated to be 7.4 billion Bbl, 6.7 trillion cubic feet of associated/dissolved natural gas, and 0.53 billion Bbl of natural gas liquids (Gaswirth, *et al*., 2013). These significant petroleum resources in the Williston Basin have sparked exploration efforts in Bakken-equivalent strata in Glacier and Choteau Counties in north-central Montana. There, the time equivalent Sappington and Exshaw Formations contain facies similar to the Bakken Formation in the Williston Basin. The Exshaw Formation also extents north in the Western Canadian Basin of Alberta and British Columbia (Smith and Bustin, 2000: Rokosh, *et al*., 2009).

Despite the magnitude of petroleum exploration and production in the Williston Basin, few studies to date have attempted to apply a sequence stratigraphic approach to the Bakken Formation and its equivalents. Considering the heterogeneity in initial production rate in the Williston Basin (Theloy and Sonnenberg, 2013) (**Fig. 1**), existing depositional models that represent the Bakken Formation as having a layer-cake stratigraphy do not adequately reflect the degree of facies complexity within the formation. This inconsistency suggests that the application of a more sophisticated sequence stratigraphic approach will improve understanding of the depositional fill history of Devonian-Mississippian strata across the region and, from this, better predictability of their production potential.

1.3. Lithostratigraphy

The Late Devonian (Famennian) to Early Mississippian (Tournaisian) strata in Montana include the Bakken Formation in the Williston Basin, the Exshaw Formation in the Western Canadian Basin, the Sappington Formation in central Montana, and the Cottonwood Canyon Member of the Lodgepole Formation in southern Montana (Sandberg and Klapper, 1967; Baars, 1972; Peterson, 1986; Smith and Bustin, 2000) (**Fig. 2**).

Lithologically, the Sappington Formation in central Montana consists of a calcareous/dolomitic to sandy/silty middle interval bounded below and above by mudstone intervals. Prior work on the Sappington Formation has divided it into five different lithostratigraphic units: (1) a basal black, organic-rich mudstone; (2) a lower argillaceous, calcareous siltstone or silty argillaceous limestone; (3) a middle gray, laminated, calcareous mudstone; (4) an upper yellowish gray to brownish orange, flaggy to massive, calcareous siltstone; and (5) an uppermost dark gray to black, sandy, organic-rich mudstone (e.g. Achauer, 1959; Gutschick *et al*., 1962; McMannis, 1962: Sandberg, 1965) (**Fig. 3 and Fig. 4**). Lithostratigraphically, units 2 through 4 have been described by these early workers as forming the middle member of the Sappington Formation, whereas units 1 and 5 comprise the lower and upper members respectively.

Like the Sappington Formation, the Bakken Formation in the Williston Basin is characterized by three distinct lithofacies: a calcareous/dolomitic sandy-silty middle member bounded below and above by thinly-laminated, organic-rich mudstone members (e.g. Smith and Bustin, 1998, 2000; Sonnenberg *et al*., 2011; Angulo and Buatois, 2012) (**Fig. 3**). In the Williston Basin, the middle member of the Bakken Formation has been subdivided into as many as six different lithofacies (e.g. Smith and Bustin, 1998, 2000; Sonnenberg *et al*., 2011; Angulo and Buatois, 2012) (**Fig. 3**). In southern Alberta and British Columbia, the Exshaw Formation consists of a lower organic-rich mudstone member and an upper siltstone/sandstone member (e.g. Savoy, 1992; Smith and Bustin, 2000; Rokosh, *et al*., 2009) (**Fig. 3**). These two units, together with the lowermost organic-rich mudstone of the Banff Formation, have been lithostratigraphically correlated to the Bakken Formation (e.g. Smith and Bustin, 2000; Rokosh, *et al*., 2009) (**Fig. 3**). Only the upper unit of the Cottonwood Canyon Member of the Lodgepole Formation, which consists of dolomitic/calcareous siltstone or silty argillaceous dolostone, is present in Montana at the base of the Lodgepole limestone (Sandberg and Klapper, 1967).

1.4. Biostratigraphy

Overall biostratigraphic correlation of Devonian-Mississippian strata in Montana is based on conodont zones (e.g. Savoy and Harris, 1993; Kaufmann, 2006; Johnston *et al*., 2010) (**Fig. 5**). These biostratigraphic data suggest that the basal Sappington Formation is

time equivalent to the lower member of the Bakken and Exshaw Formations, where organic-rich mudstone is present. The middle and upper members of the Sappington Formation are time equivalent to the lower part of the middle Bakken Formation and the upper part of the lower Exshaw Formation. On top of the middle and upper members of the Sappington Formation, there are two missing conodont zones (*Siphonodella Sulcata* and lower *S. Dupulicata)*, which early workers interpreted as an unconformity that spans the Devonian-Mississippian boundary (e.g. Achauer, 1959; Gutschick *et al*., 1962; McMannis, 1962; Sandberg and Klapper, 1967). In contrast, the Bakken and Exshaw Formations contain the two missing conodont zones (**Fig. 5**). The upper unit of the Cottonwood Canyon Member of the Lodgepole Formation unconformably overlies the Sappington Formation in central Montana and is partly time equivalent to the upper member of the Bakken Formation and the lower Banff Formation (Sandberg and Klapper, 1967; Baars, 1972) (**Fig. 5**).

1.5. Paleogeography, Paleoclimate, and Tectonic Settings

During the Late Devonian (Famennian) to Early Mississippian (Tournaisian), the western margin of the North America craton was located between the equator and 30° N and was characterized by a subtropical climate (Scotese and McKerrow, 1990; Smith and Bustin, 1998). Smith and Bustin (1998) inferred that an east-directed equatorial undercurrent provided nutrients to the western margin of the continent through a series of interconnected basins that included the Williston Basin (**Fig. 6**). At this time, the tectonic emplacement of an allochthon along the western margin of the North American continent caused the Antler Orogeny to develop, forming a mountainous 'Antler Highlands' separated from the western margin of the craton by a relatively deep marine basin (**Fig. 6**). The timing of the Antler Orogeny is reasonably well established by studies in Nevada and Utah (e.g. Sandberg, *et al*., 1983; Giles and Dickenson, 1995; Warme *et al*., 2008) and Alberta (Kevin, 2001). However, considerably less is known about the Antler Orogeny along tectonic strike at the present-day latitude of western Montana and central Idaho due to the structurally complex nature of the geology there, widespread erosion of the Paleozoic section (particularly in northwestern Montana), and overlap by Cenozoic volcanics (Dorobek *et al*., 1991, Dorobek, 1995).

Prior regional geologic analysis has suggested that, in addition to the Antler highlands and foredeep to the west, paleogeographic and tectonic elements in Montana included three major highlands and three major basins or troughs (Baars, 1972; Peterson, 1986; Smith and Bustin, 2000) (**Fig. 6**). These paleogeographic elements and the role they played in controlling Devonian-Mississippian depositional systems have led to differing interpretations regarding the distribution of lithostratigraphic units across the region. For instance, Sonnenberg *et al.* (2011) described the Bakken Formation in the Williston Basin as extending to the Elk Point Basin in the Western Canadian Basin where the Exshaw Formation is present, whereas Smith and Bustin (1998) suggested that the Bakken Formation in the Williston Basin extends through the Central Montana Trough (CMT) where the Sappington Formation is present. Although lateral variations of the Sappington Formation are not well documented due to poor or non-existent surface exposures, early work on the formation concluded that the Sappington deposited in a west-east trending basin in central Montana and it thins both to the north and south (e.g. Gutschick *et al*., 1962; McMannis, 1962; Rau, 1962).

1.6. Objectives

The main objectives of this study are: (1) to develop a facies model for the Sappington Formation in central Montana; (2) to establish a sequence stratigraphic framework for the Sappington Formation in the same area; and (3) to extend the interpretation outside the depositional basin of the Sappington Formation into the subsurface.

2. METHODS

2.1. Outcrop Investigation

Outcrops of the Sappington in central Montana were studied to document facies and sedimentary stacking patterns. The Sappington outcrops were measured at centimeter to decimeter scale to provide detailed sedimentologic and stratigraphic information including lithology, grain size, sedimentary structures, fabrics, ichnofacies, and

bioturbation index. Samples were systematically collected from the measured sections for detailed petrographic and geochemical analysis. The Sappington outcrops were measured at Dry Hollow (DH) in the northern Tobacco Roots Mountains, Hardscrabble Peak, Bridger Range (BR), and along Crystal Lake Road in the northern Big Snowy Mountains (BS) in central Montana (**Fig. 2**).

Because the Sappington Formation contains intimate mixtures of siliclastic and carbonate lithologies, a combination of published textural-based classifications was used in this study. Samples that were dominated by siliciclastics (% vol > 50) were classified according to Potter *et al*. (1980). Samples dominated by carbonate lithologies (% vol > 50) were classified according to Embry and Klovan (1972) (**Fig. 7**).

A hand-held scintillometer (RS-125 Super-SPEC) was used to measure natural radioactivity of the Sappington outcrops in central Montana to construct gamma ray (GR) logs and to understand how sedimentologic information in the rocks is expressed on the GR logs. The scintillometer measures a total GR in nanosievert per hour (nSv/h) and a spectral GR of potassium (K) in percent (%) and uranium (U) and thorium (Th) in parts per million (ppm). The relative contribution to the total GR readings is that 1 ppm uranium corresponds to 3.65 ppm thorium and 2.70 % potassium (Bjorlykke, 2010). The correlation between uranium and the organic content in the rocks is significant, and the correlation between clay minerals and elemental concentrations is the largest for thorium and potassium (Ellis and Singer, 2007). The thorium log provides a better estimate of clay content in the rocks because clay minerals have a high cation exchange capacity and thus can retain trace amounts of radioactive minerals such as thorium, whereas potassium is associated with clay minerals but also with other components of mudstone such as feldspars (Ellis and Singer, 2007; Bjorlykke, 2010).

At each outcrop, the GR spectrometer was stabilized by repeatedly measuring a known sample until individual readings varied within a few nSv/h. To take a single measurement, the scintillometer was held at the target strata for 90 seconds. Measurements were taken roughly at 30 cm intervals for fine-grained strata and at 50 cm intervals for other lithologies. GR measurements were transferred into excel spreadsheet to construct GR logs by depth for each outcrop.

2.2. Petrographic and Geochemical Analysis

Outcrop samples were analyzed petrographically and geochemically. Oriented thin sections representative of different lithofacies were prepared by Spectrum Petrographics, Inc., Vancouver, Washington. Each thin section sample was vacuum impregnated with blue-dyed epoxy, ground to standard 30 μm thickness, and polished prior to observation using a petrographic microscope (LEICA DM LP Polarizing microscope). Photomicrographs were taken using SPOT Software and SPOT Insight Digital Camera to document petrographic information.

In order to determine the mineralogy of samples representing each facies, quantitative X-ray diffraction (XRD) analysis using a PANalytical X'Pert PRO X-ray diffractometer was conducted for 59 samples from the Sappington outcrops. Fresh pieces of samples were powdered using a ball mill (LEESON, Model: A4S17DZ32C). Powdered samples were mounted in 27 mm back-mounted powder mounts and loaded for multiple sequential analyses. The X-rays were generated using a copper tube with a nickel filament at 45 kV and 40 mA, and each sample analysis involved three 11 minute scans from 2 to 70 two-theta. Once samples were scanned, data were collected using X'Pert Data Collector software and analyzed using X'Pert HighScore Plus software by applying the six following steps: (1) Merge scans after making sure all three scans look alike: Treatment → Merge Scans → Simple Sum → Select the scans to merge → Sum → Replace; (2) Determine the background of the scans: Treatment → Determine Background (Granularity = 12 and Bending Factor = 4) → Accept; (3) Determine the peaks present in the scans: Treatment → Search Peaks → Insert Peaks (if necessary); (4) Identify mineralogy in the samples: Analysis → Search & Match → Subset (mineral subset consisting of 17 minerals (**Table 1**) was used in this study); (5) Resolve the peaks by matching candidate minerals from the highest score; and (6) Make quantitative analysis: Analysis → Rietveld → Refinement → Default.

Total organic carbon (% TOC) was quantitatively analyzed by Elemental Analyzer (CE Instruments EA 1110 CHNS-O) for 78 samples from the Sappington outcrops. Fresh pieces of samples were collected and ground into power using a ball mill. Approximately 5-10 milligrams of the powdered samples were transferred into silver capsules and weighed using an electronic balance to the nearest 0.01 mg. Hydrochloric acid (HCl) was used to

dissolve inorganic carbon in the samples prior to the analysis by adding 0.1 ml of 50 % concentrated HCl to each weighed and loaded sample and drying the sample in the oven for 24 hours. This acid treatment was repeated twice for each sample. After the acid treatment, the silver capsules with samples were folded for analysis by Elemental Analyzer to determine the organic content in the samples. The Elemental Analyzer was operated by Environmental Biogeochemistry Laboratory at the Department of Geosciences, The University of Montana.

2.3. Well Log Analysis

After investigation of the Sappington outcrops, well log analysis based on GR logs was conducted using Petrel well correlation software. The main purpose of this geophysical work was to extend the sequence stratigraphic framework for the formations of interest away from the outcrop locations. Well log analysis was conducted by identifying stacking patterns and correlating lithological boundaries and significant sequence stratigraphic surfaces. The most prominent, least disputed, and regionally most traceable of these surfaces are the sequence boundary (SB) and the maximum flooding surface (mfs) (e.g. Van Wagoner *et al*., 1988; Catuneanu, O., 2006). GR logs, which measure natural radioactivity of sedimentary strata, are commonly used to understand stacking patterns and identify sequence stratigraphic surfaces (e.g. Davies and Elliot, 1996; Catuneanu, O., 2006; Catuneanu *et al*., 2009).

Seventy-three GR logs that cut through the Sappington, Bakken, or underlying Three Forks Formations, were identified in a western half of Montana (**Fig. 8**). Raster versions of the GR logs were obtained through MJ Systems. Additionally, digitized GR logs were obtained from Rosetta Resources Inc. in Glacier County. The majority of logs were from wells in the Williston Basin and northwestern Montana, with wells distributed across central Montana being less dense. The well logs used in this study were not normalized and thus were evaluated independently to understand the log facies relative to the GR logs constructed from the Sappington outcrops.

The GR logs were uploaded into Petrel and placed in the UTM coordinate system using the following attributes: Well Name, API Number, Easting, Northing, and Kelly Bushing (KB) elevation. Longitude and latitude were converted into Easting and Northing

using the spreadsheet for UTM conversion downloaded from the website of Prof. Steve Dutch, University of Wisconsin - Green Bay (http://www.uwgb.edu/dutchs/usefuldata/utmformulas.htm). In the UTM coordinate system, these logs were distributed across Zones 12 and 13. Lithological boundaries and significant sequence stratigraphic surfaces of the Sappington Formation and its equivalents were placed by inserting New Well Tops under Insert. These surfaces allowed well log analysis and correlation using Petrel.

Isopach maps for the Sappington and each systems tract recognized as part of the Sappington Formation were created to understand the regional depositional patterns in central Montana, using the following attributes described in x-y-z axis: Easting in x-axis; Northing in y-axis; and Thickness of the target interval in z-axis. The thickness was calculated as the elevation difference between top and bottom surfaces of the intervals and treated as depth. These x-y-z attributes were incorporated into Petrel and used for creating isopach maps by Make Edit Surface under Process tab with the following settings: Grid size and position: Automatic; Boundary: Make boundary from the input and extends it with 3 nodes; and Algorithm: Convergent interpolation. The state map of Montana was incorporated into the isopach maps for reference.

3. RESULTS AND INTERPRETATIONS

3.1.1. Facies Analysis

The Sappington Formation in central Montana can be subdivided into eight facies (including three sub-facies in Facies 1) based on lithology, sedimentary structures, microfabrics, ichnology, mineralogical (XRD), geochemical (TOC), and petrophysical (GR) characteristics. Each facies is described below and placed in the measured sections of the Sappington Formation for the DH, BR, and BS localities (**Fig. 9**).

Facies 1: Organic-rich Mudstones

The mudstone facies can be subdivided into three different sub-facies representative of distinct depositional processes. Although all the sub-facies are organic-

rich mudstones, they show heterogeneity in sedimentary structures, bioturbation, and mineralogy, which led to different interpretations of deposition processes of the mudstones.

Facies 1A: Organic-rich Mudstone with Microfossils

Facies 1A consists of organic-rich mudstone containing medium to coarse silt detrital quartz and microfossils in a clay-rich matrix. The mudstone is homogeneous and structureless with a bioturbation index of 0. (**Fig. 10)**.

The XRD analysis of Facies 1A reveals an average of 30.0 % quartz (σ = 4.11), 22.8 % K-feldspar (σ = 3.07), 32.5 % illite (σ = 2.87), 12.0 % mixed illite/smectite (σ = 8.69), 0.5 % calcite (σ = 0.32), and 1.9 % dolomite (σ = 1.40) (N = 3). TOC, on average, is 10.35 %, which is the highest of any facies, ranging from 7.47 % to 14.78 % (N = 3, σ = 5.06).

The total GR log of Facies 1A is the highest of any facies, ranging from 197.3 to 616.9 [nSv/h]. Total GR log is characterized by a significant increase at the bottom (~34 m) and decrease at the top (~33.3 m) with a maximum of 616.9 [nSv/h] in the middle (~33.5 m). The spectral GR logs show a significant increase in uranium concentration in the middle (~34 m) with a maximum of 68.5 [ppm] and decrease at the top (~33.3 m). The thorium curve shows a maximum of 15.9 [ppm] (~34 m), and the potassium curve is relatively constant with a maximum of 7.4 [%] (~33.5 m).

The spectral GR response of the uranium curve is consistent with high TOC (average 10.35 %), and the response of the thorium and potassium curves are consistent with high clay content (average 44.5 %) and relatively constant and high K-feldspar content (average 22.8 %, σ = 3.07) verified by XRD.

The sedimentary process inferred for deposition of Facies 1A is suspension settle-out of dominantly pelagic clay minerals and additional hemiplegic silt-sized siliciclastic grains under anoxic bottom conditions. An ancient analog for Facies 1A was described from the Upper Devonian Sonyea Group of New York, which contains massive, homogeneous mudstone facies, interpreted as being deposited through rapid suspension settle-out, probably as a consequence of clay flocculation due to concentrated suspensions (Schieber, 1999).

Facies 1B: Organic-rich Mudstone with Pinch and Swell Lamination

Facies 1B consists of organic-rich mudstone containing medium to coarse silt-sized detrital quartz in a clay-rich matrix and pinch and swell lamination consisting of medium silt to upper very fine-grained sand-sized radiolaria, which are mostly spherical, silicified, and/or phosphatized (**Fig. 11**). The pinch and swell lamination ranges in thickness from 0.5 to 2.0 mm thick and are characterized by either sharply truncated or irregular surfaces (**Fig. 11**). The bioturbation index of Facies 1B is 0.

The XRD analysis of Facies 1B reveals an average of 31.6 % quartz (σ = 12.05), 24.9 % K-feldspar (σ = 10.26), 28.7 % illite (σ = 9.11), 10.2 % mixed illite/smectite (σ = 10.41), 1.6 % chlorite (σ = 2.28), 1.6 % calcite (σ = 2.36), and 1.5 % dolomite (σ = 1.99) (N = 8). TOC, on average, is 3.50 %, which is the second highest of any facies, ranging from 0.26 % to 13.69 % (N = 8, σ = 3.89).

The total GR log response at the DH locality ranges from 108.2 to 265.7 [nSv/h] and is characterized by a maximum of 265.7 [nSv/h] in the middle (~ 40.5 m). The spectral GR logs generally correspond to the total GR log pattern with uranium maximum of 5.2 [ppm], thorium maximum of 11.9 [ppm], and potassium maximum of 6 [%] (~ 40.5 m). The total GR log at the BR locality ranges from 195.0 to 578.3 [nSv/h] and is characterized by gradually increasing GR measurements with a maximum of 578.3 [nSv/h]. The spectral GR logs show a gradual increase in uranium concentration with a maximum of 34.5 [ppm] (~34 m), a thorium peak in the middle (~34.5 m) with a maximum of 12.5 [ppm], and a relatively constant potassium curve (average 5.4 %).

The spectral GR response of the uranium curve at the DH locality is consistent with high TOC (2.34 %), and the response of thorium and potassium curves are consistent with relatively high clay (~20 %) and K-feldspar (~30-40 %) verified by XRD. The spectral GR response of the uranium curve at the BR locality is consistent with increasing organic content (1.17-13.69 %) as documented by TOC results, and the responses of thorium and potassium curves are consistent with high clay content (~50%) corresponding to the thorium peak and relatively constant K-feldspar content (~20-30 %) verified by XRD.

The sedimentary processes inferred for Facies 1B is a combination of suspension settle-out of dominantly pelagic clay minerals with subordinate hemiplegic silt-sized detrital quartz minerals under anoxic bottom conditions and delivery of medium silt to

upper very fine-grained sand-sized radiolarian grains partly through traction transport or suspension settle-out. Delivery of some radiolarian grains was likely a product of turbidity current deposition because some silt- and sand-bearing laminae are characterized by basal sharp truncation surfaces and normal grading towards top surfaces. Other radiolarian grains were likely a product of suspension settle-out because of the absence of basal sharp truncation surfaces. An ancient analog for Facies 1B was described from the Upper Devonian Sonyea Group of New York, which contains mudstone showing wavey lenticular silt lamina alternating with clay layers, interpreted as deposited through traction transport of silt grains within suspension settle-out of clay minerals occurring between traction transport events (Schieber, 1999).

Facies 1C: Bioturbated, Organic-rich Calcareous/Dolomitic Mudstone

Facies 1C consists of bioturbated, calcareous/dolomitic mudstone containing siliciclastic and carbonate mud matrix and medium to coarse silt-sized detrital quartz grains and dolomite rhombs (**Fig. 12)**. This mudstone is thinly-bedded (3 to 5 cm thick). The bioturbation index ranges from 1 to 2, and ichnofacies identified in this facies include mainly *Chondrites* but also local *Planolites*. Backfilled burrows are typically filled with coarser sediments composed of detrital quartz in a clay-rich matrix.

The XRD analysis of Facies 1C reveals an average of 34.6 % quartz (σ = 5.05), 15.7 % K-feldspar (σ = 4.65), 16.7 % illite (σ = 1.17), 0.3 % mixed illite/smectite (σ = 0.06), 9.9 % calcite (σ = 9.28), and 21.7 % dolomite (σ = 17.45) (N = 3). TOC, on average, is 3.04 %, which is the third highest of any facies, ranging from 0.19 % to 8.50 % (N = 9, σ = 2.73).

The total GR log at the BR locality ranges from 192.7 to 251.2 [nSv/h] and is characterized by an abrupt increase at the bottom (~16 m) and decrease at the top (~15 m) with a maximum of 251.2 [nSv/h] in the middle (~15.5 m). The spectral GR logs show uranium maximum of 14.1 [ppm] and thorium maximum of 17.2 [ppm] (~15-15.5 m) and secondary maximum at the top (~15 m) and a relatively constant potassium curve (average of 6.1 %). The total GR log at the BS locality ranges from 116.3 to 184.5 [nSv/h] and is characterized by an abrupt increase at the bottom and decrease at the top with a maximum of 184.5 [nSv/h] within the interval of Facies 1C (~1.8-2 m). The spectral GR logs

generally track the total GR log pattern with uranium maximum of 10.7 [ppm], thorium maximum of 11.4 [ppm], and potassium maximum of 5.2 [%].

The spectral GR response of the uranium curve at the BR locality is consistent with the highest TOC (3.18 %) (~16 m), and the response of thorium and potassium curves are consistent with relatively high clay content (~15-20 %). The K-feldspar content (~15-20 %) documented by XRD is consistent with the potassium curve of the spectral GR. The spectral GR response of the uranium curve at the BS locality is consistent with the highest TOC (8.50 %) at the bottom (~2 m) but does not reflect the second highest TOC (5.51 %) at the top (~1.8 m). No XRD data are available for the BS locality.

The dominant sedimentary process inferred for Facies 1C is suspension settle-out of pelagic clay minerals and additional hemiplegic silt-sized detrital quartz under dysoxic conditions capable of supporting a sparse infauna. The presence of *Chondrites*, which typically represents the last trace fossil in a bioturbation sequence and whose burrow system can occur within the sediment in the anaerobic zone (Bromley and Ekdale, 1984), is consistent with the sedimentation processes inferred for Facies 1C. An ancient analog for Facies 1C was described by Scheiber (1999) from the Upper Devonian Sonyea Group of New York, which contains bioturbated mudstone characterized by a variety of burrows such as subhorizontal tubes, vertical burrows with diffuse margins, and *Chondrites*. Schieber (1999) interpreted the presence of these burrows and the co-occurrence of *Chondrites* as indicating feeding and dwelling structures of some permanence, implying low rates of sediment accumulation.

Facies 2: Bioturbated, Calcareous/Dolomitic Muddy Siltstone

Facies 2 consists of bioturbated, calcareous/dolomitic muddy siltstone containing siliciclastic and carbonate mud and medium to coarse silt-sized detrital quartz grains and dolomite rhombs (**Fig. 13**). This muddy siltstone is thinly-bedded (3 to 5 cm thick) and locally interlaminated with silty dolostone. The bioturbation index ranges from 0 to 3, and ichnofacies identified in this facies include *Palaeophycus*, *Planolites* and *Teichichnus*. Backfilled burrows are typically filled with coarser sediments composed of detrital quartz and dolomite rhombs in a clay matrix.

XRD analysis of Facies 2 reveals an average of 25.0 % quartz ($\sigma = 3.95$), 4.0 % K-

feldspar (σ = 3.43), 19.1 % illite (σ = 7.42), 1.4 % mixed illite/smectite (σ = 4.19), 1.2 % chlorite (σ = 1.20), 20.5 % calcite (σ = 9.48), 26.5 % dolomite (σ = 16.00), and 2.3 % ankerite (σ = 2.69) (N = 17). TOC, on average, is 0.23 % ranging from 0.14 % to 0.35 % (N = 24, σ = 0.074).

The total GR log at the DH locality ranges from 83.0 to 114.5 [nSv/h] in the lower interval (~36-40 m) with the local maximum in the middle (~37.5 m) and ranges from 120.0 to 133.9 [nSv/h] in the upper interval (~29.5-34 m) with the local maximum in the middle (~31.5 m). The total GR is characterized by a series of local maxima and minima within an overall gradually decreasing log patterns. The spectral GR logs in the lower interval generally track the total GR log pattern, within which the thorium curve shows the greatest variation. In the upper interval, the spectral GR logs show an inverse relationship between the uranium and thorium curves, meaning local maxima of the uranium curve corresponds to the local minima of a thorium curve and vice versa. The potassium curve of the spectral GR logs tracks the total GR log pattern.

The total GR log at the BR locality contains an isolated reading of 121.8 [nSv/h] at the base of a 0.5 m thick interval of Facies 2 (~26.5-27 m) and ranges from 116.5 to 146.8 [nSv/h] in the upper interval (~23.5-26 m) with a local maximum at the top (~23.5 m). The total GR is characterized by a series of local maxima and minima within an overall gradually increasing log patterns in the upper interval. In the lower interval, an isolated reading of the spectral GR shows a local minimum on the uranium curve and local maxima on the thorium and potassium curves. In the upper interval, the spectral GR logs show an inverse relationship between the uranium and thorium curves similar to that observed at the DH locality. The potassium curve gradually increases upsection in the upper interval.

The dominant sedimentary process inferred for Facies 2 is suspension settle-out of clay minerals and silt-sized detrital quartz. Presence of several different trace fossils implies deposition under oxygenated conditions, and a dominance of *Cruziana* ichnofacies of *Planolites* and *Teichichnus* suggests sublittoral zone in marine environments (Catuneanu, O., 2006; MacEachern, *et al*., 2010). An ancient analog for Facies 2 has been described from the Upper Cretaceous Wyandot Formation, offshore Nova Scotia, which contains bioturbated, very-fine grained, calcareous mudstone with identified ichnofacies of *Chondrites*, *Palaeophycus*, *Planolites*, *Thalassinoides*, and *Zoophycos* (Phillips and

Mcllroy, 2010). Phillips and Mcllroy (2010) interpreted the calcareous mudstone as deposited through background sedimentation of fine-grained siliciclastics when primary carbonate production lessened or terrigenous sediments input increased.

The spectral GR response of the uranium curve in the lower interval at the DH locality (~36-40 m) is consistent with low TOC value (0.14-0.18 %), and the response of the thorium curve is consistent with relatively high clay content (~20 %), as verified by XRD. The response of the potassium curve was not verified by XRD, however, since K-feldspar was not detected in the lower interval. The spectral GR response of the uranium curve in the lower interval at the BR locality (~26.5-27 m) is consistent with low TOC value (0.19-0.20 %), and the response of the thorium and potassium curves is consistent with relatively high clay content (~10 %). The presence of K-feldspar (~3 %) there is verified by XRD. In the upper intervals at the DH (~29.5-34 m) and at the BR (~23.5-26 m) localities, the uranium curves of the spectral GR logs are consistent with relatively low TOC (0.15-0.31 % at DH; 0.28-0.35 at BR), and the response of thorium and potassium curves is consistent with relatively high clay content (~15-45 %;~10-20 % at BR) and presence of K-feldspar (~1-11 % at DH; ~1-7% at BR), as verified by XRD.

The inverse relationship between the uranium and thorium curves of the spectral GR in the upper intervals at the DH (~29.5-34 m) and BR (~23.5-26 m) localities implies deposition of clay-rich layers containing relatively lower weight percentages of organic matter alternating with less clay-rich layers containing relatively higher weight percentages of organic matter. Since the uranium curve maxima correspond to a relatively higher quartz content (~25-30 % at DH and BR), this relationship could be a potential predictor of organic matter preservation. The potassium curves appear to track the total GR log pattern since the uranium and thorium curves effectively offset each other.

Facies 3: Bioturbated, Wavy-laminated/Lenticular Silty Dolostone with Interbedded/Interlaminated Mudstone

Facies 3 consists of a bioturbated, wavy-laminated/lenticular silty dolostone containing medium silt- to lower very fine-grained sand-sized grains of detrital quartz and dolomite rhombs interbedded/interlaminated with mudstone (**Fig. 14**). The silty dolostone beds are thin thinly (1 to 5 cm thick), wave-laminated/lenticular-bedded, and laterally

continuous without cross-cutting others (**Fig. 14**). The interbedded mudstone is bounded and sharply truncated by the wave-rippled beds, and the interlaminated mudstone typically drapes wave-rippled beds (**Fig. 14**). The bioturbation index ranges from 0 to 1, and ichnofacies identified in this facies include *Planolites* and *Skolithos*.

XRD analysis of Facies 3 reveals an average of 31.1 % quartz (σ = 4.21), 5.0 % K-feldspar (σ = 3.28), 12.8 % illite (σ = 7.45), 1.7 % mixed illite/smectite (σ = 4.98), 1.3 % chlorite (σ = 1.46), 16.6 % calcite (σ = 11.26), 29.0 % dolomite (σ = 12.50), and 2.6 % ankerite (σ = 3.16) (N = 13). TOC, on average, is 0.23 % ranging from 0.14 % to 0.35 % (N = 13, σ = 0.074).

The total GR log at the DH locality (~25.5-29.5 m) ranges from 85.1 to 117.1 [nSv/h] with major peaks at the bottom (~29 m) and top (~27 m). The total GR log of Facies 3 at the BR locality (~22-23.5 m) ranges from 122.7 to 164.5 [nSv/h] with a local maximum at ~22.5 m followed by an abrupt decrease at the top (~22 m). Similar to the GR log patterns of Facies 2, the spectral GR logs at both DH and BR localities show an inverse relationship between the uranium and thorium curves, and the potassium curve generally tracks the total GR log pattern.

The spectral GR response of the uranium curve at the DH locality is consistent with relatively low TOC value (0.10-0.15 %), and the response of thorium and potassium curves is consistent with relatively high clay content (~10-40 %) and presence of K-feldspar (~0-7 %) verified by XRD. The spectral GR response of the uranium curve at the BR locality is consistent with relatively low TOC value (0.22-0.65 %), and the response of thorium and potassium curves is consistent with relatively high clay content (~5-25 %) and the presence of K-feldspar (~3-10 %), consistent with XRD data. The inverse relationship between the uranium and thorium curves and tracking of the potassium curve to the total GR observed in Facies 2 also characterizes Facies 3.

Facies 3 is interpreted as a product of storm deposition during which medium silt- to lower very fine-grained sand-sized particles of detrital quartz were introduced and deposited above storm wave base but below fair-weather wave base. The sharp basal contact characteristic of silty dolostone beds in Facies 3, the presence of combined flow ripples in the dolostone, and the presence of overlying mud drapes are consistent with deposition by a waning storm event with suspension settle-out of clay minerals taking place

below fair-weather wave base between storm events. An ancient analog for Facies 3 was described from the Cretaceous (Turonian) Cardium Formation of Alberta, which contains bioturbated very fine sandy and silty beds interstratified with mudstone and is interpreted as representing a gradational shoreface succession from offshore transition to lower shoreface (Plint, 2010).

Facies 4: Hummocky Cross-Stratified (HCS) Silty Dolostone

Facies 4 consists of hummocky cross-stratified (HCS) silty dolostone containing medium silt- to lower very fine-grained sand-sized detrital quartz grains and dolomite rhombs, and finely crystalline calcite cement (**Fig. 15**). HCS beds are typically a few decimeters thick and each bed displays stacked low-angled cross-lamination with sharp basal contacts (**Fig. 15**). Facies 4 locally contains soft sediment deformation (SSD) beds. The bioturbation index is 0.

XRD analysis of one representative sample of Facies 4 reveals 20.9 % quartz, 0.3 % K-feldspar, 2.5 % illite, 3.5 % calcite, 63.2 % dolomite, 7.3 % ankerite, and 2.3% anhydrite (N = 1, σ not available since N = 1). TOC, on average, is 0.24 % ranging from 0.12 % to 0.33 % (N = 4, σ = 0.11).

The total GR logs of Facies 4 ranges from 66.7 to 122.0 [nSv/h] and are typically characterized by local minima (e.g., ~21 m, ~24 m at DH; ~21.5 m at BR). The spectral GR log patterns of uranium, thorium, and potassium curves generally track the total GR log pattern. The local maxima of the total GR logs occur when the spectral GR logs of uranium and/or thorium curves also show local maxima (e.g., ~25.5 m at DH; ~30 m at BR).

The spectral GR response of the uranium curves is consistent with low TOC (0.12-0.28 %) at the local GR minima, but it is not consistent with the low TOC when the uranium curve shows local maxima. Likely, this inconsistency results from the very low TOC percentages for this facies and a decrease in the signal/noise ratio within the scintillometer readings. The spectral GR responses of thorium and potassium are consistent with low clay (2.5 %) and K-feldspar (0.3 %) contents verified by XRD data from the BR locality (~30 m).

Facies 4 is interpreted as a product of storm-related deposition resulting from

storm-generated combined flow currents and associated waning flow. HCS beds with sharp basal contact represents the main storm deposits. When HCS beds are associated with SSD beds above, the deposition represents rapid sedimentation through storm-related processes.

Ancient analogs for Facies 4 have been described from the Neoproterozoic Nuccaleena Formation of the lowermost Ediacaran deposits (~635 Ma) (Rose and Maloof, 2011) and the Warcowie dolomite of the Yudnamutana Subgroup of Sturtian age during Cryogenian (Heron, *et al*., 2011) in South Australia. Both of these units are reported to contain low-angled HCS beds and/or SCS beds, interpreted as representing storm-dominated deposition in an offshore to offshore-transitional environment.

Facies 5: Bioturbated, Ripple-laminated, Calcareous/Dolomitic Siltstone-Silty Dolostone

Facies 5 consists of bioturbated, ripple-laminated, calcareous/dolomitic siltstone-silty dolostone containing medium silt- to lower very fine-grained sand-sized detrital quartz grains and dolomite rhombs, and a finely crystalline calcite cement (**Fig. 16**). The silty dolostone beds are wave-rippled, thinly bedded (a few cm thick), and laterally continuous without cutting across each other. The sedimentary structures and bedding surfaces are disturbed by bioturbation and backfilled burrows (**Fig. 16**). Current-ripples occur locally (**Fig. 16**). Some rippled beds are separated by silt parting or mud drapes (**Fig. 16**). The bioturbation index ranges from 1 to 3, and ichnofacies identified in this facies include *Chondrites, Planolites, Teichichnus, Thalassinoides, and Rosselia*. Facies 5 contains the most diverse suite of ichnofauna of all observed facies in this study.

XRD analysis of four representative samples of Facies 5 revealed an average of 41.1 % quartz (σ = 10.9), 4.7 % K-feldspar (σ = 3.8), 7.5 % illite (σ = 3.2), 0.2 % mixed illite/smectite (σ = 0.5), 27.5 % calcite (σ = 16.5), 17.5 % dolomite (σ = 20.7), and 1.6 % ankerite (σ = 3.6) (N = 4). TOC, on average, is 0.17 % ranging from 0.09 to 0.23 % (N = 7, σ = 0.06).

The total GR logs of Facies 5 ranges from 56.6 to 96.0 [nSv/h] with local maxima (e.g., ~16-19 m, ~34-36 m at DH; ~17.5-19.5 m at BR) along with the spectral GR log patterns of thorium and potassium curves that generally track the total GR log patterns. In places, the uranium curve contains a local maxima of notable amplitude where thorium and

potassium curves show a corresponding local minimum (e.g., ~35 m at DH; ~16.5 m, 18 m at BR). Conversely, in places the thorium curves show local maxima where uranium and potassium curves have local minima (e.g., ~26 m at BR). At the top of middle Sappington member at the BR locality (~16.5 m), the spectral GR log shows a thorium peak, whereas the measurements of uranium and potassium were below detection.

The spectral GR response of the uranium curves is consistent with low TOC (0.09-0.23 %). The response of thorium and potassium curves is consistent with a presence of clay (average 7.7 % clays) and K-feldspar (average 4.7 %) contents verified by XRD.

The dominant sedimentary process inferred for Facies 5 is episodic wave reworking of medium silt- to lower very fine-grained sand-sized detrital quartz grains above fair-weather wave base. The presence of several different trace fossils implies deposition under oxygenated conditions, and a dominance *Cruziana* ichnofacies including *Palaeophycus, Teichichnus, Thalassinoides,* and *Rosselia* suggests deposition in a sublittoral marine environment (Catuneanu, O., 2006; MacEachern, *et al*., 2010).

The late Ordovician Bighorn dolomite in Wyoming is inferred to be an ancient analog for Facies 5. Holland and Patzkowsky (2009, 2012) described the Bighorn dolomite as containing bioturbated dolostone with abundant biota and pervasive *Thalassinoides* burrows that obliterated primary sedimentary structures and interpreted it as being deposited in an open, shallow subtidal zone. The late Permian Khuff Formation in Al Qasim Province, Saudi Arabia, is another ancient analog for Facies 5. Khalifa (2005) described the Khuff Formation as containing dolostone with *Skolithos* and infaunal burrows that obliterated primary sedimentary structures and interpreted it as being deposited in the intertidal or subtidal zones (Khalifa, 2005).

Facies 6: Ripple-laminated Silty Dolostone

Facies 6 consists of ripple-laminated silty dolostone containing medium silt- to lower very fine-grained sand-sized detrital quartz grains and dolomite rhombs, and finely crystalline calcite cement (**Fig. 17**). Beds of silty dolostone in Facies 6 are generally 1 to 5 cm thick and commonly wave-rippled but also characterized locally by current-ripples (**Fig. 17**). The rippled beds locally contain brachiopod and echinoderm skeletal debris and are locally separated by silt partings or mud drapes (**Fig. 17**). The bioturbation index for

Facies 6 is 0.

XRD analysis of four representative samples of Facies 6 revealed an average of 27.2 % quartz ($\sigma = 7.14$), 0.2 % K-feldspar ($\sigma = 0.18$), 8.6 % illite ($\sigma = 5.93$), 17.2 % calcite ($\sigma = 28.00$), 43.6 % dolomite ($\sigma = 27.23$), and 3.2 % ankerite ($\sigma = 2.17$) ($N = 4$). TOC, on average, is 0.17 % ranging from 0.17 % to 0.29 % ($N = 4$, $\sigma = 0.06$). TOC, on average, is 0.20 % ranging from 0.17 % to 0.29 % ($N = 4$, $\sigma = 0.06$).

Total GR logs of Facies 6 range from 66.7 to 109.2 [nSv/h] with local maxima (e.g., ~19.5 m, ~22.5 m at DH; ~20 m at BR) along with the spectral GR log patterns of thorium and potassium curves that generally track the total GR log patterns. In one place, the uranium curve contains a local maximum of notable amplitude where thorium and potassium curves show a corresponding local minima (28 m at BR).

The spectral GR response of the uranium curves is consistent with low TOC (0.09-0.23 %) except for the strata where the uranium curve contains a local maximum of a notable amplitude. The response of thorium and potassium is consistent with the presence of clay (average 8.6 % clays) and K-feldspar (average 0.2 %) contents, as verified by XRD.

The dominant sedimentary process inferred for Facies 6 is wave reworking of medium silt- to lower very fine-grained sand-sized detrital quartz grains above fair-weather wave base. Absence of ichnofacies in Facies 6 implies relatively high rates of sediment accumulation and/or physical reworking.

An ancient analog for Facies 6 was described from the Neoproterozoic Nuccaleena Formation of the lowermost Ediacaran deposits (~635 Ma), which contains wave-rippled dolostone, interpreted as deposited on the lower slope above wave base (Hoffmann, *et al*., 2007).

Facies 7: Planar-bedded Silty Dolostone

Facies 7 consists of planar-bedded silty dolostone containing coarse silt- to lower very fine-grained sand-sized detrital quartz grains and dolomite rhombs (**Fig. 18**). Secondary porosity due to dissolution of dolomite rhombs is common (**Fig. 18**). Dolostone beds are typically 1 to 2 cm thick, parallel to each other, and separated by sharp contacts. Internally, beds display planar horizontal lamination (**Fig. 18**). The bioturbation index of Facies 7 is 0.

XRD analysis of one representative sample of Facies 7 reveals 36.4 % quartz, 4.6 % K-feldspar, 1.5 % illite, 42.1 % calcite, 15.4 % dolomite (N = 1, σ not available since N = 1). TOC, on average, is 0.28 % ranging from 0.21 % to 0.29 % (N = 3, σ = 0.08).

The total GR logs of Facies 7 ranges from 70.5 to 83.9 [nSv/h] with local minima (e.g., ~23 m at DH; ~21 m at BR) or characterizes inflection points between local minima and maxima (~20 m at DH) or vice versa (~16.5 m at DH). The spectral GR logs of the uranium and potassium curves generally show little variations, and the thorium curve shows more variability, corresponding to the relatively high variability of the total GR log patterns.

The spectral GR response of the uranium curve for Facies 7 is consistent with its low TOC (0.21-0.29 %), although local minima or transitions on the uranium curves do not appear to co-vary with TOC. The response of the thorium and potassium curves are consistent with clay (1.5 % illite) and K-feldspar (4.6 %) contents verified by XRD.

The dominant sedimentary process inferred for Facies 7 is traction transport and deposition of silt and sand-sized particles in upper plane bed flow. The sedimentary environments inferred for Facies 7 include foreshore deposition, geostrophic current deposition in a shoreface environment, combined flow deposition during storm events, and some type of sediment gravity flow such as turbidite (Boggs, 1992; Plint, 2010). The absence of ichnofacies in Facies 6 implies relatively high rates of sediment accumulation or high energy environments, consistent with the depositional processes inferred for Facies 7.

Ancient analogs for Facies 7 include the Neoproterozoic Nuccaleena Formation of the lowermost Ediacaran deposits in Southern Australia (~635 Ma), which contains planar-laminated dolostone in association with deep water foreslope facies (Rose and Maloof, 2011), and middle Devonian dolomitic strata in the northwestern Holy Cross Mountains in central Poland, which contains planar-laminated dolostone (Narkiewicz and Retallack, 2014).

Facies 8: Oncolitic, Fossil-bearing Floatstone

Facies 8 consists of oncolitic, fossil-bearing floatstone. The matrix consists of siliciclastic and carbonate mud, medium to coarse silt-sized detrital quartz grains and

dolomite rhombs, calcite cement, and organic debris (**Fig. 19**). This floatstone is rich in oncoids and fossils. Oncoids commonly contain brachiopods and bryozoans as nuclei, and algal coatings occurring around these bioclasts can be either rounded or irregular (**Fig. 19**). Oncoids also contain irregular-shaped carbonate clasts as nuclei and, in many oncolites, multiple generations of encrustation (**Fig. 19**). Most oncoids are a few cm in size but individual oncoids as large as ~10 cm wide were observed (**Fig. 19**). Brachiopods, bryozoans, and echinoderms are the most commonly identified fossils in the floatstone facies, but gastropods and ostracods also were identified (**Fig. 19**). These fossils are typically delicately preserved but also occur as broken fragments (**Fig. 19**). A bioclastic layer consisting dominantly of brachiopod and echinoderm fragments is locally present (**Fig. 19**).

The floatstone beds are massive and thicker (~3 m) at the BR locality and interbedded with calcareous/dolomitic mudstone beds (Facies 3) at the DH locality. At the BR locality, such oncolitic, fossil-bearing floatstone becomes less fossil-bearing and more fine-grained and matrix dominant upsection. The bioturbation index of Facies 8 ranges from 0 to 1.

XRD analysis of four representative samples of Facies 8 revealed an average of 21.1 % quartz ($\sigma = 6.75$), 1.6 % K-feldspar ($\sigma = 1.96$), 7.7 % illite ($\sigma = 4.22$), 0.1 % mixed illite-smectite ($\sigma = 0.13$), 0.1 % chlorite ($\sigma = 0.27$), 30.8 % calcite ($\sigma = 32.85$), 35.9 % dolomite ($\sigma = 28.90$), 2.4 % ankerite ($\sigma = 1.56$), and 0.4 % gypsum ($\sigma = 0.81$) ($N = 5$). TOC, on average, is 0.24 %, ranging from 0.21 % to 0.29 % ($N = 5$, $\sigma = 0.04$).

The total GR logs of Facies 8 ranges from 83.0 to 121.1 [nSv/h] with local minima (~39.5 m at DH; ~31 m at BR) along with the spectral GR log patterns of thorium and potassium curves that generally track the total GR log patterns. At the BR locality, the spectral GR logs for uranium and thorium co-vary, and the potassium curve is consistently low throughout Facies 8.

The spectral GR response of the uranium curve for Facies 8 is consistent with low TOC values. The response of the thorium curve is consistent with clay content (average 7.8 % clays), and the low potassium readings are consistent with low K-feldspar content (average 1.6 %) verified by XRD.

Facies 8 is interpreted as being deposited along the flanks of a carbonate build-up

where heterotrophic filter feeders were abundant within a photic zone. The abundance of delicately-preserved fossils suggests deposition of the floatstone proximal to the source area, and the locally-truncated, highly irregular algal laminae in many of the oncoids indicate occasional reworking. The fine-grained matrix in the floatstone implies deposition in a low energy environment through suspension settle-out and in part an entrapment by organisms living in the carbonate build-up. A bioclast layer consisting of fossil fragments suggests occasional changes in energy level.

Analogous oncoids to those in Facies 8 were described in grainstone from the Jurassic (Bajocian) strata in Bourgogne, northwestern France, which contain a mixture of irregularly shaped oncoids with variable shape and size, suggesting occasional reworking (Flügel, E, 2010). Similar, analogous oncoids were described in rudstone from the Late Jurassic strata, Switzerland, which contains large oncoids with irregular algae surfaces whose shapes are controlled by the shape of the cores (Flügel, E, 2010). Flügel (2010) interpreted these oncoids as deposited in moderately high-energy, shallow water environment near a platform edge.

3. 2. Facies Associations

Based on facies analysis of the Sappington Formation in central Montana, four facies associations are defined and interpreted to represent specific sedimentary environments. Each facies association is described below along with the evidence supporting the sedimentary environment inferred for each association.

Facies Association 1: Partly Restricted Offshore Marine Environment

Facies Association 1 (FA1) consists of organic-rich mudstone (Facies 1) and occurs in the lower and upper members of the Sappington Formation at the DH, BR, and BS localities (**Fig. 9**). FA1 is interpreted as deposited in a partly restricted offshore marine environment.

The absence of bioturbation and high organic content in the lower mudstone member suggests anoxic conditions prevailed long enough to severely limit biological activities throughout deposition. Overall thicker and more organic-rich mudstone at the BR locality (2.1 m thick, average TOC = 6.97 %, max. TOC = 14. 78 %) relative to the DH

locality (1.0 m thick, average TOC = 1.09 %, max. TOC = 2.74 %) implies that paleogeographically the anoxic basin deepened from west to east between the two localities. Additionally, lower clay content and organic-matter preservation in the lower mudstone member at the DH locality relative to the BR locality DH average 23.6% clay, N=3; BR average 48.3 % clay, N=8) implies that the deposition of the DH locality was shallower and more prone to wave mixing or bottom current activity and dysoxic, rather than anoxic, conditions.

The presence of bioturbation and relatively high organic content in the upper mudstone member at the BR and BS localities (combined average TOC = 3.04%, N=9) suggests deposition in an offshore to offshore transition environment under dysoxic conditions capable of supporting a sparse infauna.

(2) Open Marine Carbonate Build-up Environment

Facies Association 2 (FA2) consists of oncolitic, fossil-bearing floatstone (Facies 8) and occurs in the lower unit of the middle Sappington Formation (**Fig. 9**). FA2 is interpreted as deposited along the flanks of a carbonate build-up in a relatively low energy, open marine environment. The presence of a nearby carbonate build-up is suggested by the abundance of delicately-preserved heterotrophic filter feeders and the formation of oncoids by photosynthetic algae. The diverse suite of filter-feeders including brachiopods, bryozoans, and echinoderms observed in the floatstone implies deposition in an open marine environment with relatively consistent temperature, salinity, and current activity, and low levels of turbidity. The presence of photosynthesizers strongly suggests a shallow subtidal environment within the photic zone. The abundance of fine-grained sediments in the floatstone is interpreted to have been in part trapped by these organisms but also deposited through suspension settle-out, suggesting a low energy setting. The very loose packing of the allochems, which generally float in a fine-grained matrix of mixed siliciclastic and carbonate sediments, suggests that the facies association represents an allochthonous mixture of sediment that includes contributions from a nearby, active carbonate build-up as well as contributions from continental weathering.

(3): Open Marine Offshore to Offshore Transition Environment

Facies Association 3 (FA3) includes bioturbated, calcareous/dolomitic muddy siltstone (Facies 2) and wavy-laminated/lenticular silty dolostone with interbedded/interlaminated mudstone (Facies 3). FA3 occurs in the lower and middle units of the middle Sappington member at the DH and BR localities (**Fig. 9**). FA3 is interpreted as deposited in an open marine offshore to offshore transition environment. The presence of a *Cruziana* ichnofacies assemblage and relatively low TOC content (<0.65%) in the middle mudstone member suggests that the basin was generally well oxygenated and existed in an open marine setting. The calcareous/dolomitic muddy siltstone generally represents deposition in an offshore environment through suspension settle-out, and the deposition of silty dolostone with interbedded/interlaminated mudstone reflects a decrease in mud content associated with shallower water of an offshore transition zone.

(4): Open Marine Storm-dominated Shoreface Environment

Facies Association 4 (FA4) includes HCS silty dolostone (Facies 4), bioturbated, ripple-laminated silty dolostone (Facies 5), ripple-laminated silty dolostone (Facies 6), and planar bedded silty dolostone (Facies 7) and occurs in the lower and upper units of the middle Sappington member at the DH, BR, and BS localities (**Fig. 9**). FA4 is interpreted as reflecting deposition in an open marine storm-dominated environment ranging from lower to middle shoreface.

The high degree of bioturbation in the ripple-laminated silty dolostone within the lower unit of the middle Sappington Formation suggests a rate of deposition that was low enough to allow for the establishment of a thriving infauna. The presence of a storm bed locally observed at the BR locality implies storm influence.

In the upper unit of the middle Sappington member, FA4 commonly represents a vertical succession of facies interpreted to reflect deposition by individual storm events as well amalgamation of depositional events from multiple storms. As such, a sharp basal contact of HCS silty dolostone is interpreted as representing the initial energy increase associated with the storm. Overlying silty dolostone containing HCS, combined flow ripples, and local soft sediment deformation is interpreted to represent storm deposition. All three structures are consistent with rapid sedimentation during waning storm

deposition, and locally observed unidirectional current ripples that cap the succession imply decreasing energy levels possibly associated with post-storm relaxation and/or geostrophic flow. In some parts of FA4, HCS silty dolostone is overlain by ripple-laminated silty dolostone and/or is associated with planar-bedded silty dolostone, which are interpreted to be storm-related. Succession of planar-bedded silty dolostone, overlain by ripple-laminated beds, are interpreted as reflecting relaxation or geostrophic current flow associated with waning storm events, followed by wave reworking of the upper deposit. Cm-scale interbeds of bioturbated, ripple-laminated silty dolostone are interpreted to reflect wave reworking and infaunal colonization during intervening periods of relatively fair weather.

3.3. Sequence Stratigraphic Framework

At present, three main sequence stratigraphic models are routinely used to analyze the sediment fill history of a basin. These three models are similar in terms of their use of correlative chronostratigraphic surfaces to study stratigraphy in a time-dependent framework. They differ, however, in their placement of boundaries between discrete stratigraphic intervals. For example, in the depositional sequence model (e.g. Mitchum *et al*, 1977; Vail *et al*., 1977; Posamentier *et al.*, 1988), sequences are bound by surfaces that reflect the transition from a regressive phase to a transgressive phase, and are composed of an subaerial unconformity in many up-dip positions and a correlative marine conformities in more distal positions; genetic stratigraphic sequences (Galloway, 1989) in contrast are bound by maximum flooding surfaces that mark the transition from an overall transgression to a regression; and the transgressive-regressive sequence (Embry and Johannessen, 1992) bases the distinction of individual depositional sequences on the identification of composite surfaces including subaerial unconformities on the basin margin and the marine portion of maximum regressive surfaces in more distal positions.

In this study, the depositional sequence approach was taken because sequence boundaries, flooding surfaces, and maximum flooding surfaces were easily recognized within the Sappington Formation and the identification of these surfaces allowed the definition of systems tracts that reflect a full depositional cycle.

3.3.1 Sequence Stratigraphic Surfaces

Flooding surface are identified where there is evidence of an abrupt landward shift of facies, indicating an increase in base level or a decrease in sediment supply (Catuneanu, O., 2006; Catuneanu *et al*., 2009). Transgressive ravinement surfaces are flooding surfaces that show clear indication of erosion due to wave or tidal scouring. Transgressive ravinement surfaces are commonly related to base-level rise and landward migration of the shoreline (Hunt and Tucker, 1992). Maximum flooding surfaces are placed where a change from retrogradational to progradational stacking patterns are recognized (Catuneanu, O., 2006; Catuneanu *et al*., 2009). Forced regressive surfaces are placed where there is evidence of an abrupt facies shift that may indicate base-level fall or an increase in sediment supply (Catuneanu, O., 2006; Catuneanu et al., 2009). Sequence boundaries are the most significant surfaces related to the basinward regression of the depositional system and mark the end of base level fall. Sequence boundaries are composed of subaerial unconformities in the up-dip portion of the depositional system and its marine correlative conformity in the sub-aqueous part (Catuneanu, O., 2006; Catuneanu et al., 2009).

3.3.2 Systems Tracts

Systems tracts represent contemporaneous depositional intervals within a given sequence (e.g. Van Wagoner *et al*., 1988, 1990; Galloway, 1989; Hunt and Trucker, 1992). A depositional sequence can contain the Highstand Systems Tract (HST), Falling Stage Systems Tract (FSST), Lowstand Systems Tract (LST), and Transgressive Systems Tract (TST), but not all systems tracts may be recognized at any given location within a depositional system.

The HST is defined as a combination of aggradational and progradational stacking patterns during the late stage of base-level rise when the sedimentation rate exceeds the rate of base-level rise (Catuneanu, O., 2006). The HST is bounded by the maximum flooding surface at the base and typically a composite surface at the top formed by the subaerial unconformity, the basal surface of forced regression, and the oldest portion of the regressive surface of marine erosion (Catuneanu, O., 2006). Highstand sedimentary wedges generally consist of fluvial, coastal, and shoreface deposits, located relatively close to the basinal margin (Catuneanu, O., 2006).

The FSST is composed of shallow and deep water deposits that accumulated in the basin during a forced basinward regression of the depositional system (Hunt and Tucker, 1992; Catuneanu, O., 2006). The FSST is bounded at its base by the surface of forced regression and the oldest portion of the regressive surface of marine erosion. The top of the FSST is marked by a composite surface including a subaerial unconformity, its marine correlative conformity, and the youngest portion of the regressive surface of marine erosion (Catuneanu, O., 2006).

The LST is composed of aggradational and progradational stacked facies that were deposited during the early stage of base-level rise (Hunt and Tucker, 1992; Catuneanu, O., 2006). The LST is bounded by the subaerial unconformity and its marine correlative conformity at the base and by the maximum regressive surface, which defines the change from shoreline regression to subsequent transgression, at the top (Catuneanu, O., 2006).

The TST is composed of retrogradational stacked facies deposited during base-level rise (Catuneanu, O., 2006). The TST is bounded by the maximum regressive surface at the base and by the maximum flooding surface at the top, (Catuneanu, O., 2006).

3.3.3. The Sappington Formation in Southwestern-Central Montana

3.3.3.1. Dry Hollow (DH) Section

The Sappington Formation at the Dry Hollow locality (DH) is approximately 25 meter thick. It is bound by the uppermost limestone bed of the Three Forks Formation at the base and by the thick bioclastic limestones of the Lodgepole limestone at the top (**Fig. 20**). The Sappington-Three Forks contact is a regional unconformity recognized throughout much of Montana. Several conodont zones are missing across this boundary (**Fig. 5**) and the hiatus is interpreted as a sequence boundary (SB).

The lower organic-rich mudstone of the Sappington Formation represents an abrupt shift of facies from the underlying shallow marine limestone of the Three Forks formation. Within the lower organic-rich mudstone, facies are interpreted to be retrogradational and accompanied by an increase of TOC and increase in total GR measurements. The contact between the lower organic-rich mudstone and the overlying oncolitic, fossil-bearing floatstone is interpreted as a regionally correlative maximum flooding surface (mfs). The

mostly fine-grained mudstone and the highest total GR measurements were observed immediately below the contact between these two facies. As such, the retrogradationally stacked facies reflecting a partly restricted offshore marine environment, bounded by the fs at the base and mfs at the top, is interpreted as representing a TST.

The lower unit of the middle Sappington member, consisting of oncolitic, fossil-bearing floatstone, calcareous/dolomitic muddy siltstone, and silty dolostone, represents a shoaling-upward succession above the mfs. The interpreted sedimentary environments shoal from carbonate build-up, to offshore, to offshore transition, and finally to shoreface deposits in an open marine environment. The shoaling upward succession is topped by a regional correlative fs, and is interpreted as a HST.

The middle unit of the middle Sappington member consists of calcareous/dolomitic muddy siltstone overlying the silty dolostone of the HST. The abrupt shift of facies from the silty dolostone to the muddy siltstone of the middle Sappington member is interpreted as representing a regional correlative SB that marks the end of base-level fall as well as a regional correlative fs that indicates the beginning of base-level rise. The muddy siltstone generally fines upward, consistent with an increase in total GR values. The surface with the highest clay content was interpreted as mfs, forming the top boundary of the TST. The muddy siltstone transitions into interbedded/interlaminated silty dolostone, interpreted to represent a shoaling-upward succession above the mfs at its base. Within this shoaling-upward succession, facies are stacked progradationally and are accompanied by a decreasing total GR measurements and overall change within an open marine setting from offshore to offshore transition depositional environments. The contact between the shoaling-upward succession and the overlying silty dolostone is interpreted as representing a regional correlative forced regressive surface (FRS), as suggested by an abrupt shift of facies from muddy siltstone to silty dolostone. This shoaling-upward succession, bounded by the mfs at the base and FRS at the top, is interpreted as representing a HST.

The upper unit of the middle Sappington member is interpreted as another shoaling-upward succession. Above the FRS at the base, facies are stacked aggradationally to progradationally consistent with an overall decrease in GR. The upper contact between this shoaling-upward succession and the overlying Lodgepole limestone is interpreted to be a SB. It is marked by an abrupt shift of facies from silty dolostone to limestone. This

shoaling-upward succession, bounded by the FRS at the base and SB at the top, is interpreted as representing a FSST.

3.3.3.2. Bridger Range (BR) Locality

The Sappington Formation at the Bridger Range (BR) locality is approximately 20.5 meter thick. It is bounded below by crinoidal limestone of the Three Forks Formation and above by bioclastic limestone of the Lodgepole Formation (Madison Group_ (**Fig. 20**). The basal Sappington mudstone in the Bridger section is the most organic-rich observed in this study. The contact between this organic-rich mudstone and the underlying carbonate beds of the Three Fork Formation is interpreted to be a major flooding surface (fs). This flooding surface forms a composite surface with a sequence boundary at the same contact that was identified by previous conodont biostratigraphy work. Within the lower organic-rich mudstone, facies fine upward from the base to 2 m above the flooding surface, accompanied by an increase of TOC and increase in total GR measurements. The contact between the lower organic-rich mudstone and the overlying oncolitic, fossil-bearing floatstone is interpreted to be a regionally correlative maximum flooding surface (mfs). The most fine-grained mudstone, the highest total GR measurements, and the highest TOC content all were observed immediately below the contact between these two facies. As such, these retrogradationally stacked facies are interpreted to reflect a partly restricted offshore marine environment, bounded by the fs at the base and mfs at the top, and are interpreted to represent a TST.

The lower unit of the middle Sappington member, consisting of oncolitic, fossil-bearing floatstone, calcareous/dolomitic muddy siltstone, and silty dolostone, represents a shoaling-upward succession above the mfs just below it. Within this shoaling-upward succession, facies are stacked progradationally and accompanied by a decrease in total GR measurements. The sedimentary environment changes from carbonate build-up to shoreface deposits in an open marine environment. The contact between the shoaling-upward succession and the overlying calcareous/dolomitic mudstone is interpreted to be a regional correlative fs and is represented by a shift from silty dolostone to mudstone facies. The change in lithologies from floatstone to silty dolostone within the shoaling-upward succession is interpreted to represent a gradational change to clastic deposition, because an

allochthonous mixture of sediment contributed from continental weathering was observed in the floatstone. This shoaling-upward succession, bounded by the mfs at the base and fs at the top, is interpreted as representing a HST.

The middle unit of the middle Sappington member consists of calcareous/dolomitic muddy siltstone in a fining-upward succession. The abrupt shift of facies from the silty dolostone to the muddy siltstone of the middle Sappington member is interpreted as representing a regional correlative SB that marks the end of base-level fall as well as a regional correlative fs that indicates the beginning of base-level rise. Within the fining-upward succession, facies are stacked retrogradationally, consistent with an increase in total GR measurements. The mfs was place in the interval containing the highest clay content. These retrogradationally stacked, open marine offshore deposits are interpreted as TST, bounded by a fs at its base and a mfs at its top.

The middle unit of the middle Sappington member consists of calcareous/dolomitic muddy siltstone interbedded/interlaminated with silty dolostone that represents a shoaling-upward succession above the mfs. Facies within this overall shoaling upward succession change from offshore to offshore transition zone. Although total GR measurements are increasing within this shoaling-upward succession, lithological changes with increasing interbedded/interlaminated silty dolostone upsection suggests a progradational stacking pattern. The contact between the shoaling-upward succession and the overlying silty dolostone is interpreted as representing a regional correlative forced regressive surface (FRS), as suggested by an abrupt shift of facies from muddy siltstone to silty dolostone. This shoaling-upward succession, bounded by the mfs at the base and FRS at the top, is interpreted as representing a HST.

The upper unit of the middle Sappington member consists of shoaling-upward succession above the FRS. Within this shoaling-upward succession, silty-dolostone facies are stacked aggradational to progradationally, consistent with an overall decrease in total GR measurements. The abrupt shift of facies from silty dolostone to the bioturbated, organic-rich calcareous/dolomitic mudstone of the upper Sappington member is interpreted as representing a regional correlative SB that marks the end of base-level fall. This shoaling-upward succession, bounded by the FRS at the base and SB at the top, is interpreted as representing a FSST.

The upper organic-rich mudstone of the Sappington Formation represents an abrupt shift of facies from the underlying silty dolostone, and the contact between the two lithologies is interpreted to be a regional correlative fs. Within the upper organic-rich mudstone, facies are stacked retrogradationally and are accompanied by an increase in total GR measurements. A regional correlative mfs was placed where the finest mudstone and the highest total GR measurements were observed. The retrogradationally stacked, restricted offshore marine facies is interpreted as a TST. It is bounded by the fs at the base and mfs at the top.

A coarsening-upward succession within the upper organic-rich mudstone, above the mfs, represents the onset of a subsequent HST that continues in the overlying Lodgepole limestone.

3.3.3.3. Big Snowy (BS) Locality (Incomplete Section)

The Big Snowy locality contains an approximately 7.5 meter thick interval of the upper Sappington Formation, bounded by the Sappington-Lodgepole contact. (**Fig. 20**).

The upper unit of the middle Sappington member consists of a shoaling upward succession of silty dolostone, reflected by a decrease in total GR. The contact between the shoaling-upward succession and the overlying organic-rich upper mudstone is a wavy surface with mud rip-up clasts. This surface was interpreted as a sequence boundary (SB) and a transgressive wave ravinement surface (TRS) (**Fig. 21**). This shoaling-upward succession is interpreted as representing either a HST or FSST.

The upper organic-rich mudstone of the Sappington Formation represents an abrupt shift of facies from the underlying silty dolostone, and the contact between the two lithologies is interpreted to be a regionally transgressive ravinement surface (TRS). Within the upper organic-rich mudstone, facies are stacked retrogradationally and are accompanied by an increase in total GR. A regionally correlative maximum flooding surface (mfs) was placed where the most fine-grained mudstone and the highest total GR measurements were observed. The retrogradationally stacked facies reflect a partly restricted offshore marine environment, bounded by the TRS at the base and mfs at the top, and is interpreted to represent a TST.

The subsequent coarsening-upward succession within the upper organic-rich

mudstone, above the mfs, was interpreted as a HST with an upper bounding surface somewhere in the Lodgepole limestone.

3.3.4. The Sappington Formation in the Subsurface of Central and Western Montana (Well Log Analysis)

Outcrop GR measurement allowed for calibration of the subsurface data set to be used for the sequence stratigraphic interpretation. The most important surfaces recognized on log are listed below, in stratigraphic order. An abrupt shift from generally low GR values to very high GR values mark the contact between the Three Forks Formation and the Sappington Formation. The surface reflected by this GR shift was interpreted to represent a composite surface that is both a sequence boundary (SB) and flooding surface (fs) and was used to mark the base of the lower member of the Sappington Formation. A maximum flooding surface (mfs) was placed at the overlying peak in total GR measurements. Above the mfs, the total GR measurements show an overall decreasing log pattern up to the next fs at the base of middle mudstone member. Within the middle member, a mfs was approximately placed either at the end of increasing total GR measurements (e.g., DH locality) or in the middle of increasing total GR measurements (e.g., BR section) reflecting heterogeneity within the middle mudstone facies. A forced regressive surface (FRS) can be difficult to pinpoint from the total GR log patterns because of inconsistency based on outcrop observations. For instance, FRS can be pinpointed in the BR type log pattern because it coincides with the abrupt fall in total GR measurements, whereas it can be difficult to pinpoint in the DH type log pattern because the FRS occurs at the end of one of the decreasing total GR measurements. Above the FRS, the total GR measurements show an overall decreasing log pattern until it reaches another SB either at the base of the upper organic-rich mudstone or at the Sappington-Lodgepole contact. If the upper mudstone is present, a fs was placed at the base of the upper organic-rich mudstone, and a mfs was placed approximately at the peak of the total GR measurements. The Sappington-Lodgepole contact can be placed approximately where an overall decrease in total GR measurements reach the base-line for the overlying Lodgepole limestone.

The overall GR log pattern revealed in outcrop and the stratigraphic surfaces picked within it using outcrop observations were carried into the subsurface, where similar

sequence stratigraphic surfaces were recognized and mapped. For example, a GR well log from State 16A-36 (25-013-21033) in central Montana shows a similar stacking pattern as observed at the Sappington outcrops at the DH and BR localities (**Fig. 22**). From stratigraphic bottom to up, the well log shows a significant increase in total GR measurements at the base, interpreted as a fs at the base and a mfs at the top of the peak. Above the mfs, the total GR log shows a progradational stacking pattern until it transitions into a retrogradationally stacked log pattern, indicating the presence of a fs at this transition. Since the retrogradationally stacked log pattern is similar to the stacking pattern at the BR locality, a next mfs was approximately placed below the total GR peak. Following the mfs, the total GR log measurements show a progradational stacking pattern, as observed at the DH locality, until reaching a minimum value which marks the contact with the overlying Lodgepole limestone, interpreted to be a SB. In case of State 16A-36, the top Sappington Formation, or the SB, was noted on the well log.

3.4. Depositional History of the Sappington Formation in Western and Central Montana (Summary)

Based on the well log correlation, a series of isopach maps for the Sappington Formation and its equivalents in central and western Montana were created. These isopach maps summarize the results of the sequence stratigraphic analysis and depict the regional depositional patterns and depositional history of these strata.

The total isopach map shows regional depositional basins of the Sappington in central Montana, the Exshaw Formation in northwestern Montana, and major paleogeographic features such as the Central Montana Uplift (CMU) and the Beartooth Uplift (**Fig. 23**). This map shows depositional centers of the Sappington Formation to be elongate in an east-west direction and to be closely associated with the Central Montana Trough (CMT) (**Fig. 23**). Other depositional centers were identified in western and northwestern Montana, including Cascade, Teton, Glacier, and Toole Counties (**Fig. 23**).

The oldest depositional sequence, consisting of the lower member and the lower unit of the middle member, contains the TST and HST and generally deposited in a west-east trending CMT as well as semi-isolated basins in western and northwestern Montana (**Fig. 24**). Deposition of the partly restricted marine interval during the TST is consistent

with the regional depositional pattern indicated by the isopach map (**Fig. 24**). In central Montana, the CMT was surrounded by the paleohighs and had a semi-closed end westward, which would have helped establish basin-wide oxygen dysoxic to anoxic conditions for the preservation of the organic-rich mudstone. The presence of the semi-isolated basins in western and northwestern Montana during the TST implies deposition in a partly restricted offshore marine environment. Deposition of the open marine interval during the HST is consistent with the regional depositional pattern indicated by the isopach map, showing the depositional basins in central and western Montana having open-end westward, suggesting oxygenation of these basins due to a connection to the open marine westward (**Fig. 24**). Depositional basin in northwestern Montana appeared to be separated from the deposition in central and western Montana by paleohighs during the HST **(Fig. 24**).

The second depositional sequence, consisting of the middle and upper units of the middle member, contains the TST, HST, and FSST. Deposition of the open marine interval during the TST is consistent with the regional depositional pattern indicated by the isopach map, showing the depositional basins in central and western Montana with an open-ended connection to the west (**Fig. 24**). During the following HST and TST, deposition of the open marine interval is consistent with the regional depositional pattern indicated by the isopach map, showing an open-end westward (**Fig. 24**). Additionally, the isopach map indicated that the CMT was deepening to the west and implied expansion of the CMT to both south-central and north-central Montana (**Fig. 24**). Such changes in regional depositional patterns implies potential tectonic influence on basin geometry either due to reactivations of old fault zones or the Antler Highlands approaching from the west. Depositional basin in northwestern Montana appeared to be separated from the deposition in central and western Montana by paleohighs during the second sequence **(Fig. 24**).

The youngest depositional sequence, consisting of the upper member, contains the TST and HST. Deposition of the partly restricted marine interval during this sequence is consistent with the regional depositional pattern by the isopach map, showing semi-isolated basin in central, western, and northwestern Montana (**Fig. 24**). However, the low regional density of well logs indicating the presence of the upper member suggests that some of these semi-isolated basins may be artificial.

4. CONCLUSIONS

Detailed study of the Devonian-Mississippian Sappington Formation and its equivalents in southwestern-central Montana based on sedimentologic, petrographic, petrophysical and geochemical analyses leads to the following conclusions:

(1) The Sappington Formation can be subdivided into eight facies: organic-rich mudstones (F1); bioturbated, calcareous/dolomitic muddy siltstone (F2); bioturbated, wavy-laminated silty dolostone with interbedded/interlaminated mudstone (F3); hummocky cross-stratified silty dolostone (F4); bioturbated, ripple-laminated, calcareous/dolomitic siltstone-silty dolostone (F5); ripple-laminated silty dolostone (F6); planar-bedded silty dolostone (F7); and oncolitic, fossil-bearing floatstone (F8).

(2) The Sappington Formation is interpreted as representing four facies associations: a partly restricted offshore marine environment (FA1); an open marine carbonate build-up environment (FA2); an open marine offshore to offshore transition environment (FA3); and an open marine storm-dominated shoreface environment (FA 4).

(3) Based on a depositional sequence approach, the Sappington Formation is interpreted to represent two higher order sequences with an additional sequence continuing into the overlying Lodgepole limestone. The oldest depositional sequence contains the TST and HST, the second depositional sequence contains the TST, HST, and FSST, and the youngest depositional sequence contains the TST and HST.

(5) Regional depositional patterns for the Sappington Formation and its equivalents are consistent with the interpreted sedimentary environments of these strata based on facies associations. Deposition of the partly restricted marine interval of the lower and upper members of the Sappington Formation occurred in a west-east trending semi-isolated basin. In contrast, deposition of the open marine middle member occurred in a basin having an open west end, suggesting oxygenation due to a seaway connection west to the open ocean.

5. REFERENCES

Achauer, C.W., 1959, Stratigraphy and microfossils of the Sappington Formation in southwestern Montana. In: *10th Annual Field Conference* (C.R. Hammond and H. Trapp Jr. Eds.), Billings Geological Society, p. 41-49.

Adiguzel, Z., 2012, Correlation and stratigraphic analysis of the Bakken and Sappington Formations in Montana [Master's Thesis]: College Station, Texas A&M University.

Adiguzel, Z., Grader, G.W., Doughty, T.P., and Pope, M.C., 2012, Synsedimentary deformation and erosion of the Exshaw/Sappington Formation in west-central Montana: Evidence for a brief basin polarity switch and development of paleohighs along the Western Bakken Fairway: AAPG Annual Convention and Exhibition.

Allen, G.P., Posamentier, H.W., 1993, Sequence stratigraphy and facies model of an incised valley fill: the Gironde Estuary, France: Journal of Sedimentary Petrology, v. 63, p. 378–391.

Angulo, S. and Buatois, L.A., 2012, Ichnology of a Late Devonian-Early Carboniferous low-energy seaway: The Bakken Formation of subsurface Saskatchewan, Canada: Assessing paleoenvironmental controls and biotic responses: Palaeogeography, Palaeoclimatology, Palaeoecology, v. 315-316, p. 46-60.

Asquith, G. and Krygowski, D., 2004, Gamma Ray Log. In: *Basic Well Log Analysis*, Tulsa, Oklahoma, AAPG.

Baars, D.L., 1972, Devonian System. In: *Geologic Atlas of the Rocky Mountain Region* (Mallory, W.W. Eds.), Rocky Mountain Association of Geologist, p.90-99.

Bjorlykke, Knut, 2010, Petroleum Geoscience: From Sedimentary Environments to Rock Physics: Springer-Verlag, Berlin Heidelberg.

Blakey, R., 2011, Paleogeography and Geologic Evolution of North America: http://www2.nau.edu/rcb7/nam.html (accessed January 26, 2014).

Blum, M.D., 1994, Genesis and architecture of incised valley fill sequences: a Late Quaternary example from the Colorado River, Gulf Coastal Plain of Texas. In: *Siliciclastic Sequence Stratigraphy* (P. Weimer and H.W. Posamentier Eds.): Recent Developments and Applications: AAPG Memoir, 58, p. 259–283.

Boggs, S. Jr., 1992, Sedimentary Texture, Shales. In: *Petrology of Sedimentary Rocks*, Blackburn Press, New Jersey.

Boggs, S. Jr., 2006, Principles of Sedimentology and Stratigraphy: Person Prentice Hall, New Jersey.

Brett, C.E., Baird, G.C., and Bartholomew, A.J., 2011, Sequence stratigraphy and a revised sea-level curve for the Middle Devonian of eastern North America: Palaeogeography, Palaeoclimatology, Palaeoecology, v. 304, p. 21-53.

Bromley, R.G. and Ekdale, A.A., 1984, *Chondrites*: A Trace Fossil Indicator of Anoxia in Sediments: Science, v. 224, p. 872-874.

Buggisch, W., Joachimski, M.M., Sevastopulo, G., and Morrow, J.R., 2008, Mississippian $\delta^{13}C_{carb}$ and conodont apatite $\delta^{18}O$ records - Their relation to the Late Palaeozoic Glaciation: Paleogeography, Paleoclimatology, Paleoecology, v. 268, p. 273-292.

Cant, D., 1992, Subsurface facies analysis. In: *Facies Models: Response to Sea Level Change* (Walker, R.G. and James, N.P. Eds.), Geological Association of Canada, GeoText 1, p. 27-45.

Catuneanu, O., 2006, Principles of Sequence Stratigraphy: Elsevier, Amsterdam.

Catuneanu, O., *et al*., 2009, Towards the standardization of sequence stratigraphy. Earth Science Reviews, v. 92, p. 1-33.

Chen, Z., Osadetz, K.G., Jiang, C., and Li, M., 2009, Spatial variation of Bakken or Lodgepole oils in the Canadian Williston Basin: AAPG Bulletin, v. 93, p. 829-851.

Christopher, J.E., 1962, The Three Forks Group (Upper Devonian-Kinderhookian) of southern Saskatchewan. In: 13^{th} *Annual Field Conference and Symposium* (A.R. Hansen and J.H. McKeever Eds.), Billings Geological Society, p.67-77.

Collinson, C., Rexroad, C.B., and Thompson, T.L., 1980, Conodont Zonation of the North American Mississippian: Geological Society of America Memoir 127, p. 353-394.

Davies, S.J. and Elliott, T, 1996, Spectral gamma ray characterization of high resolution sequence stratigraphy: examples from Upper Carboniferous fluvio-deltaic systems, County Clare, Ireland. In: *High resolution sequence stratigraphy: Innovations and applications* (Howell, J. A. and Aitken, J.F. Eds), Geological Society Special Publication, v. 104, p. 25-35.

Darrow, G. and Cardinal, F.L., 1962, Devonian production in northeast Montana. In: 13*th* *Annual Field Conference and Symposium* (A.R. Hansen and J.H. McKeever Eds.), Billings Geological Society, p.107-114.

Dreesen, R., Sandberg, C.A., and Ziegler, W., 1986, Review of late Devonian and early Carboniferous conodont biostratigraphy and biofacies models as applied to the Ardenne shelf: Belgian Geological Survey, p. 27-42.

Dorobek, S.L., 1995, Synorogenic carbonate platforms and reefs in foreland basins: controls on stratigraphic evolution and platform/reef morphology: SEPM Special Publication, no. 52, p. 127-147.

Dorobek, S.L., Reid, S.K., Elrick, M., Bond, G.C., and Kominz, M.A., 1991, Subsidence across the Antler foreland of Montana and Idaho: Tectonic versus eustatic effects: Kansas Geological Survey Bulletin, v. 233, p. 232-251.

Ellis, D.V. and J.M. Singer, 2007, Well Logging for Earth Scientists: Springer, Dordrecht.

Embry, A.F. and J.E. Klovan, 1972, Absolute water depth limits of late Devonian paleoecological zones: Geologische Rundschau, v. 61, p. 672-686.

Embry, A.F. and Johannessen, E.P., 1992, T-R sequence stratigraphy, facies analysis and reservoir distribution in the uppermost Triassic-Lower Jurassic succession, western Sverdrup Basin, Arctic Canada. In: Arctic Geology and Petroleum Potential (T.O. Vorren, E. Bergsager, O.A. Dahl-Stamnes, E. Holter, B. Johansen, E. Lie, and T.B. Lund, Eds.): Norwegian Petroleum Society (NPF) Special Publication 2, p. 121-146.

Fanti, F. and O. Catuneanu, 2010, Fluvial Sequence Stratigraphy: The Wapiti Formation, West-central Alberta, Canada: Journal of Sedimentary Research, v. 80, p. 320-338.

Flugel, E, 2010, Microfacies of Carbonate Rocks: Springer-Verlag, Berlin-Heidelberg.

Fuller, J.G.C.M. and Porter, J.W., 1962, Profile and stratigraphic cross-sections of Devonian strata in the northern great plains between central Alberta and eastern North Dakota. In: 13*th* *Annual Field Conference and Symposium* (A.R. Hansen and J.H. McKeever Eds.), Billings Geological Society, p.42-46.

Galloway, W.E., 1989, Genetic stratigraphic sequences in basin analysis, I. Architecture

and genesis of flooding-surface bounded depositional units: AAPG Bulletin, v. 73, p. 125-142.

Gaswirth, S.B., Marra, K.T., Cook, T.A., Charpentier, R.R., Gautier, D.L., Higley, D.K., Klett, T.R., Lewan, M.D., Lillis, L.P., Schenk, C.J., Tennyson, M.E., and Whidden, K.J., 2013, Assessment of Undiscovered Oil Resources in the Bakken and Three Forks Formations, Williston Basin Province, Montana, North Dakota, and South Dakota, 2013: U.S. Geological Survey Fact Sheet 2013–3013.

Giles, K.A. and Dickinson, W.R., 1995, The Interplay of eustasy and lithostratigraphic flexure in forming stratigraphic sequences in foreland settings: An example from the Antler foreland, Nevada and Utah: SEPM Special Publication, v. 52, p. 187-211.

Gribi, E.D. Jr., 1959, Oil developments and prospects of south Sweetgrass Arch area. In: *10th Anniversary Field Conference* (C.R. Hammond and H. Trapp Jr. Eds.), Billings Geological Society, p. 93-97.

Gutschick, R.C. and Lamborn, R., 1975, Bifungites, trace fossils from Devonian-Mississippian rocks of Pennsylvanian and Montana, U.S.A.: Paleogeography, Paleoclimatology, Paleoecology, v. 18, p. 193-212.

Gutschick, R.C., Suttner, L.J., and Switek, M.J., 1962, Biostratigraphy of transitional Devonian-Mississippian formation of southwest Montana. In: 13*th Annual Field Conference and Symposium* (A.R. Hansen and J.H. McKeever Eds.), Billings Geological Society, p.79-89.

Haq, B.U. and Schutter, S.R., 2008, A chronology of Paleozoic sea-level changes: Science, v. 322, p. 64-68.

Heron, D.P.L., Cox, G., Trundley, A., and Collins, A., 2011, Sea ice-free conditions during the Sturtian glaciation (early Cryogenian), Southern Australia: Geological Society of America, v. 39, p. 31-34.

Hoffman, P.F., Halverson, G.P., Domack, E.W., Husson, J.M., Higgins, J.A., and Schrag, D.P., 2007, Are basal Ediacaran (635 Ma) post-glacial “cap dolostones” diachronous?: Earth and Planetary Science Letters, v.258, p.114-131.

Hofmann, M.H., Wroblewski, A., and Boyd R., 2011, Mechanism controlling the clustering of fluvial channels and the compensational stacking of cluster belts: Journal of

Sedimentary Research, v. 81, p. 670-685.

Holland, S.M. and Patzkowsky, M.E., 2009, The stratigraphic distribution of fossils in a tropical carbonate succession: Ordovician Bighorn dolomite, Wyoming, USA: Palaios, v. 24, p. 303-317.

Holland, S.M. and Patzkowsky, M.E., 2012, Sequence architecture of the Bighorn dolomite, Wyoming, USA: Transition to the late Ordovician icehouse: Journal of Sedimentary Research, v. 82, p. 599-615.

Hunt, D. and Tucker, M.E., 1992, Stranded parasequences and the forced regressive wedge systems tract: deposition during base level fall: Sedimentary Geology, v. 81, p. 1-9.

Isaacson, P.E., Martinez, E.D., Grader, G.W., Kalvoda, J., Babek, O., and Devuyst, F.X., 2008, Late Devonian-earliest Mississippian glaciation in Gondwanaland and its biogeographic consequences: Paleogeography, Paleoclimatology, Paleoecology, v. 268, p. 126-142.

Jiang, C. and Li, M., 2002, Bakken/Madison petroleum systems in the Canadian Williston Basin. Part 3: geochemical evidence for significant Bakken-derived oils in Madison Group reservoirs: Organic Geochemistry, v. 33, p. 761-787.

Johnson, J.G., Klapper, G., and Sandberg, C.A., 1985, Devonian eustatic fluctuations in Euramerica: Geological Society of America Bulletin, v. 96, p. 567-587.

Johnson, J.G., Klapper, G., and Sandberg, C.A., 1986, Late Devonian eustatic cycles around margin of old red continent: Belgian Geological Survey, p. 141-147.

Johonston, D.I., Henderson, C.M., and Schumidt, M.J., 2010, Upper Devonian to lower Mississippian conodont biostratigraphy of uppermost Wabamun group and Palliser formation to lowermost Banff and Lodgepole formations, southern Alberta and southeastern British Columbia, Canada: Implications for correlations and sequence stratigraphy: Bulletin of Canada Petroleum Geology. V. 58, no. 4, p. 295-341.

Kaufmann, B., 2006, Calibrating the Devonian Time Scale: A synthesis of U-Pb ID-TIMS ages and conodont stratigraphy: Earth-Science Reviews, v. 76, p. 175-190.

Keighley, D., Flint, S., Howell, J., and Moscariello, A., 2003, Sequence Stratigraphy in Lacustrine Basins: A model for Part of the Green River Formation (Eocene),

Southwest Uinta Basin, Utah, U.S.A.: Journal of Sedimentary Research, v. 73, p. 987-1006.

Kevin, R.G., 2001. Devonian Antler fold and thrust belt and foreland basin development in the southern Canadian Cordillera: implications for the Western Canada Sedimentary Basin: Bulletin of Canadian Petroleum Geology, v. 49, no. 1, p. 7-36.

Khalifa, M.A., 2005, Lithofacies, diagenesis and cyclicity of the 'Lower Member' of the Khuff Formation (Late Permian), Al Qasim Province, Saudi Arabia: Journal of Asian Earth Sciences, v. 25, p. 719-734.

Kim, J.Y., Pickerill, R.K., and Wilson, R.A., 2001, Palaeophycus bolbitermilus isp. Nov. from the Lower Silurian Upsalquitch Formation of New Brunswick, eastern Canada: Atlantic Geology, v. 36, p. 131-137.

Klapper, G., 1966, Upper Devonian and lower Mississippian conodont zones in Montana, Wyoming, and South Dakota: The University of Kansas Paleontological Contributions, p. 1-43.

LeFever, J.A., Overview of Bakken stratigraphy and "mini-core" workshop: North Dakota Geological Survey.

LeFever, J.A. and Nordeng, S.H., 2011, Cyclic sedimentation patterns of the Mississippian-Devonian Bakken Formation, North Dakota: AAPG International Conference and Exhibition, Calgary, Alberta, September 12-15, 2010.

MacEachern, J.A., Pemberton, S.G., Gingras, M.K., and Bann, K.L., 2010, Ichnology and Facies Model. In: *Facies Models 4* (James, N.P. and Dalrymple, R.W. Eds.), Canadian Sedimentology Research Group, p. 19-58.

MacQuaker, J.H.S., Taylor, K.G., and Gawthorpe, R.L., 2007, High resolution facies analysis of mudstone: Implications for paleoenvironmental and sequence stratigraphic interpretations of offshore ancient mud-dominated successions: Journal of Sedimentary Research, v. 77, p. 324-339.

McCourt, J.H., 1955, Reagan field, Glacier County, Montana. In: *6th Annual Field Conference* (P. J. Lewis Eds.), Billings Geological Society, p. 177-181.

McMannis, W.J., 1962, Devonian stratigraphy between Three Forks, Montana and Yellowstone Park. In: *13th Annual Field Conference and Symposium* (A.R. Hansen

and J.H. McKeever Eds.), Billings Geological Society, p.4-12.

Mitchum, R.M., Jr., Vail, P.R., and Thompson, S., III, 1977, Seismic stratigraphy and global changes of sea-level, part 2: the depositional sequence as a basic unit for stratigraphic analysis. In: *Seismic Stratigraphy-Applications to Hydrocarbon Explication* (Payton, C.E. Eds.): AAPG Memoir 26, p. 53-62.

Mount, J., 1985, Mixed siliciclastic and carbonate sediments: a proposed first-order textural and compositional classification, Sedimentology, v. 32, p. 435-442.

Narkiewicz, M. and Retallack, G.J., 2014, Dolomitic paleosols in the lagoonal tetrapod track-bearing succession of the Holy Cross Mountains (Middle Devonian, Poland): Sedimentary Geology, v. 299, p. 74-87.

Obermajer, M., Osadetz, K.G., Fowler, M.G., and Snowdon, L.R., 2000, Light hydrocarbon (gasoline range) parameter refinement of biomarker-based oil-oil correlation studies: an example from Williston Basin: Organic Geochemistry, v. 31, p. 959-976.

Obernajer, M., Osadetz K.G., Fowler, M.G., Silliman J., Hansen, W.B., and Clark M., 2002, Delineating compositional variabilities among crude oils from Central Montana, USA, using light hydrocarbon and biomarker characteristics: Organic Geochemistry, v. 33, p. 1343-1359.

Oviatt, C.G., McCoy, W.D., and Nash, W.P., 1994, Sequence Stratigraphy of Lacustrine Deposits: A Quaternary Example from the Bonneville Basin, Utah: Geological Society of America Bulletin, v. 106, p. 133-144.

Osadetz, K.G., Kohn, B.P., Feinstein, S., and O'Sullivan, P.B., 2002, Thermal history of Canadian Williston basin from apatite fission-track thermochronology – implications for petroleum systems and geodynamic history: Tectonophysics, v. 349, p. 221-249.

Peterson, J.A., 1986, General stratigraphy and regional paleotectonics of the western Montana overthrust belt. In: *Paleotectonics and Sedimentation in the Rocky Mountain Regions, United States* (Peterson, J.A. Eds.): AAPG Memoir 41, p. 57-86.

Phillips, C. and Mcllroy, D., 2010, Ichnofabrics and biologically mediated changes in clay mineral assemblages from a deep-water, fine-grained, calcareous sedimentary succession: an example from the Upper Cretaceous Wyandot Formation, offshore

Nova Scotia: Bulletin of Canadian Petroleum Geology, v. 58, no. 3, p. 203-218.

Plint, A.G., 2010, Wave-and Storm-dominated Shoreline and Shallow-marine Systems. In: *Facies Models 4* (James, N.P. and Dalrymple, R.W. Eds.), Canadian Sedimentology Research Group, p. 167-199.

Pollastro, R.M., Cook, T.A., Roberts, L.N.R., Schenk, C.J., Lewan, M.D., Anna, L.O., Gaswirth, S.B., Lillis, P.G., Klett, T.R., and Charpentier, R.R., 2008, Assessment of undiscovered oil resources in the Devonian-Mississippian Bakken Formation, Williston Basin Province, Montana and North Dakota, 2008: U.S. Geological Survey Fact Sheet 2008–3021.

Posamentier, H.W., Jervey, M.T., and Vail, P.R., 1988, Eustatic controls on clastic deposition I - conceptual framework. In: Sea Level Changes - An Integrated Approach (C.K. Wilgus, B.S. Hastings, C.G.St.C. Kendall, H.W. Posamentier, C.A. Ross, and J.C. Van Wagoner, Eds.): SEPM Special Publication 42, p. 110-124.

Potter, P.E., Maynard, J.B., and Pryor, W.A., 1980, Sedimentology of Shale: Berlin-Heidelberg, New York.

Prather, B.E., Booth, J.R., Steffens, G.S., and Craig, P.A., 1998, Classification, lithologic calibration, and stratigraphic succession of seismic facies of intraslope basins, deep-water Gulf of Mexico: AAPG Bulletin, v. 82, p. 701-728.

Rahm, D., 2011, Regulating hydraulic fracturing in shale gas plays: The case of Texas: Energy Policy, v. 39, p. 2974-2981

Rau, J.L., 1962, The stratigraphy of the Three Forks Formation: In: 13th *Annual Field Conference and Symposium* (A.R. Hansen and J.H. McKeever Eds.), Billings Geological Society, p.51-66.

Rhodes, R.B., 1955, the Pakowki Lake-Sweetgrass Hills area, southeastern Alberta and north central Montana. In: *6th Annual Field Conference* (P. J. Lewis Eds.), Billings Geological Society, p. 182-188.

Rokosh, C.D., Pawlowicz, J.G., Berhane, H., Anderson, S.D.A., and Beaton, A.P., 2009, Geochemical and sedimentological investigation of the Banff and Exshaw Formations for shale gas potential: Initial results: Energy Resources Conservation Board Alberta Geological Survey.

Rose, C.V. and Maloof, A.C., 2010, Testing models for post-glacial 'cap dolostone' deposition: Nuccaleena Formation, Southern Australia: Earth and Planetary Science Letters, v. 296, p. 165-180.

Sageman, B.B., Murphy, A.E., Werne, J.P., Straeten, C.A., Hollander, D.J., and Lyons, T.W., 2003, A tale of shales: the relative roles of production, decomposition, and dilution in the accumulation of organic-rich strata, Middle-Upper Devonian, Appalachian basin: Chemical Geology, v. 195, p. 229-273.

Sandberg, C.A., 1962, Correlation of Devonian and lowermost Mississippian rocks between outcrops in western and central Montana and the Williston Basin in eastern Montana. In: 13th *Annual Field Conference and Symposium* (A.R. Hansen and J.H. McKeever Eds.), Billings Geological Society, p.33-34.

Sandberg, C.A., 1965, Nomenclature and correlation of lithologic subdivisions of the Jefferson and Three Forks Formations of southern Montana and Northern Wyoming: Geological Survey Bulletin, v. 1194, p. 1-18.

Sandberg, C.A., and Klapper, G., 1967, Stratigrapy, age. And paleotectonic significance of the Cottonwood Canyon Member of the Madison Limestone in Wyoming and Montana: Geological Survey Bulletin, v. 1251, p. 1-70.

Savoy, L.E., 1992, Environmental record of Devonian-Mississippian carbonate and low-oxygen facies transitions, southernmost Canadian Rocky Mountains and northwestern Montana: Geological Society of America Bulletin, v. 104, p.1412-1432.

Savoy, L.E., and Harris, A.G., 1993, Conodont biofacies and taphonomy along a carbonate ramp to black shale basin (latest Devonian and earliest Carboniferous), southernmost Canadian Cordillera and adjacent Montana: Earth Science 30, p. 2404-2422.

Schieber, J., 1999, Distribution and deposition of mudstone facies in the Upper Devonian Sonyea Group of New York: Society for Sedimentary Geology, v. 69, no. 4, p. 909-925.

Schieber, J., 2011, Reverse engineering mother nature – Shale sedimentology from an experimental perspective: Sedimentary Geology, v. 238, p. 1-22.

Scholten, R. and Hait, M.H. Jr., 1962, Devonian system from shelf edge to geosyncline,

southeastern Montana – central Idaho. In: 13*th* *Annual Field Conference and Symposium* (A.R. Hansen and J.H. McKeever Eds.), Billings Geological Society, p.13-22.

Scotese, C.R. and McKerrow, W.S., 1990, Revised world maps and introduction. In: *Palaeozoic Palaeogeography and Biogeography* (McKerrow, W.S. Eds.), Geol. Soc. London mem. 12, p. 1-21.

Smith, M.G. and Bustin R.M., 1998, Production and preservation of organic matter during deposition of the Bakken Formation (Late Devonian and Early Mississippian), Williston Basin: Palaeogeography, Palaeoclimatology, Palaeoecology, v. 142, p. 185-200.

Smith M.G. and Bustin R.M., 2000, Late Devonian early Mississippian Bakken and Exshaw black shale source rocks, Western Canadian Sedimentary Basin: A sequence stratigraphic interpretation: AAPG Bulletin, v. 84, p. 940-960.

Soliman, M.Y., Daal, J., and East, L., 2012, Fracturing unconventional formations to enhance productivity: Journal of Natural Gas Science and Engineering, p. 1-16.

Sonnenberg S.A. and Pramudito A., 2009, Petroleum geology of the giant Elm Coulee field, Williston Basin: AAPG Bulletin, v. 93, p. 1127-1153.

Sonnenberg, S.A., Vickery J., Theloy C., and Sarg J., 2011, Middle Bakken facies, Williston Basin, USA: A key to prolific production: AAPG Annual Convention and Exhibition, Houston, Texas, USA, April 10-13, 2011

Sonnenberg, S.A., Gantyno, A., and Sarg, R., 2011, Petroleum potential of the upper three forks formation, Williston Basin, USA. AAPG Annual Convention and Exhibition. Houston, Texas, USA, April 10-13, 2011

Straeten, C.A., Brett, C.E., and Sageman, B.B., 2011, Mudrock sequence stratigraphy: A multi-proxy (sedimentological, paleobiological and geochemical) approach, Devonian Appalachian Basin: Palaeogeography, Palaeoclimatology, Palaeoecology, v. 304, p. 54-73.

Theloy, C. and Sonnenberg, S.A., 2012, Factors influencing productivity in the Bakken play, Williston Basin: AAPG Annual Convention and Exhibition, Long Beach, California, April 22-25, 2012,

Theloy, C. and Sonnenberg, S., 2013, New Insights into the Bakken Play: What Factors Control Production?: AAPG Annual Convention and Exhibition. Pittsburgh, Pennsylvania, May 19-22, 2013.

Vail, P.R., Mitchum, R.M. Jr., and Thompson, S., III, 1977, Seismic stratigraphy and global changes of sea level, part four: global cycles of relative changes of sea level: AAPG Memoir, v. 26, p. 83-98.

Van Wagoner, J.C., 1995, Overview of sequence stratigraphy of foreland basin deposits: terminology, summary of papers, and glossary of sequence stratigraphy. In: *Sequence Stratigraphy of Foreland Basin Deposits* (J.C. Van Wagoner and G.T. Bertram, Eds.), AAPG Memoir 64, p. ix-xxi.

Van Wagoner, J.C., Mitchum, R.M. Jr., Campion, K.M., and Rahmanian, V.D., 1990, Siliciclastic sequence stratigraphy in well logs, core, and outcrops: concepts for high-resolution correlation of time and facies: AAPG Methods in Exploration Series 7, p. 55.

Van Wagoner, J.C., Posamentier, H.W., Mitchum, R.M., Jr., Vail, P.R., Sarg, J.F., Loutit, T.S., and Hardenbol, J., 1988, An overview of sequence stratigraphy and key definitions. In: *Sea Level Changes – An integrated Approach* (C.K. Wilgus, B.S. Hasting, C.G. St. C. Kedndall, H.W. Posamentier, C.A. Ross, and J.C. van Wagoner, Eds.), SEPM Special Publication, v. 42, p. 39-45.

Warme, J.E., Morrow, J.R., and Sandberg, C.A., 2008, Devonian carbonate platform of eastern Nevada: Facies, surfaces, cycles, sequences, reefs, and cataclysmic Alamo Impact Breccia: Geological Society of America Field Guide 11, p. 215-247.

Williams. C.J., Hesselbo, S.P., Jenkyns, H.C., and Morgans-Bell, H.S., 2001, Quartz silt in mudrocks as a key to sequence stratigraphy (Kimmeridge Clay Formation, Late Jurassic, Wessex Basin, UK): Terra Nova, v. 13, p. 449-455.

Wilson, J.E., 1955, Devonian correlations in northwestern Montana. In: *6th Annual Field Conference* (P. J. Lewis Eds.), Billings Geological Society, p. 70-77.

Wright, V.P. and Burchette, T.P., 1996, Shallow-water carbonate environments. In: *Sedimentary Environments: Processes, Facies and Stratigraphy* (Reading, H.G. Eds.), Blackwell Publishing, p. 325-394.

6. FIGURES AND TABLES

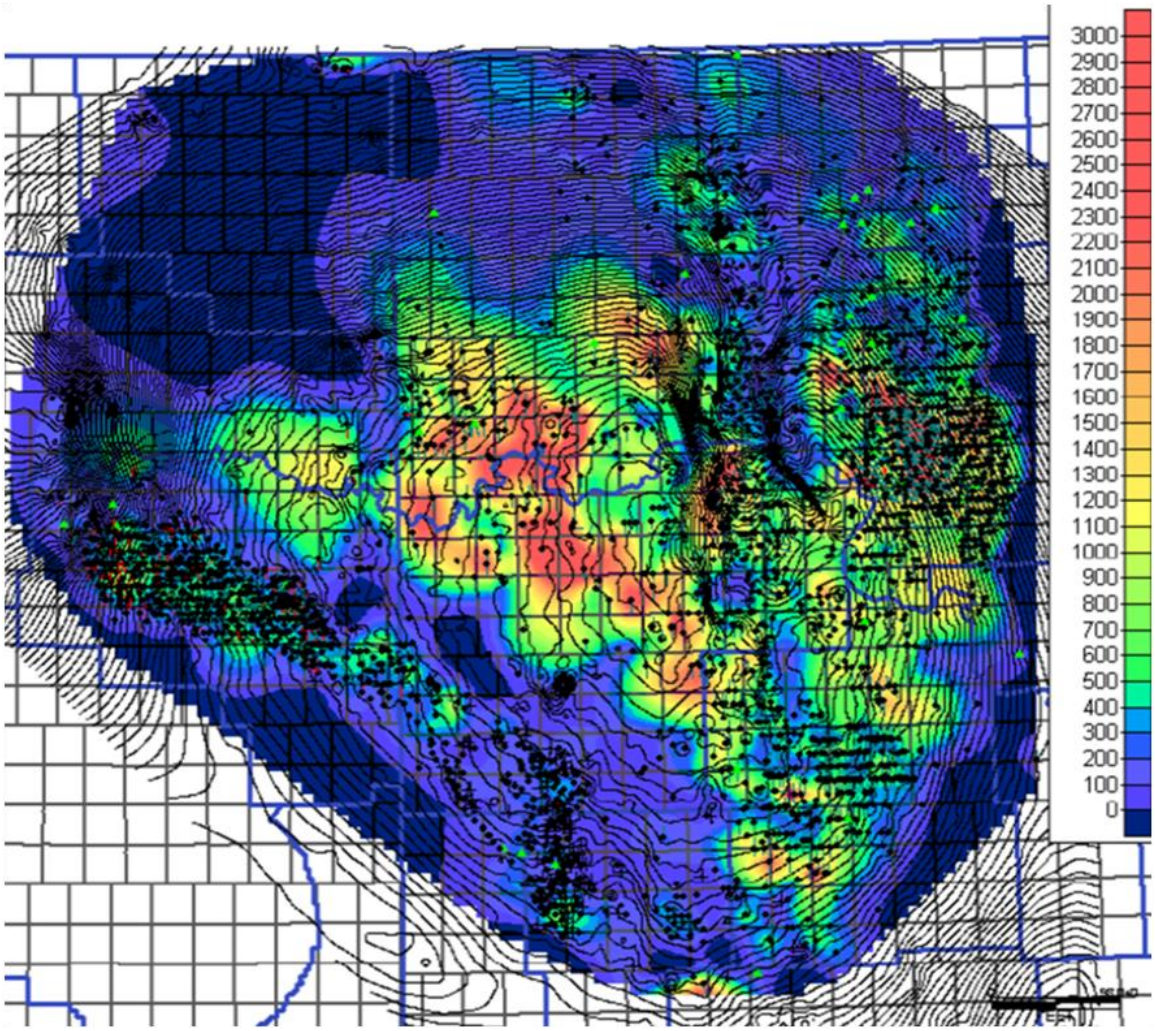

Fig. 1. Map showing an initial production rate of the Bakken Formation in the Williston Basin (Theloy and Sonnenberg, 2013).

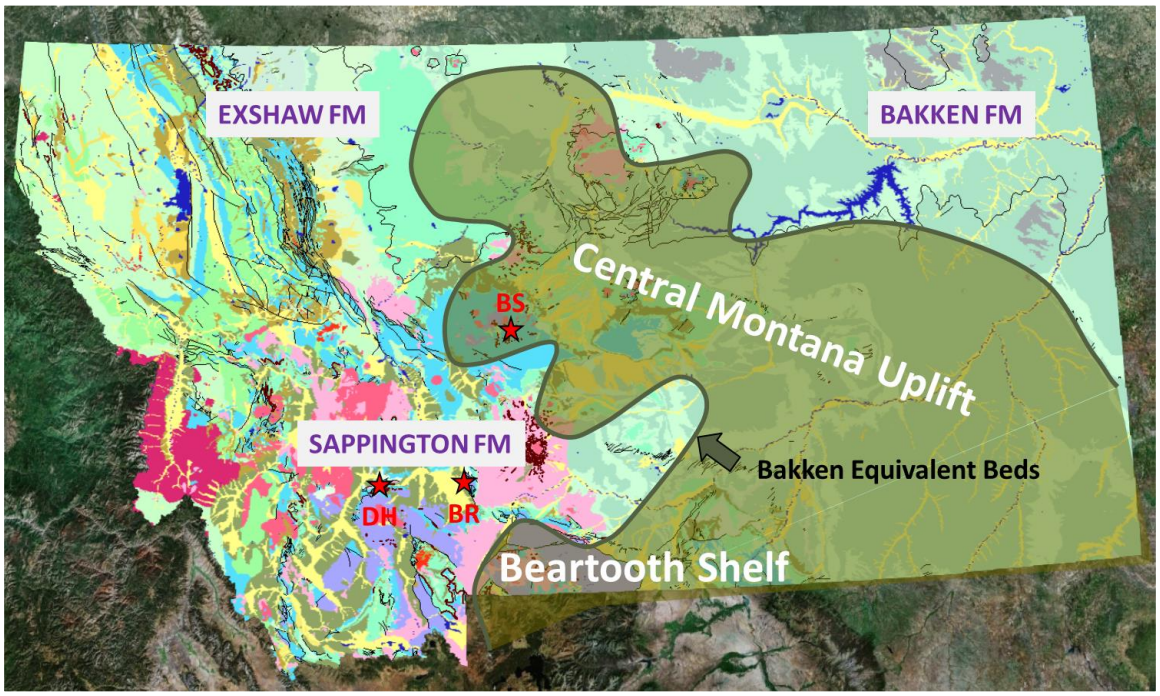

Fig. 2. Geologic map of Montana showing the Devonian-Mississippian strata including the Bakken Formation in the Williston Basin, the Exshaw Formation in the Western Canadian Basin, and the Sappington Formation in central Montana. Major paleohighs including the Central Montana Uplift and the Beartooth Shelf are shown as outlined by a facies belt of the Devonian-Mississippian strata (e.g. Baars, 1972; Peterson, 1986; Smith and Bustin, 2000). The outcrops of the Sappington Formation investigated in this study include: Dry Hollow (DH), Bridger Range (BR), and Big Snowy Mountains (BS).

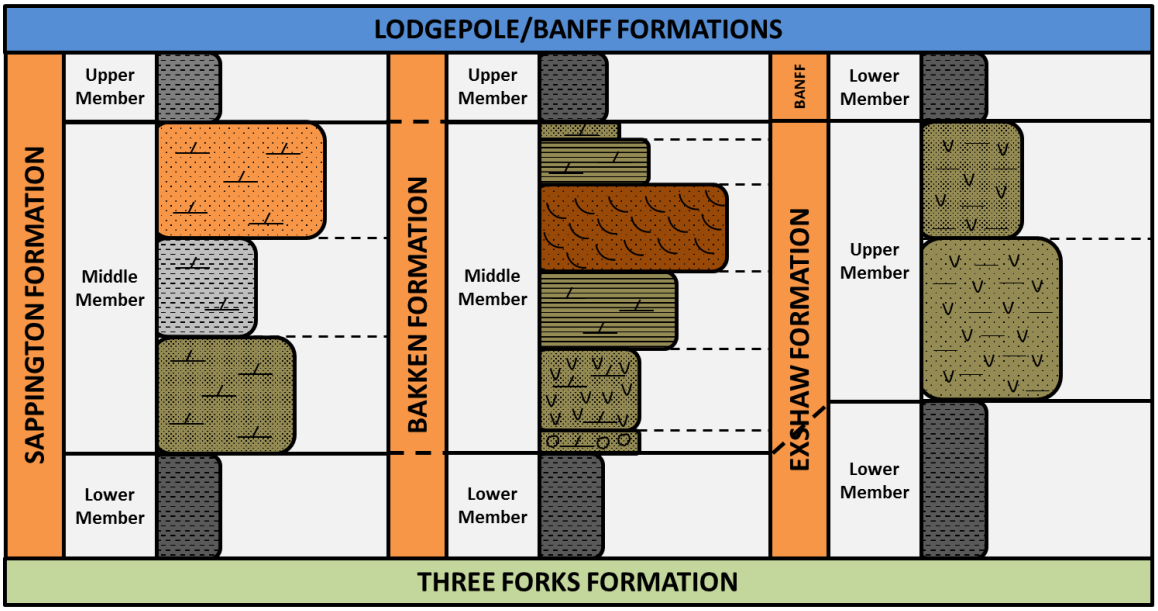

Fig. 3. Lithostratigraphic correlation of the Devonian-Mississippian strata in Montana. The Sappington Formation is described as containing lower and upper mudstone members and a middle calcareous siltstone-silty limestone member including three different lithological units (e.g. Achauer, 1959; Gutschick *et al*., 1962; McMannis, 1962: Sandberg, 1965). The Bakken Formation is described as containing lower and upper mudstone members and a calcareous/dolomitic sandy-silty middle member including six different lithofacies (e.g. Smith and Bustin, 1998, 2000; Sonnenberg *et al*., 2011; Angulo and Buatois, 2012). The Exshaw Formation is described as containing a lower mudstone member and an upper siltstone/sandstone member, and the basal Banff Formation is described as mudstone (e.g. Savoy, 1992; Smith and Bustin, 2000; Rokosh, *et al*., 2009).

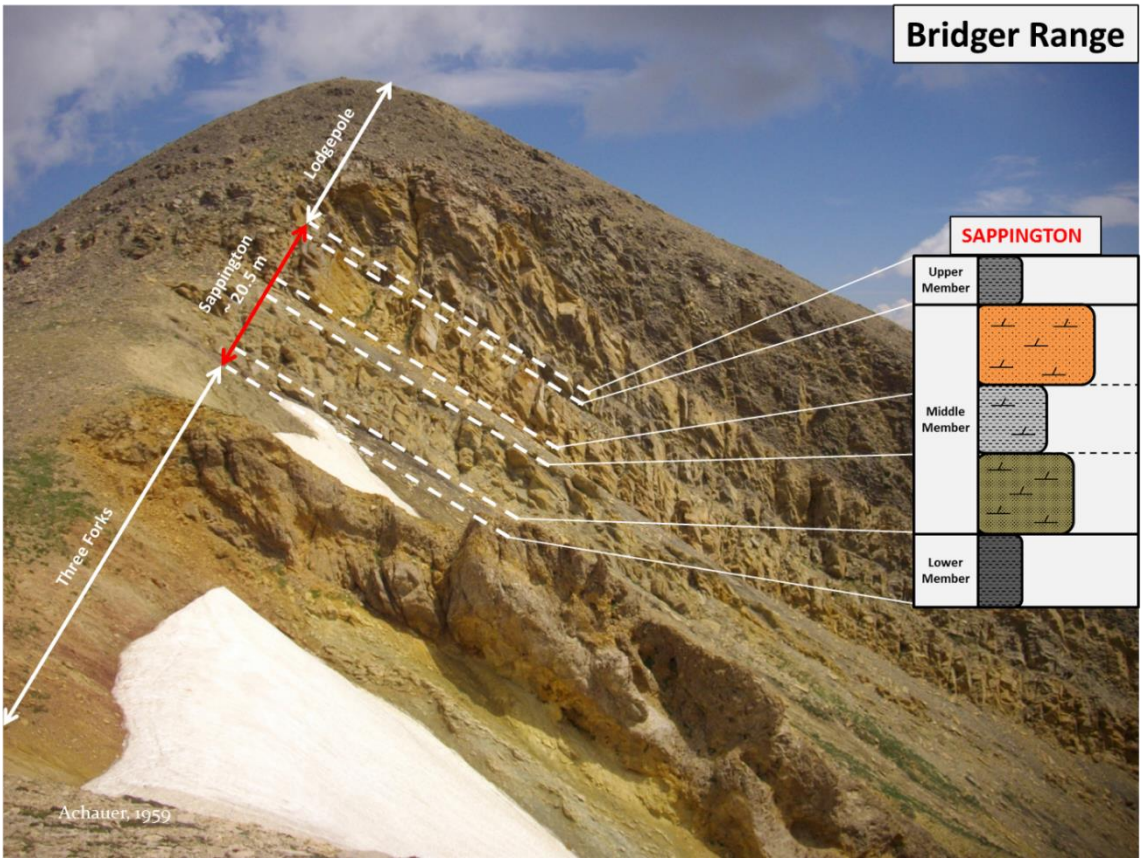

Fig. 4. Example of the Sappington Formation at the Bridger Range (BR) section, showing five distinct lithostratigraphic units, bounded below by the Three Forks Formation and above by the Lodgepole Formation: lower, middle, and upper mudstone members are slope formers, and lower and upper units of a middle calcareous siltstone-silty limestone member are cliff formers (e.g. Achauer, 1959; Gutschick *et al*., 1962; McMannis, 1962: Sandberg, 1965). View looking toward the northeast.

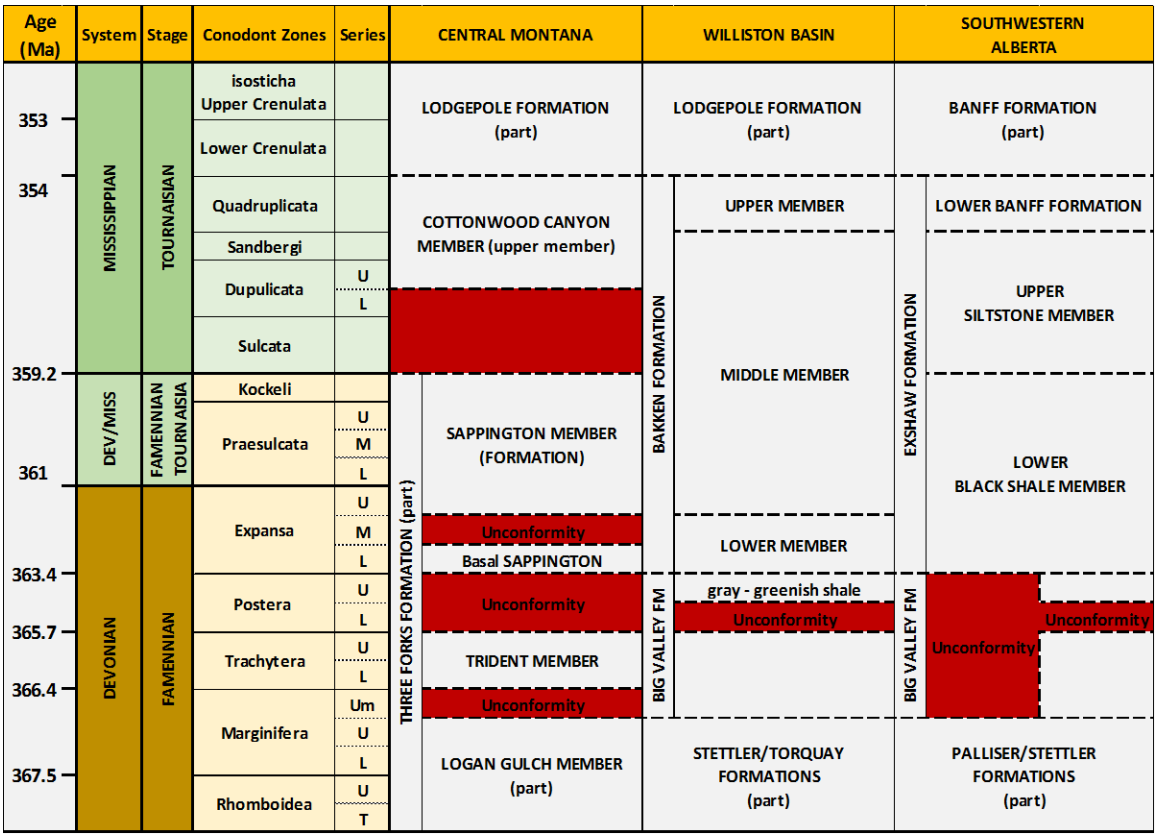

Fig. 5. Biostratigraphic correlation of the Devonian-Mississippian strata in Montana based on conodont zones (e.g. Savoy and Harris, 1993; Kaufmann, 2006; Johnston *et al*., 2010). The biostratigraphic correlation shows that the Sappington Formation is time equivalent with a lower member and a lower unit of a middle member of the Bakken Formation, and it is time equivalent with the lower member of the Exshaw Formation. The upper unit of the Cottonwood Canyon Member of the Lodgepole Formation unconformably overlies the Sappington Formation above two missing conodont zones (*Siphonodella Sulcata* and *S. Dupulicata*). Calibrations of the time scale is based on Haq and Schutter (2008) for Devonian strata and Buggisch *et al*. (2008) for the Mississippian strata. The Devonian-Mississippian boundary is placed at 359.2 Ma according to Haq and Schutter (2008), whereas Kaufmann (2006) placed the boundary at 360.7 ± 2.7 Ma, which makes the Devonian-Mississippian boundary variable.

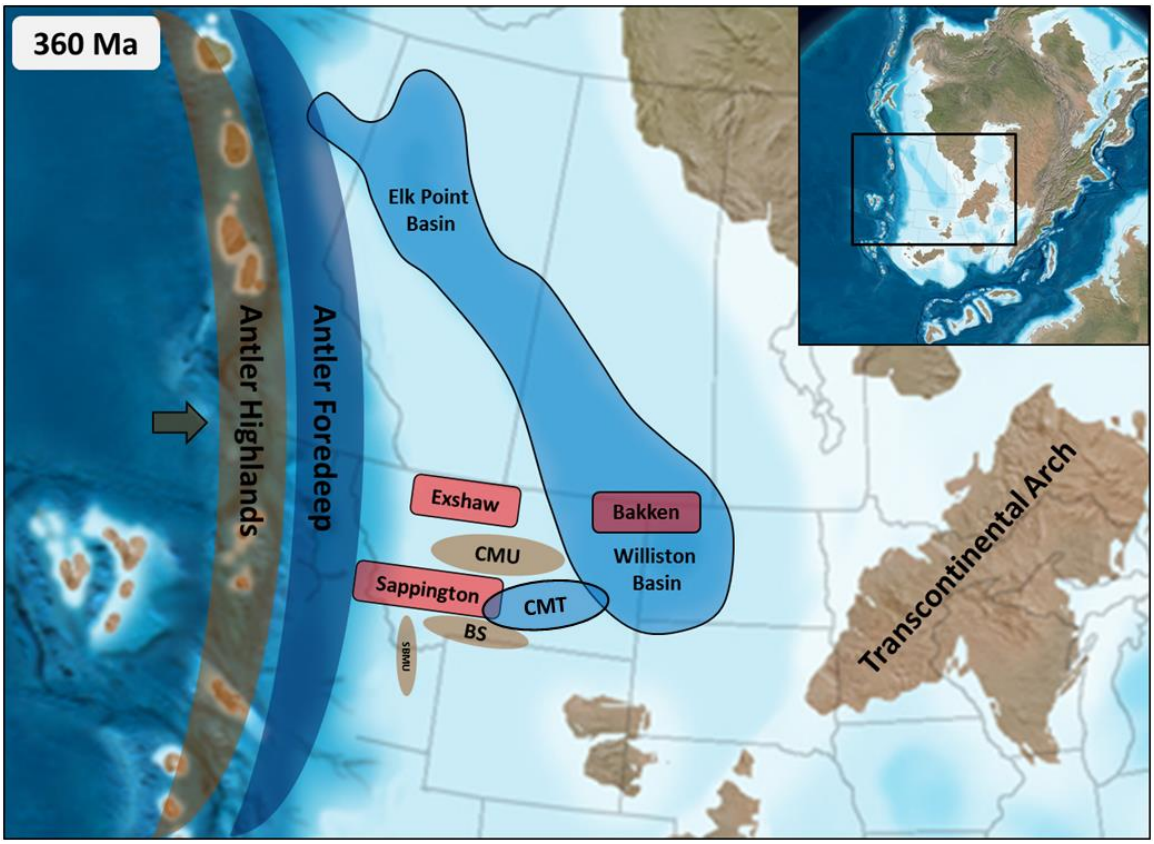

Fig. 6. Paleogeographic map of a western margin of the North American continent during the Devonian-Mississippian, showing major tectonic elements (brown), sedimentary basins (blue), and the Devonian-Mississippian strata in Montana (red) (e.g. Scotese and McKerrow, 1990; Smith and Bustin, 1998; Sonnenberg *et al.*, 2011; Blakey, 2011). CMU = Central Montana Uplift; BS = Beartooth Shelf; SBMU = Southern Beaverhead Mountains Uplift; CMT = Central Montana Trough.

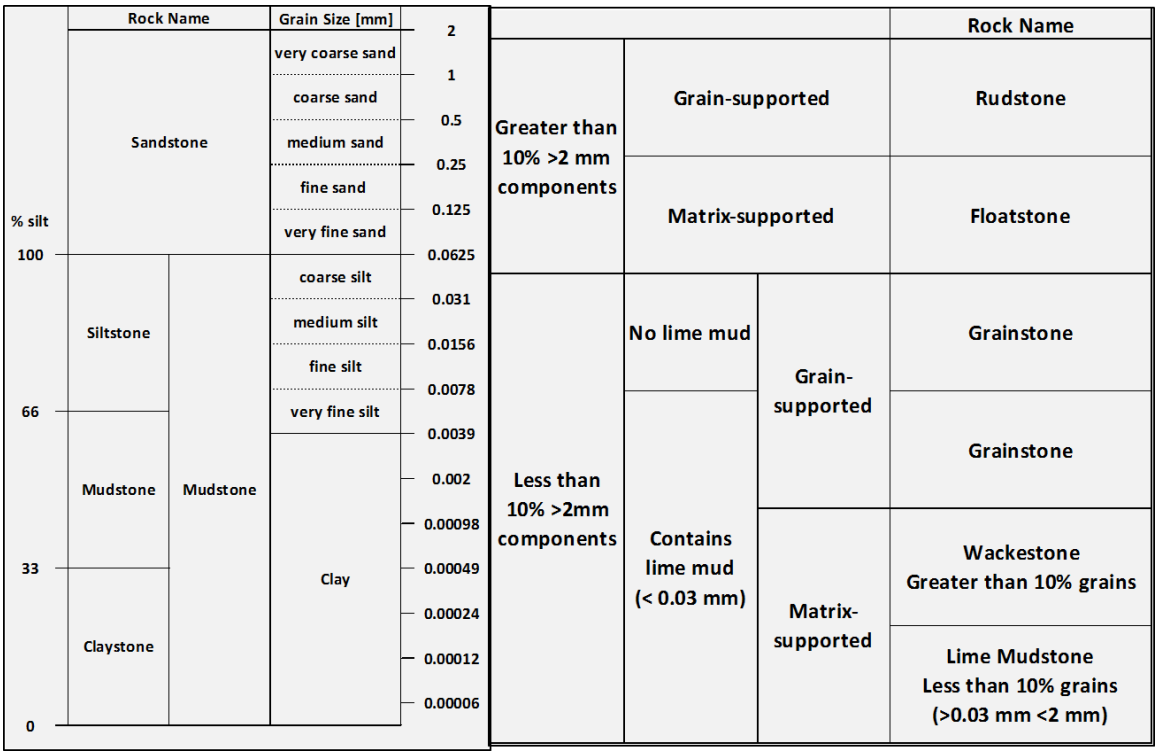

Fig. 7. Textural-based classification systems used in this study to describe mixtures of siliclastic and carbonate lithologies. Samples that were dominated by siliciclastics (% vol > 50) were classified according to Potter *et al*. (1980). Samples dominated by carbonate lithologies (% vol > 50) were classified according to Embry and Klovan (1972).

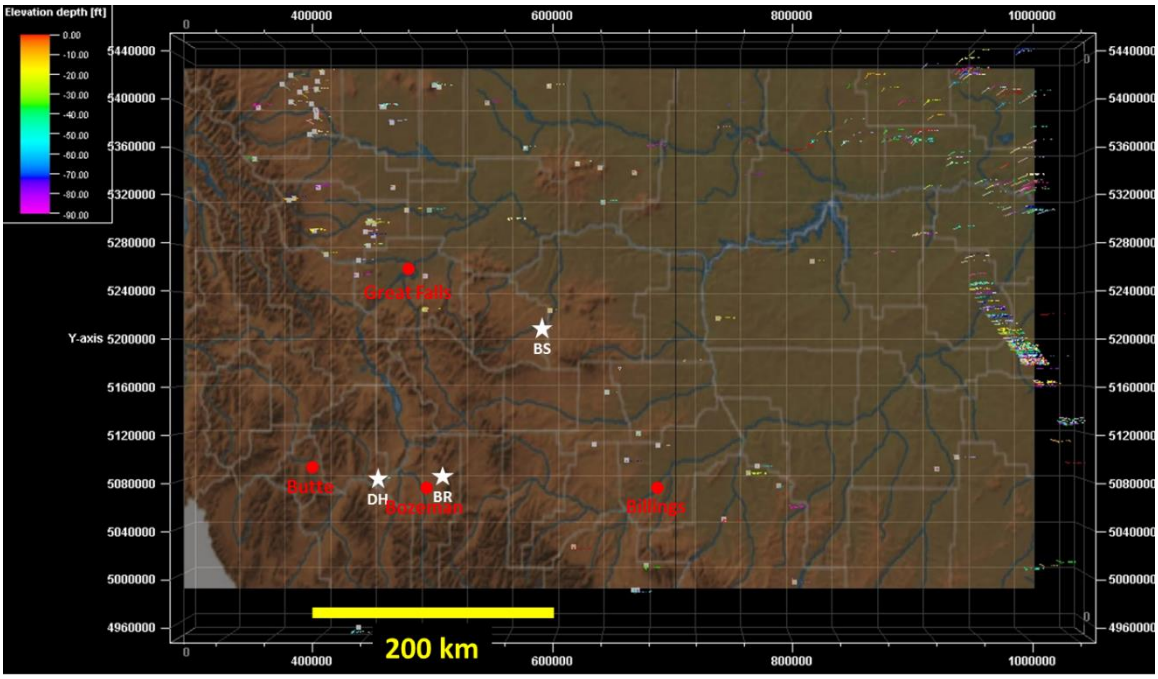

Fig. 8. Map showing locations of well logs cut through the Sappington, Bakken, or underlying Three Forks Formations, major cities in Montana, and the outcrops of the Sappington Formation measured in this study. Seventy-three well logs used in this study are highlighted by while squares.

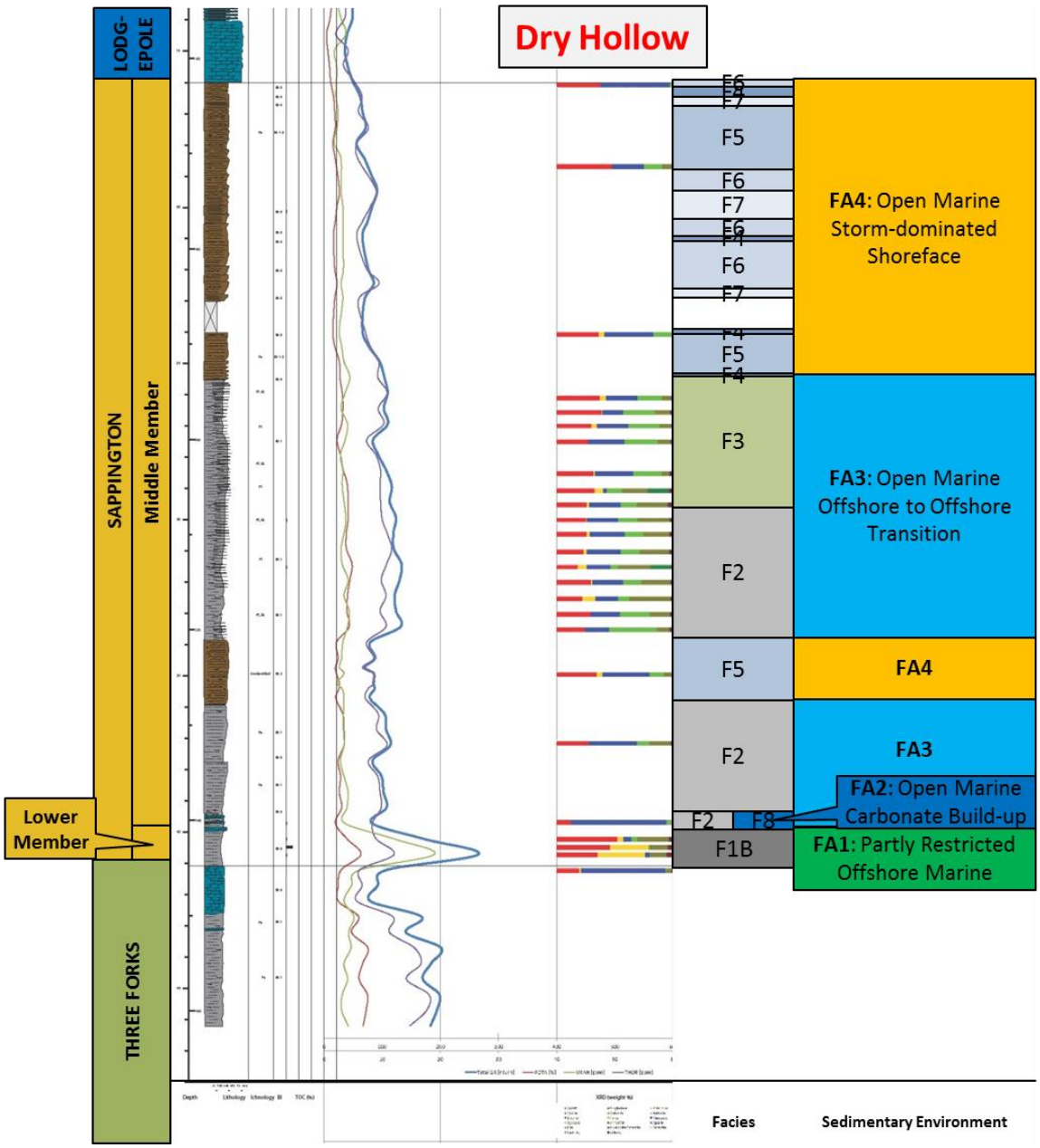
Dry Hollow
LODG-EPOLE
SAPPINGTON
Middle Member
Lower Member
THREE FORKS
F6
F7
F5
F6
F7
F6
F4
F6
F7
F4
F5
F4
F3
F2
F5
F2
F2
F8
F1B
FA4: Open Marine Storm-dominated Shoreface
FA3: Open Marine Offshore to Offshore Transition
FA4
FA3
FA2: Open Marine Carbonate Build-up
FA1: Partly Restricted Offshore Marine
Facies
Sedimentary Environment

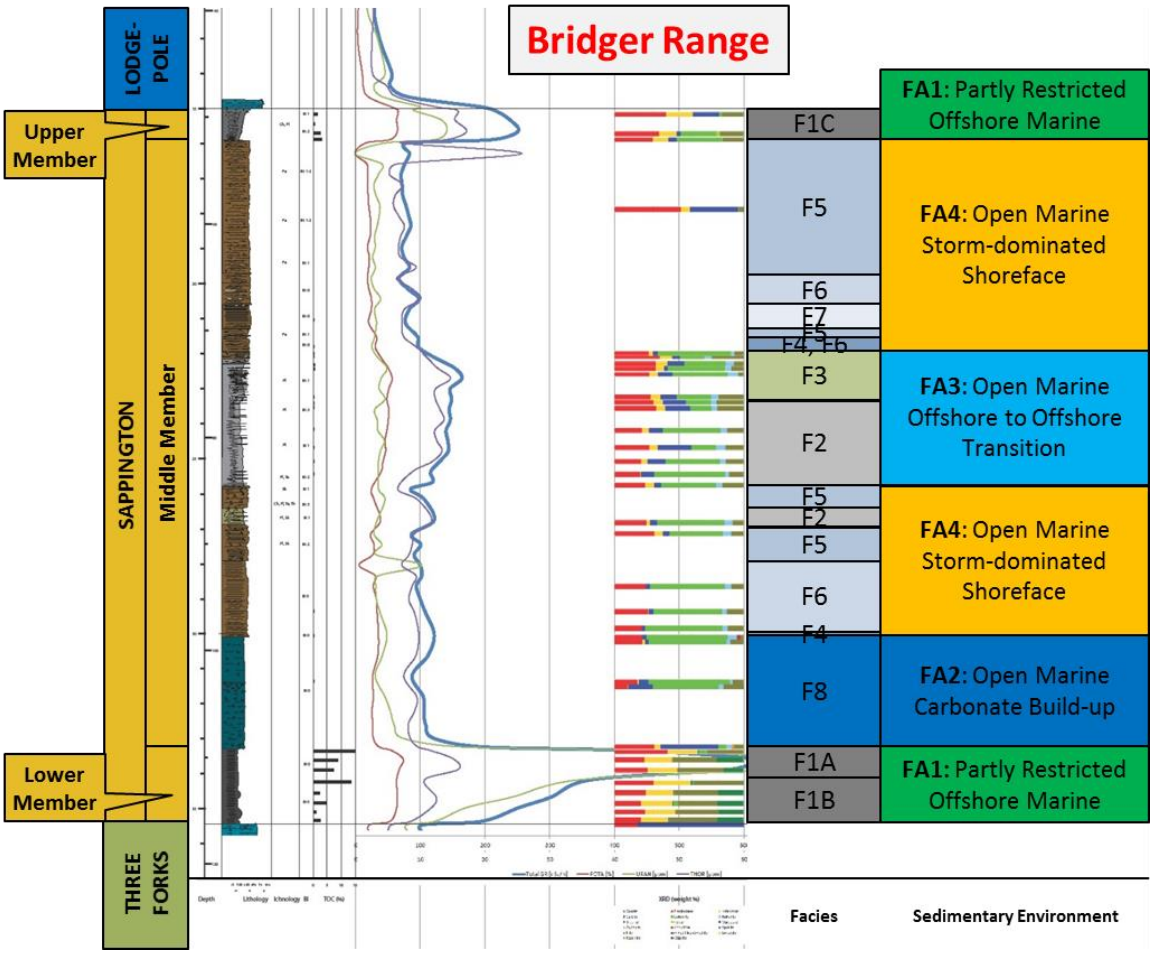
Bridger Range
LODGE-POLE
Upper Member
SAPPINGTON
Middle Member
Lower Member
THREE FORKS
F1C
F5
F6
F7
F5
F4, F6
F3
F2
F5
F2
F5
F6
F4
F8
F1A
F1B
FA1: Partly Restricted Offshore Marine
FA4: Open Marine Storm-dominated Shoreface
FA3: Open Marine Offshore to Offshore Transition
FA4: Open Marine Storm-dominated Shoreface
FA2: Open Marine Carbonate Build-up
FA1: Partly Restricted Offshore Marine
Facies
Sedimentary Environment

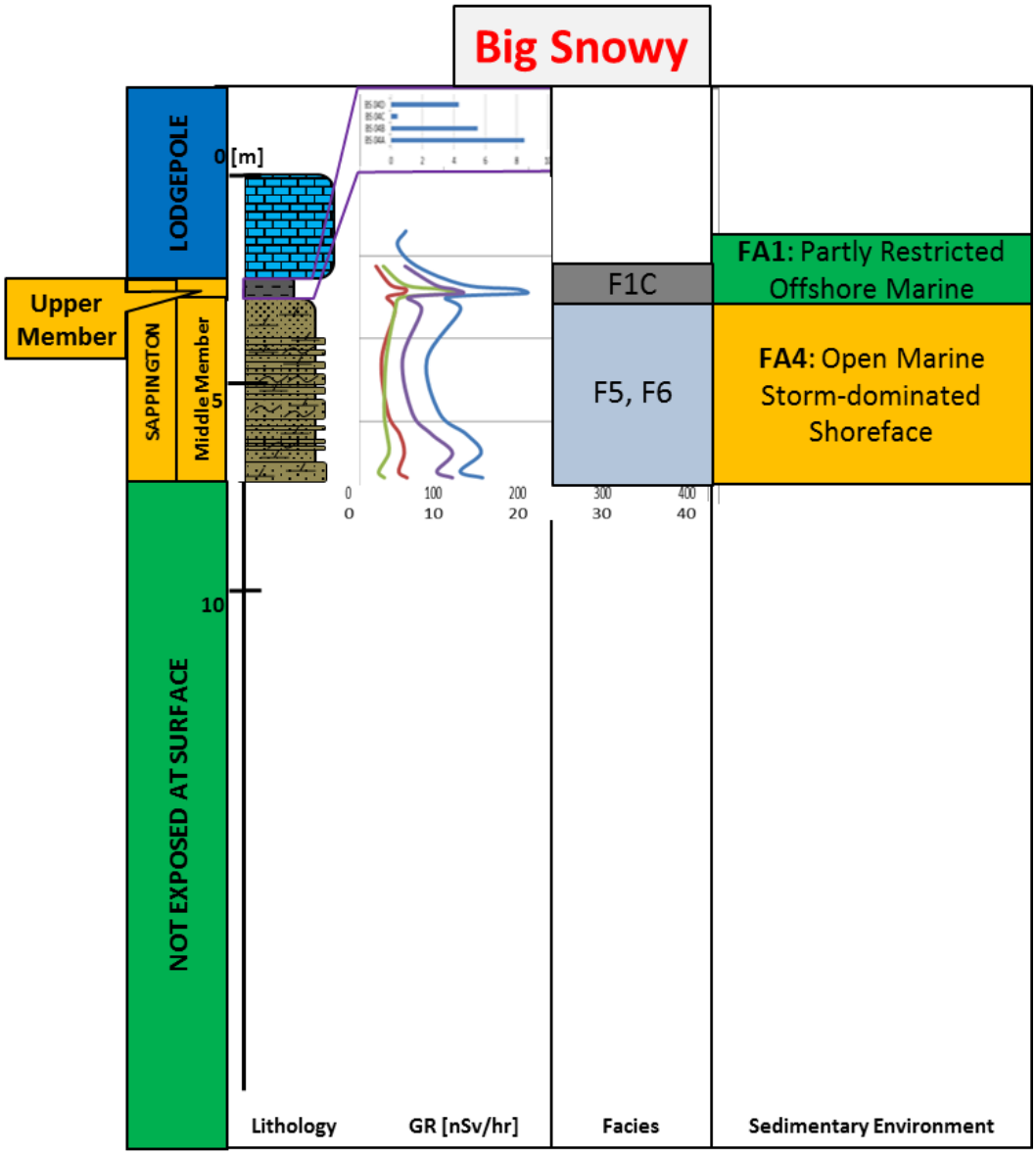

Fig. 9. Measured stratigraphic sections of the Sappington Formation at Dry Hollow (DH) and Bridger Range (BR) sections, showing stratigraphic, sedimentologic (lithology, grain size, sedimentary structures, fabrics, ichnofacies, and bioturbation index), petrophysical (total and spectral gamma ray logs), geochemical (total organic carbon and mineralogy) information, facies descriptions, and facies associations.

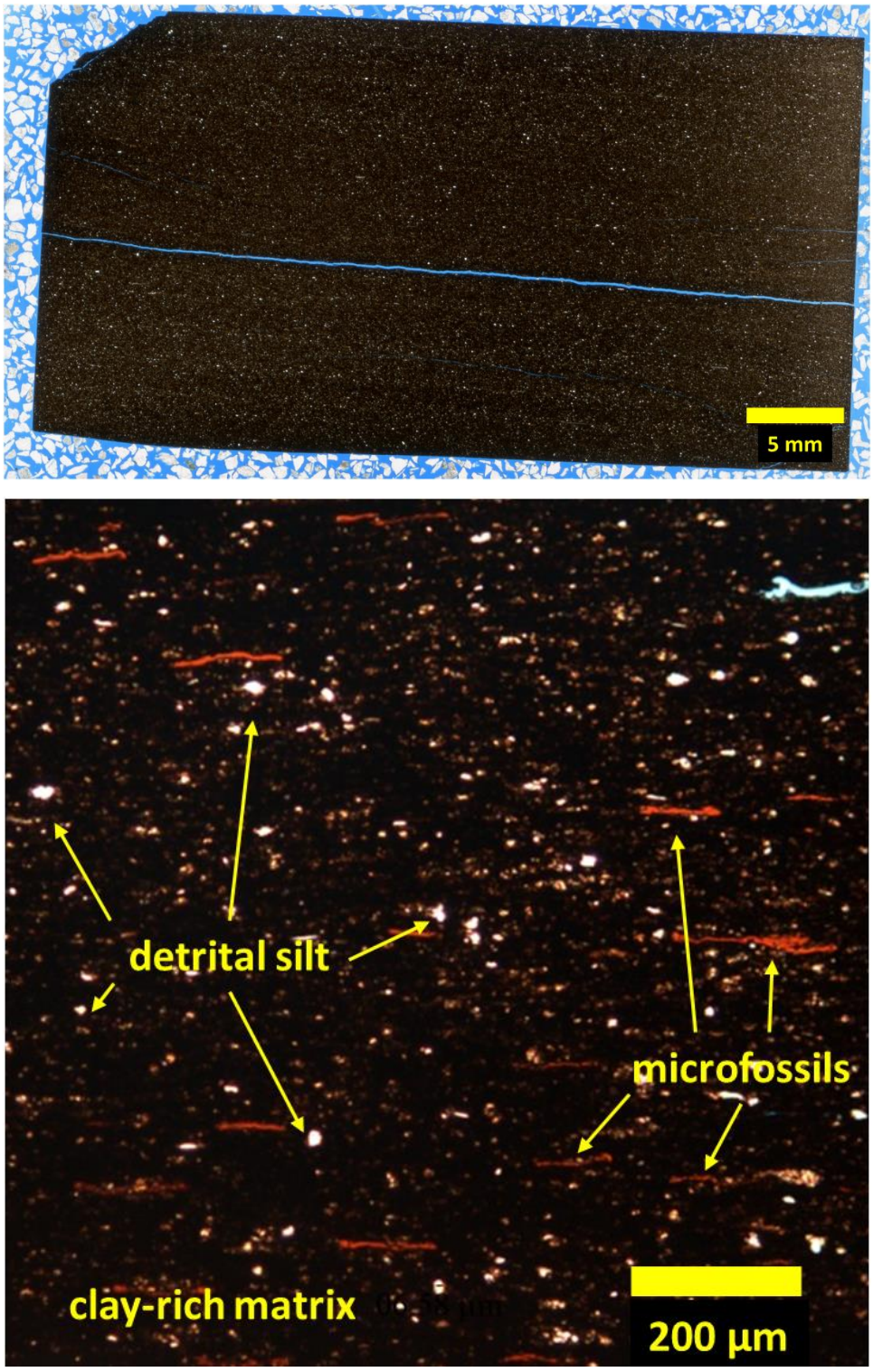

Fig. 10. Thin section and photomicrograph of an organic-rich mudstone with microfossils (Facies 1A), showing medium to coarse silt detrital quartz and microfossils in homogeneous, clay-rich mud matrix.

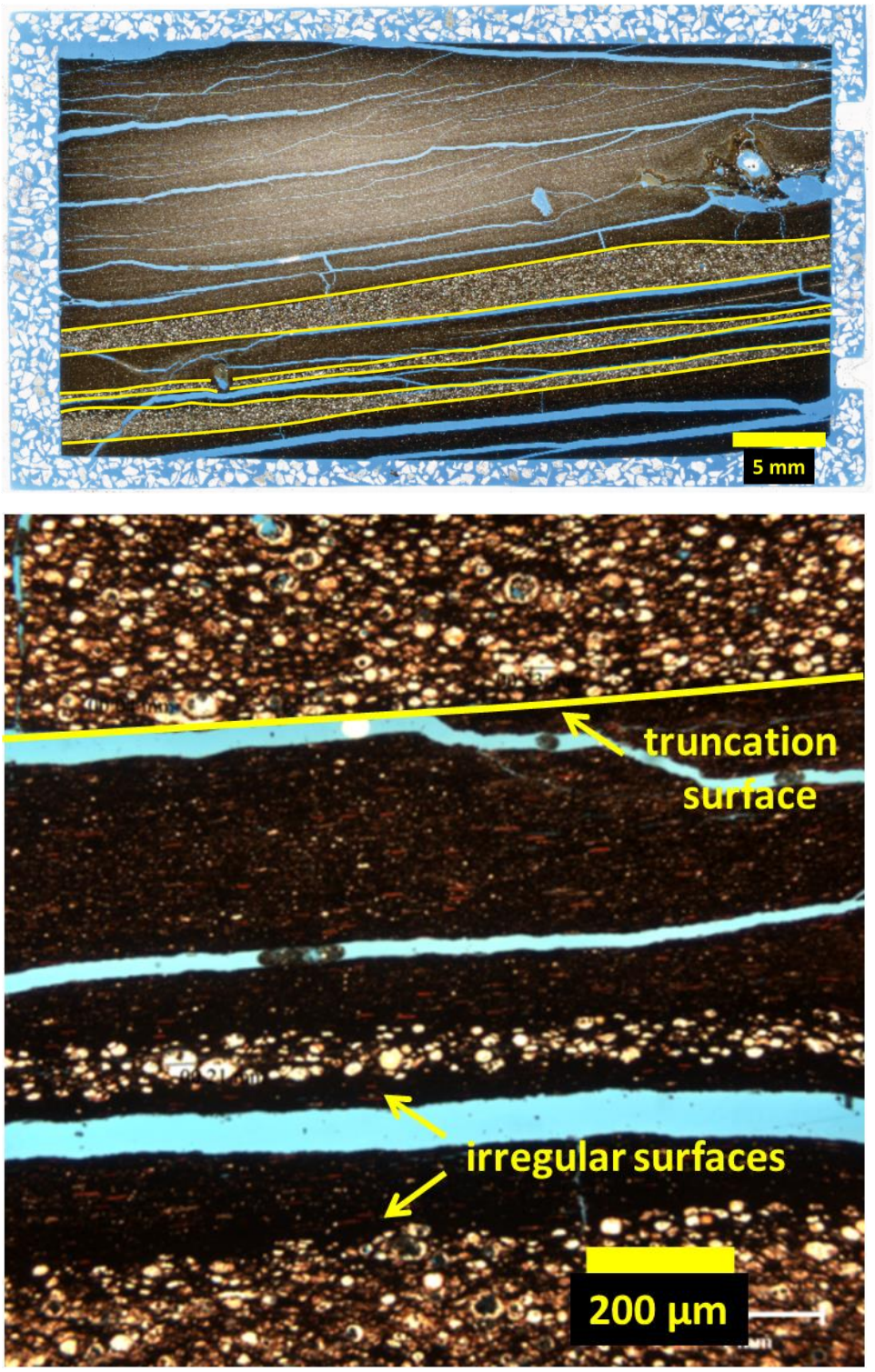

Fig. 11. Thin section (top) and photomicrograph (bottom) of an organic-rich mudstone (Facies 1B), showing pinch and swell lamination (highlighted in yellow) consisting of medium silt to upper very fine-grained sand-sized radiolarian grains and clay-rich mud matrix containing medium to coarse silt detrital quartz and microfossils. The pinch and swell lamination is characterized by either sharply truncated or irregular surfaces.

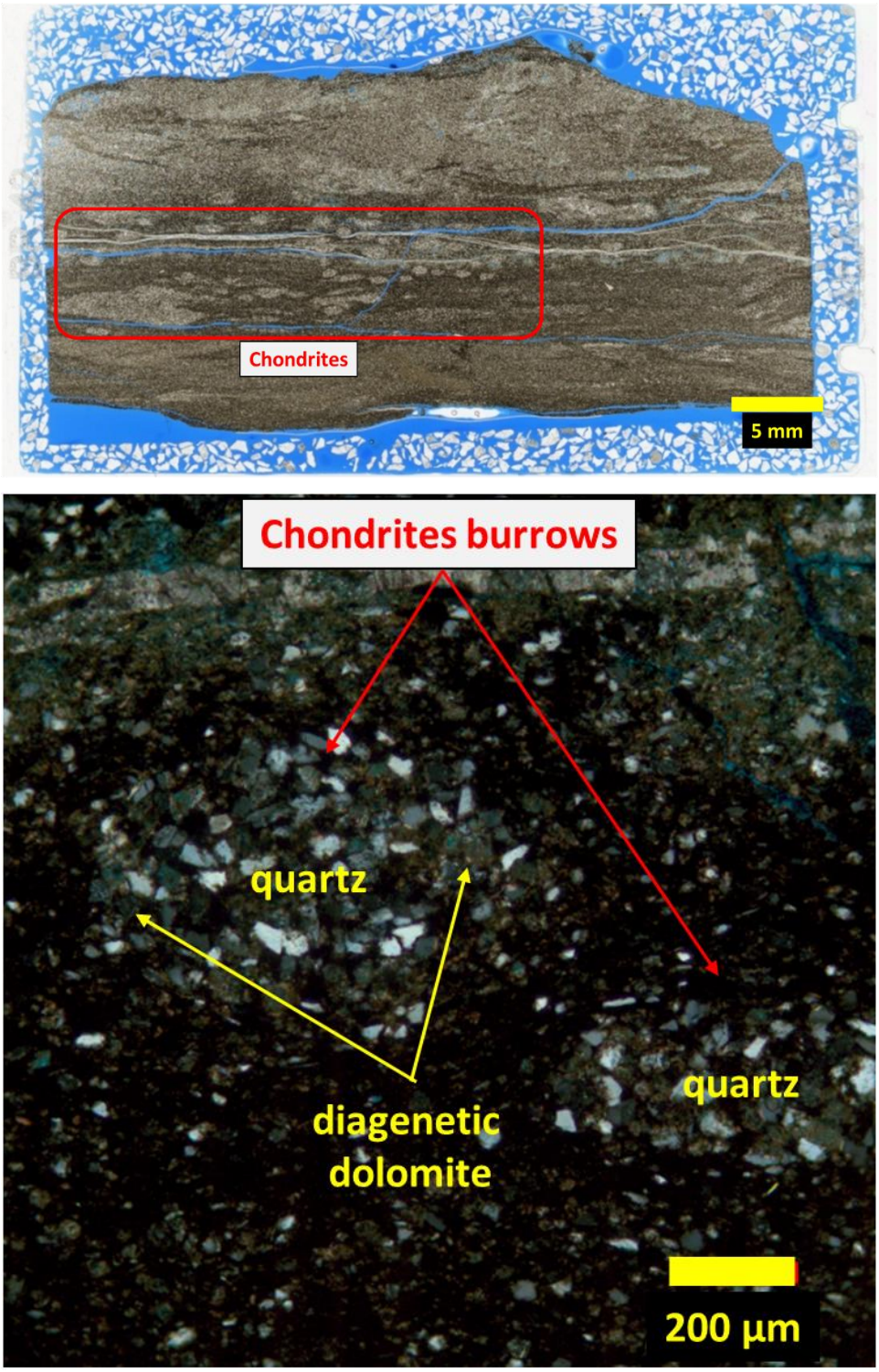

Fig. 12. Thin section (top) and photomicrograph (bottom) of bioturbated, organic-rich, calcareous/dolomitic mudstone (Facies 1C), showing *Chondrites* burrows backfilled with silt-sized detrital quartz and diagenetic dolomite in siliciclastic and carbonate mud matrix.

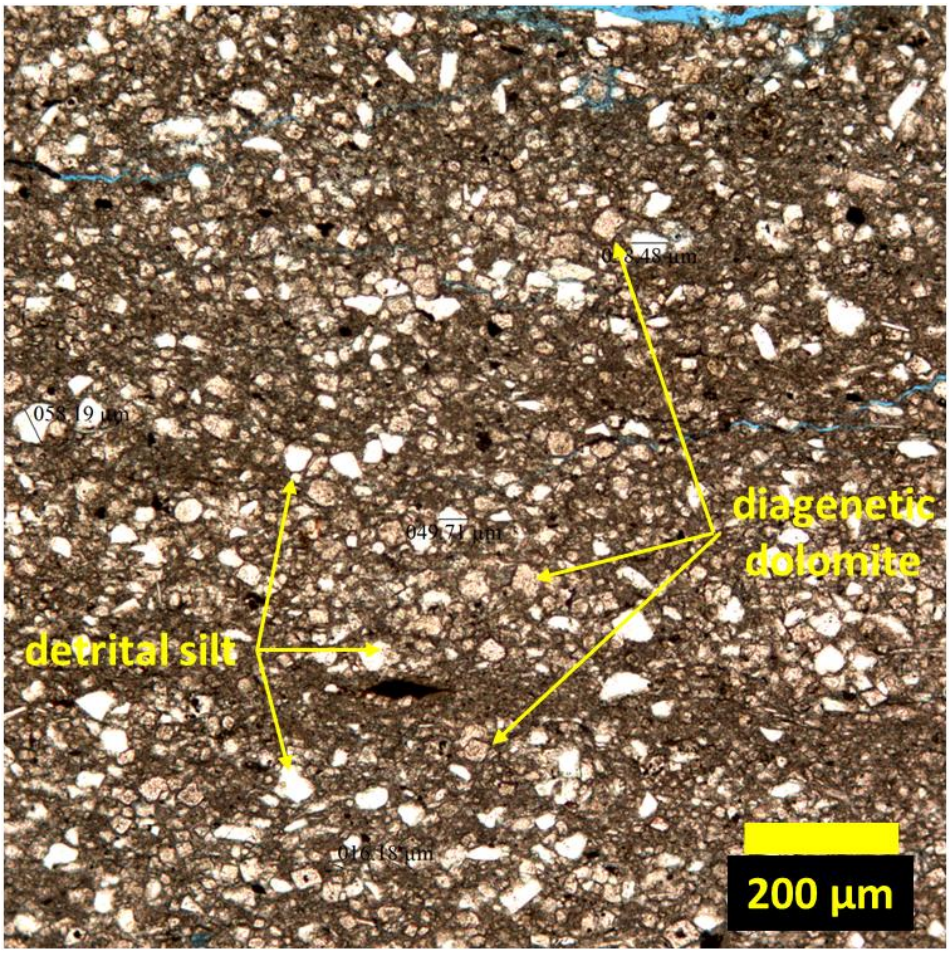

Fig. 13. Photomicrographs of bioturbated, calcareous/dolomitic mudstone-siltstone (Facies 2), showing silt-sized detrital quartz and diagenetic dolomite in siliciclastic and carbonate mud matrix.

Fig. 14. Field photo of a bioturbated, wavy-laminated/lenticular silty dolostone with interbedded/interlaminated mudstone (Facies 3), showing major (highlighted in yellow) and minor truncation surfaces (highlighted in orange) of wavy and lenticular beds.

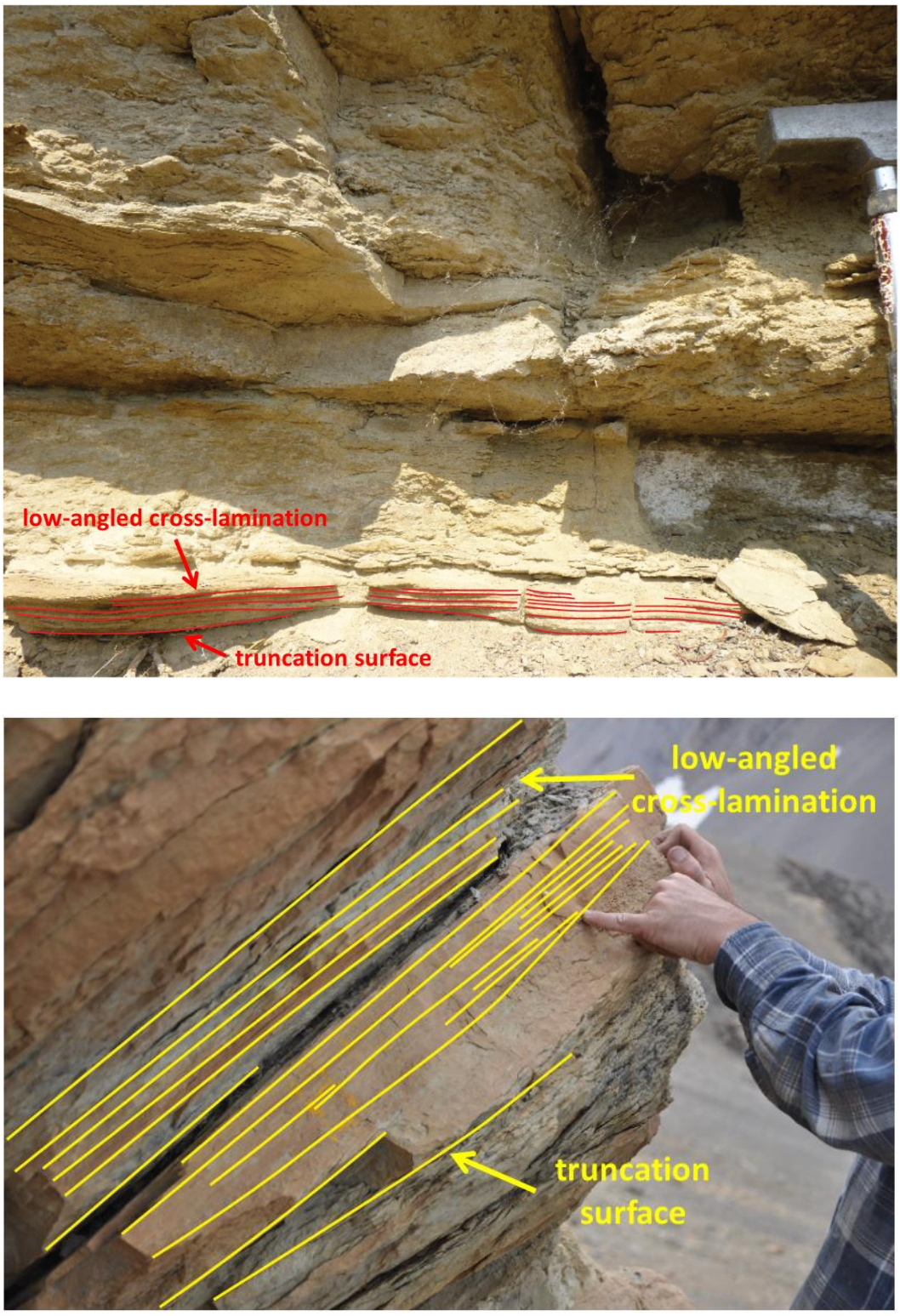

Fig. 15. Field photos of a hummocky cross-stratified (HCS) silty dolostone (Facies 4), showing stacked low-angled cross-lamination (fingertip) with sharp basal contacts (yellow arrows).

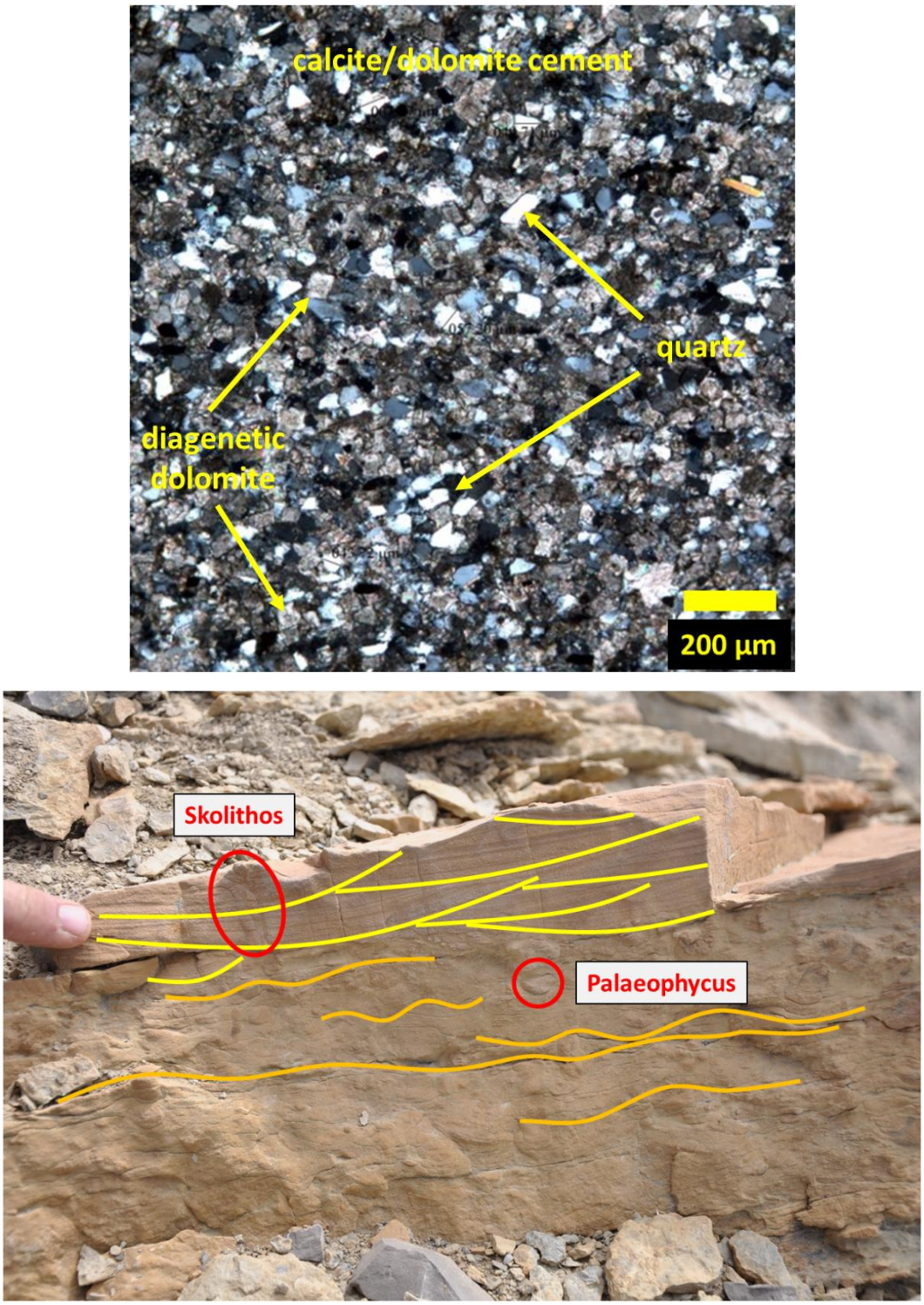

Fig. 16. Field photo (bottom) of a bioturbated, ripple-laminated, calcareous/dolomitic siltstone-silty dolostone (Facies 5), showing wave-ripples (highlighted in orange), current-ripples (highlighted in yellow), and ichnofacies including *Palaeophycus* and *Skolithos* burrows. Photomicrographs (top) of Facies 5 shows silt-sized detrital quartz grains and diagenetic dolomite in finely crystalline calcite/dolomite cement.

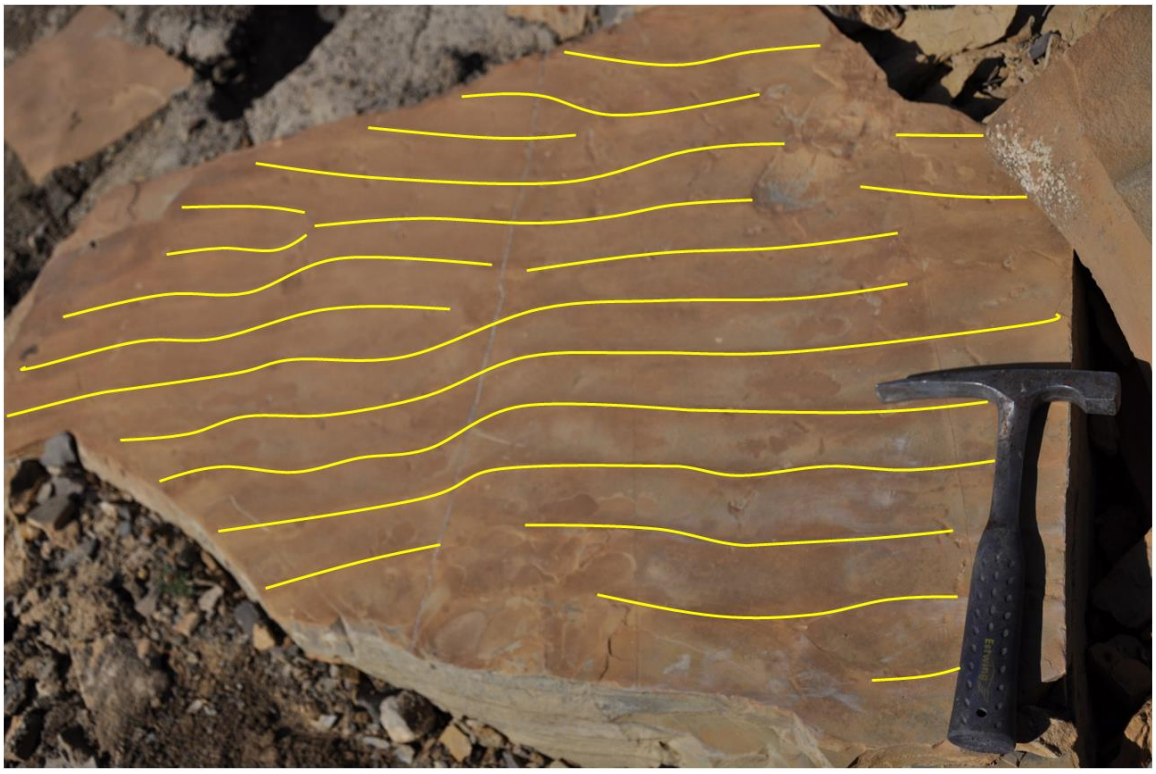

Fig. 17. Field photos of ripple-laminated silty dolostone (Facies 6), showing symmetric wave-ripples (highlighted in yellow).

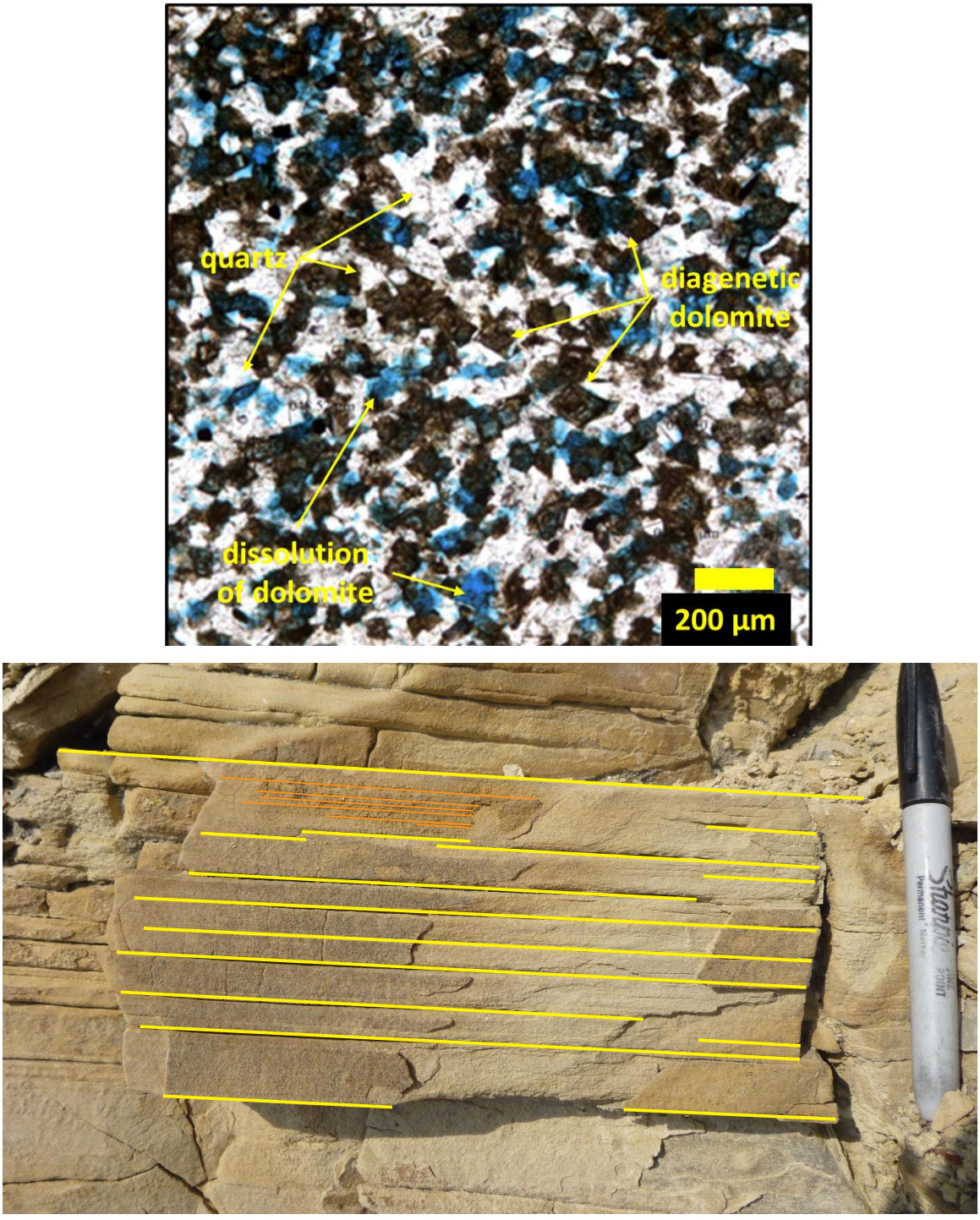

Fig. 18. Field photo of planar-bedded silty dolostone (Facies 7), showing planar beds (highlighted in yellow) and internal planar horizontal lamination (highlighted in orange). Photomicrograph of Facies 7 shows coarse silt- to lower very fine-grained sand-sized detrital quartz grains, diagenetic dolomite, and secondary porosity due to dissolution of diagenetic dolomite.

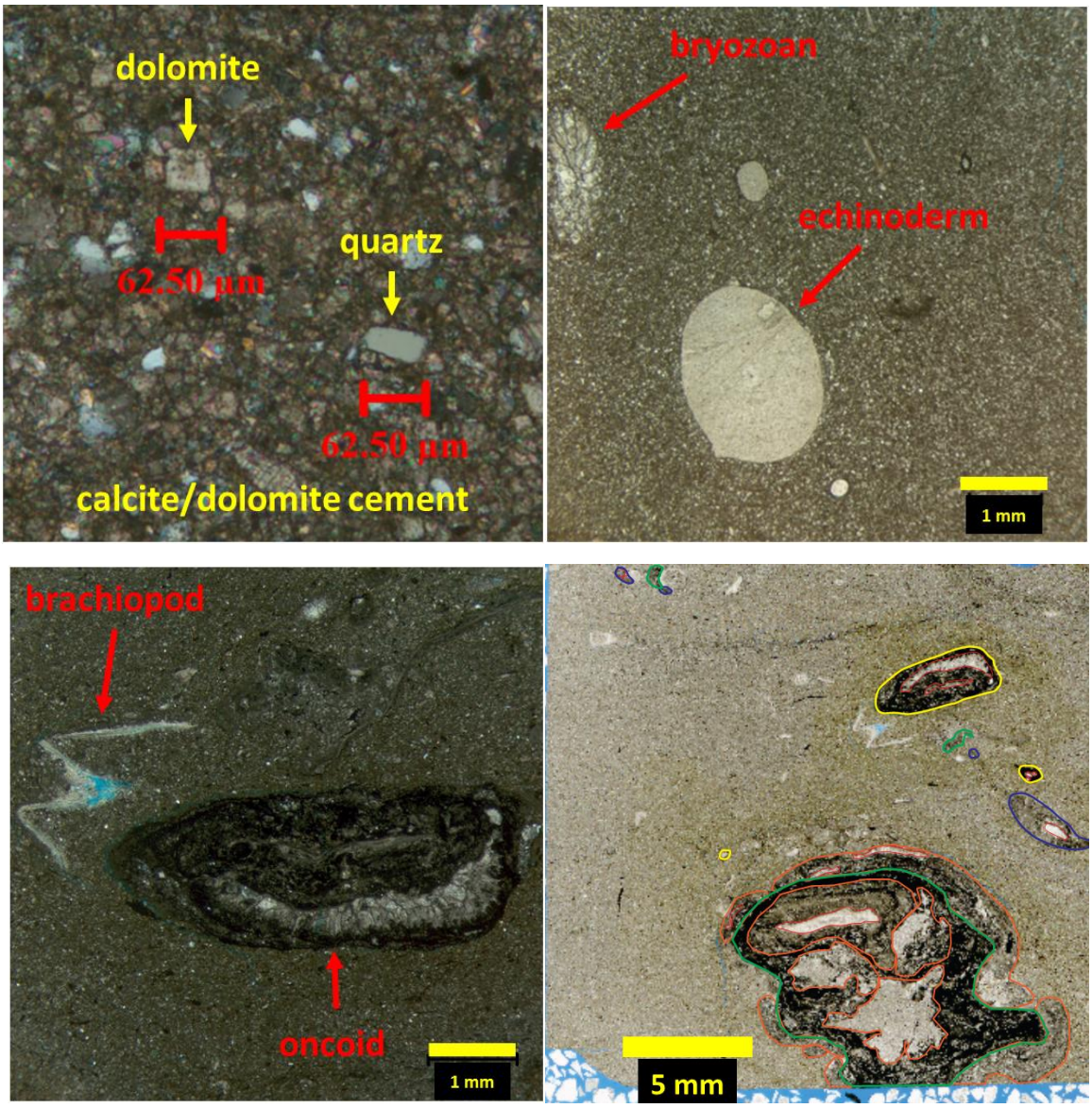

Fig. 19. Photomicrographs of oncolitic, fossil-bearing floatstone (Facies 8), showing diagenetic dolomite and detrital quartz in fine-grained matrix consisting of finely crystalline calcite/dolomite cement and siliciclastic/carbonate mud (left top), commonly identified fossils including bryozoan, echinoderm, brachiopod, and oncoid (right top and left bottom), and an encrusted oncoid containing irregular-shaped body of carbonate clasts and bryozoans as nuclei (right bottom).

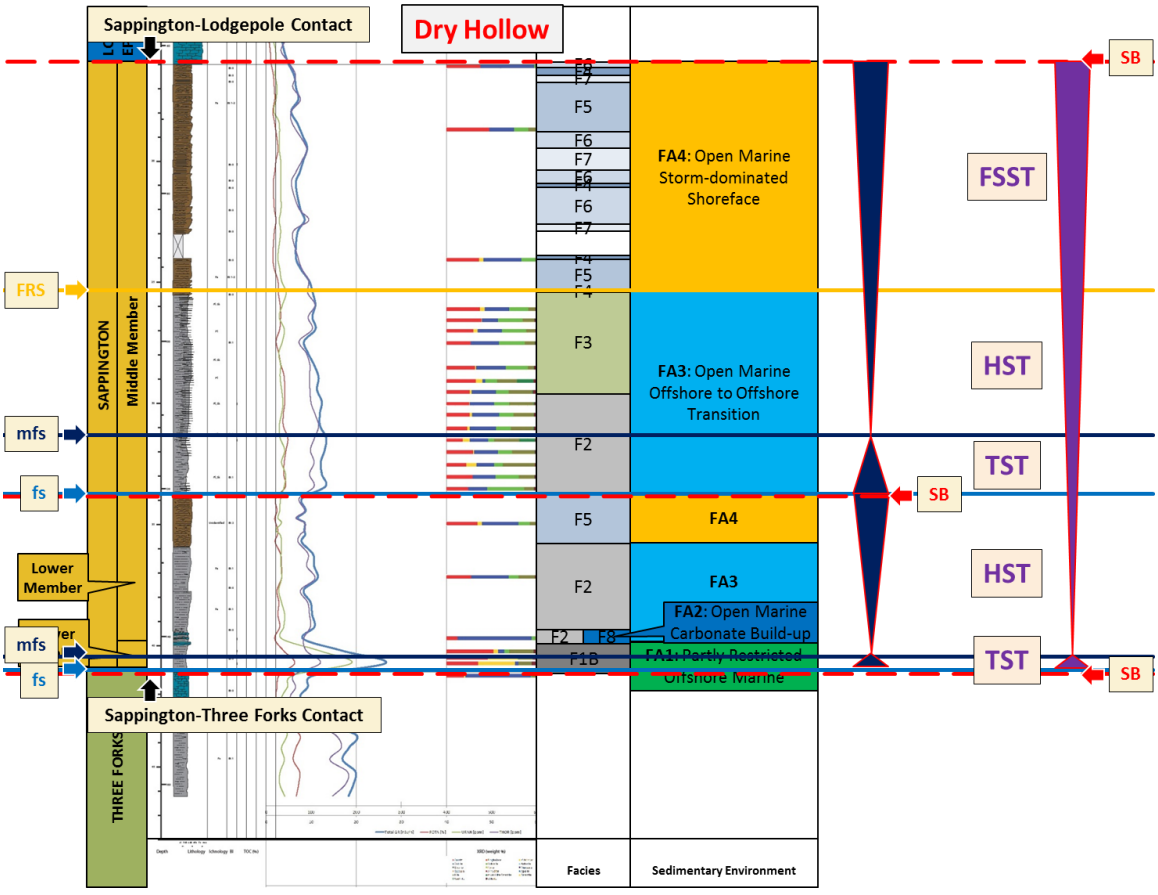
Sappington-Lodgepole Contact
Dry Hollow
SB
FSST
FRS
SAPPINGTON
Middle Member
F5
F6
F7
F3
F2
F1B
FA4: Open Marine Storm-dominated Shoreface
FA3: Open Marine Offshore to Offshore Transition
FA4
FA3
FA2: Open Marine Carbonate Build-up
FA1: Partly Restricted Offshore Marine
HST
TST
mfs
fs
SB
Lower Member
HST
mfs
fs
TST
SB
Sappington-Three Forks Contact
THREE FORKS
Facies
Sedimentary Environment

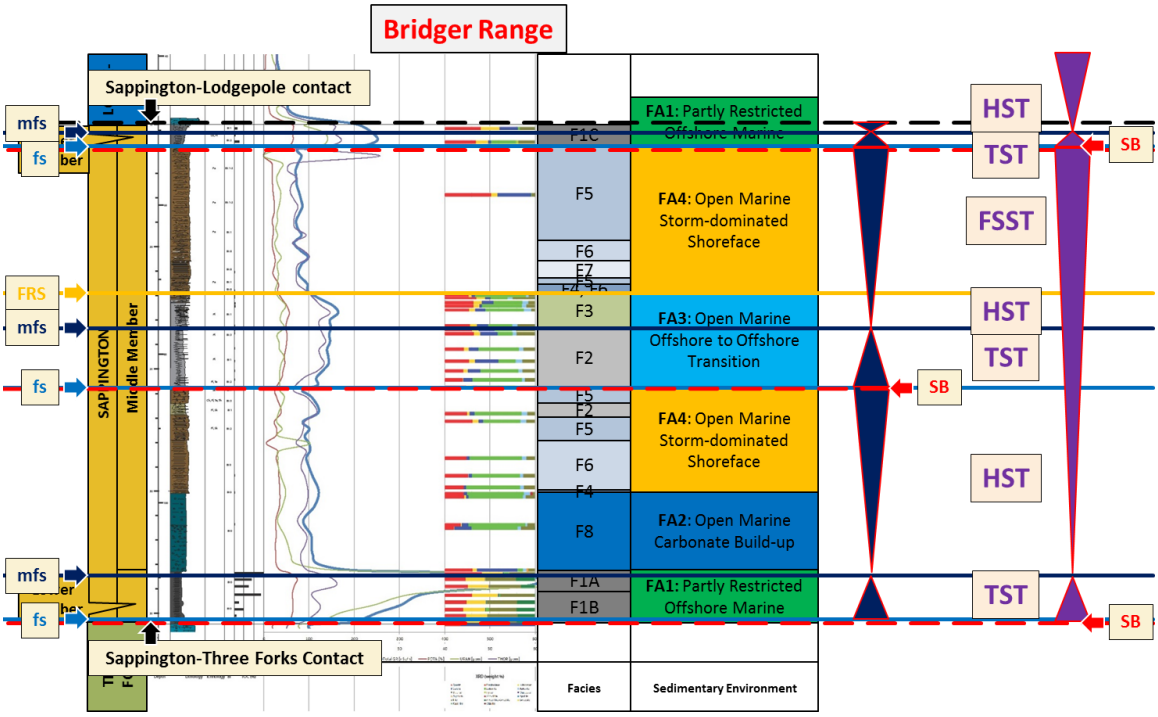
Bridger Range
Sappington-Lodgepole contact
Sappington-Three Forks Contact
mfs
fs
FRS
mfs
fs
mfs
fs
Middle Member
F1C
F5
F6
F7
F3
F2
F5
F2
F5
F6
F4
F8
F1A
F1B
FA1: Partly Restricted Offshore Marine
FA4: Open Marine Storm-dominated Shoreface
FA3: Open Marine Offshore to Offshore Transition
FA4: Open Marine Storm-dominated Shoreface
FA2: Open Marine Carbonate Build-up
FA1: Partly Restricted Offshore Marine
Facies
Sedimentary Environment
HST
TST
FSST
HST
TST
SB
HST
TST
SB
SB

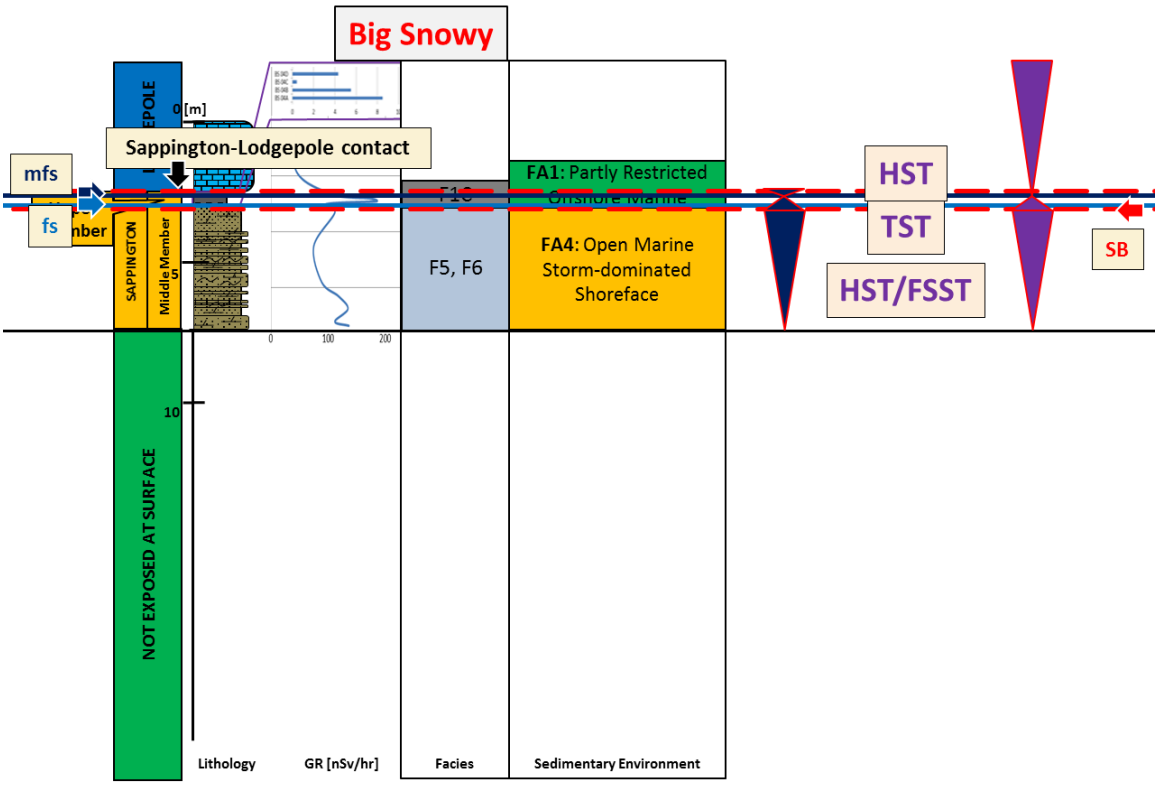

Fig. 20. Measured stratigraphic sections of the Sappington Formation at the DH, BR, and BS sections, showing stacking patterns of the Sappington intervals in higher order sequence (dark blue) and lower order sequence (purple). Up-pointing triangles show fining-upward trend, and down-pointing triangles show coarsening-upward trend. Described sequence stratigraphic surfaces including the flooding surface (fs), the maximum flooding surface (mfs), the sequence boundary (SB), the forced regressive surface (FRS), and the transgressive ravienment surface (TRS). Described systems tracts including highstand (HST), falling stage (FSST), lowstand (LST), and transgressive systems tracts (TST).

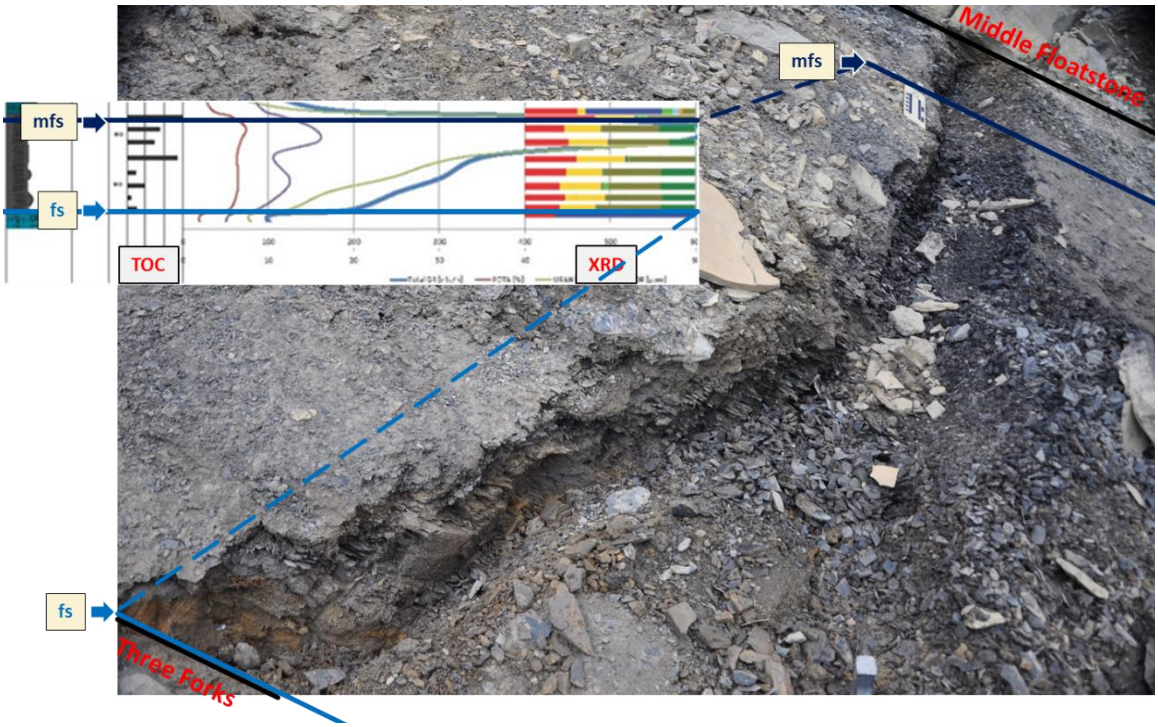
mfs
fs
TOC
XRD
mfs
Middle Floatstone
fs
Three Forks


Middle Silty Dolostone
FRS
Middle Muddy Siltstone

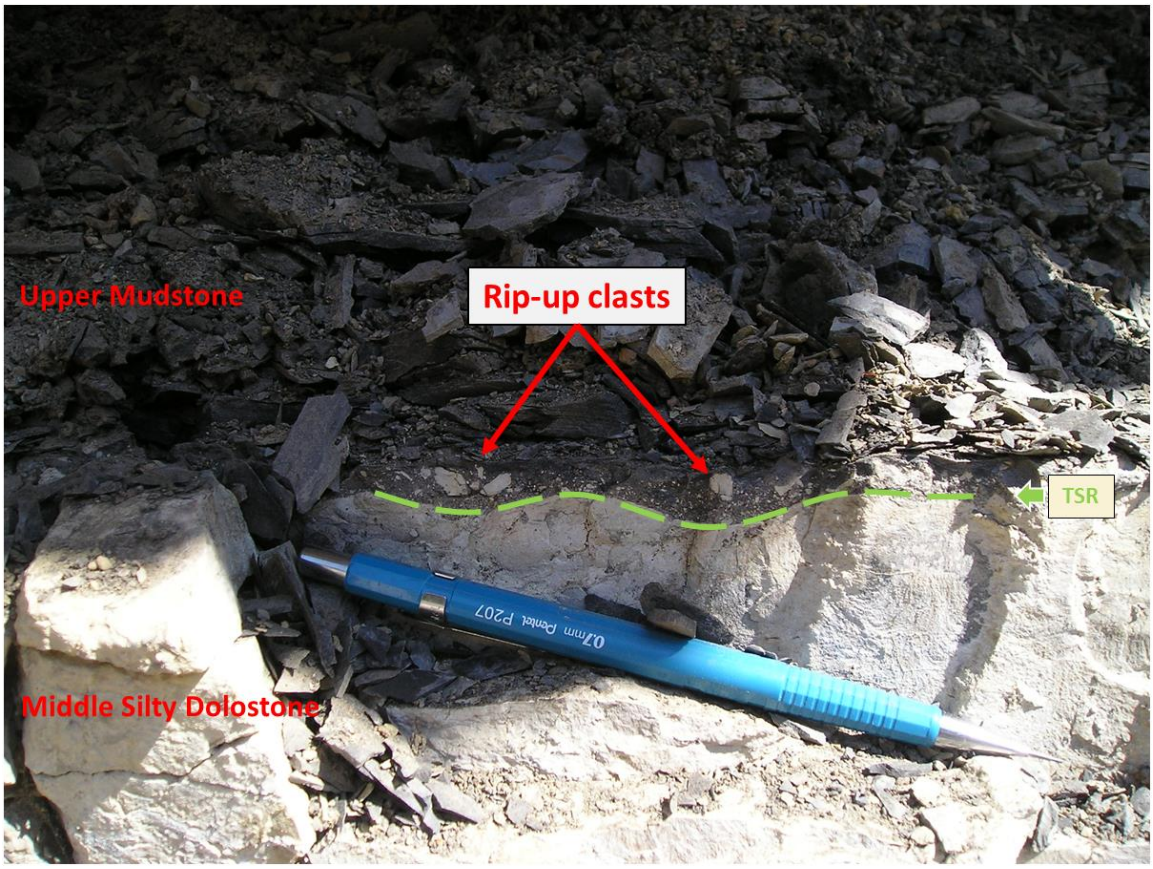

Fig. 21. Examples of sequence stratigraphic surfaces observed from the outcrops of the Sappington Formation: flooding surface (fs) and maximum flooding surface (mfs) (top); forced regressive surface (FRS) (middle); and transgressive ravinement surface (TRS) and rip-up clasts (bottom).

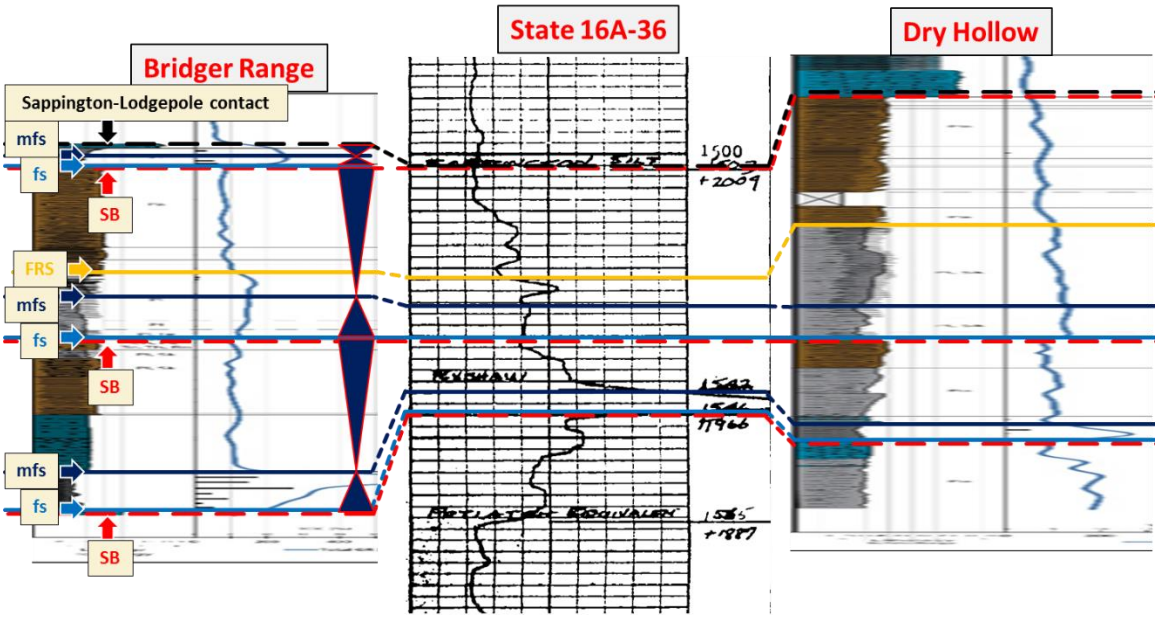

Fig. 22. Well log correlation of the outcrops of the Sappington Formation at the DH and BR sections and an example of total gamma ray log (State 16A-36; Murray 1) using sequence stratigraphic surfaces. Note: Individual well logs are not laterally on scale.

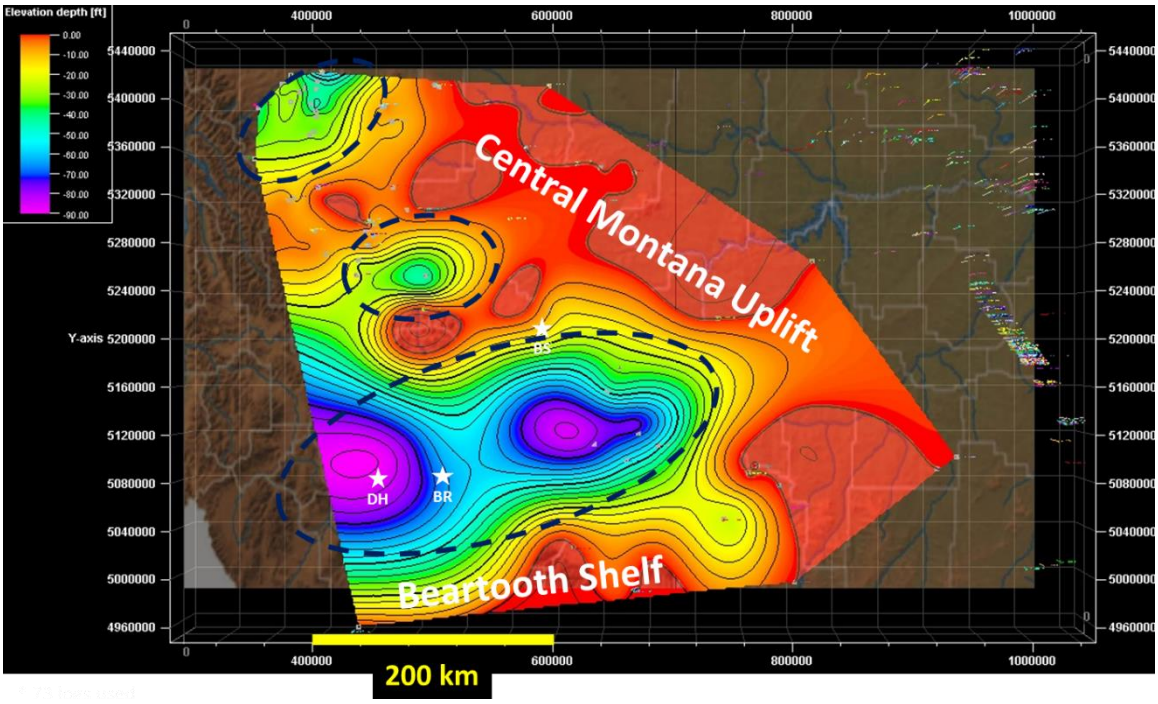

Fig. 23. Total isopach map of the Sappington Formation and its equivalents in western half of Montana based on well log analysis, showing depositional basins in central, western, and northeastern Montana (dashed blue circles), paleohighs including the Central Montana Uplift and the Beartooth Shelf. Scale: 0 (red) – 90 (purple) [ft].

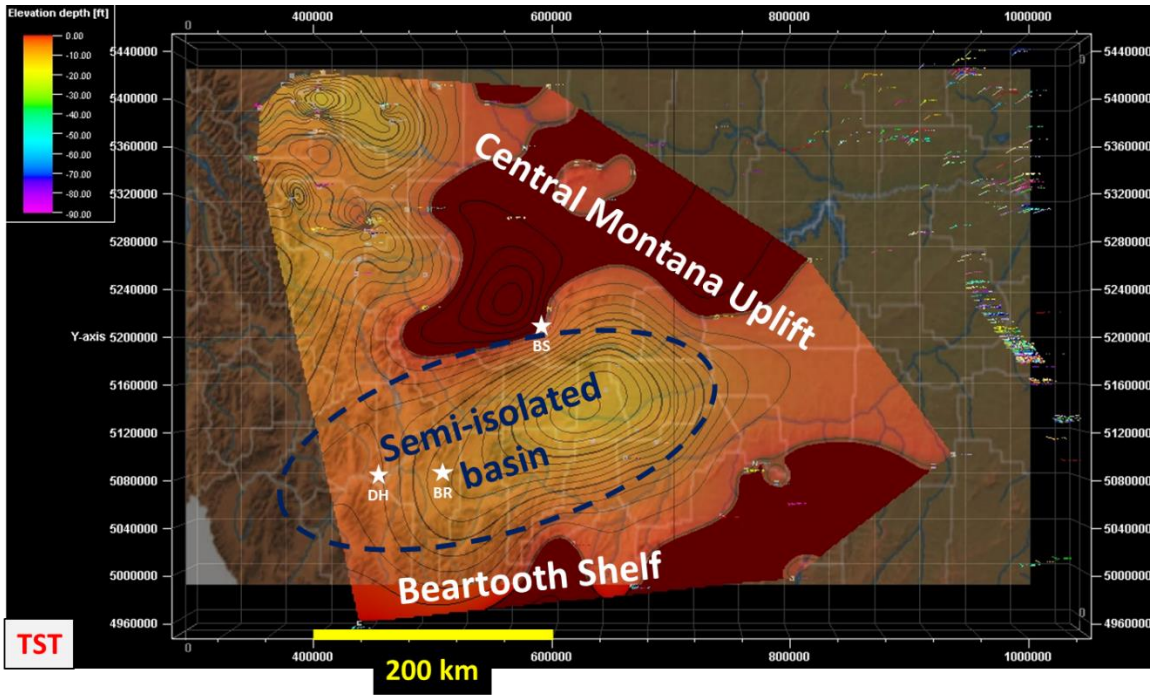
Elevation depth [ft]
0.00
-10.00
-20.00
-30.00
-40.00
-50.00
-60.00
-70.00
-80.00
-90.00
Central Montana Uplift
BS
Semi-isolated
basin
DH
BR
Beartooth Shelf
TST
200 km
Y-axis

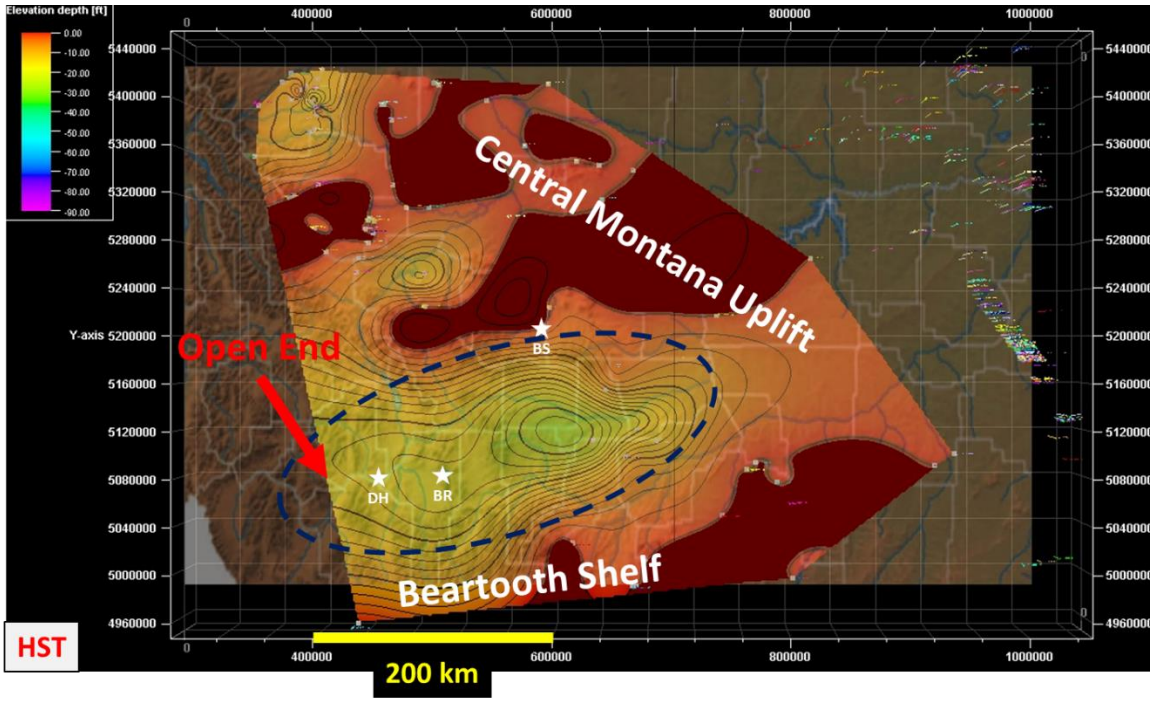
Elevation depth [ft]
0.00
-10.00
-20.00
-30.00
-40.00
-50.00
-60.00
-70.00
-80.00
-90.00
Central Montana Uplift
Open End
BS
DH
BR
Beartooth Shelf
HST
200 km
Y-axis

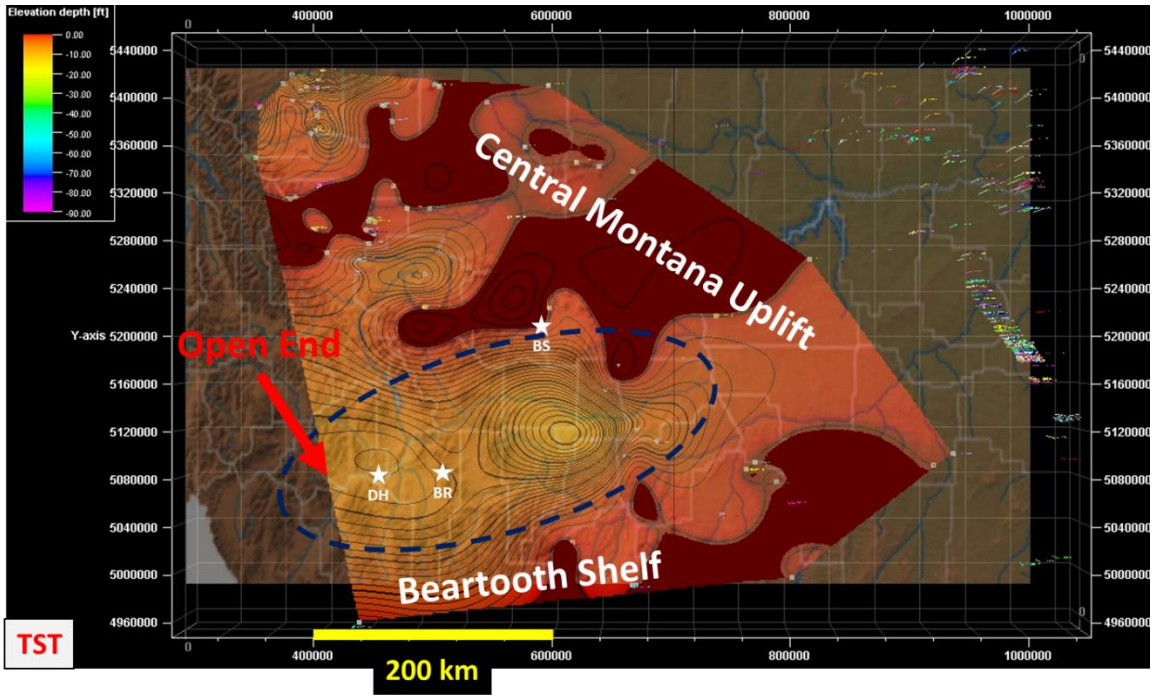
Elevation depth [ft]
0.00
-10.00
-20.00
-30.00
-40.00
-50.00
-60.00
-70.00
-80.00
-90.00
Central Montana Uplift
Open End
BS
DH
BR
Beartooth Shelf
TST
200 km
Y-axis

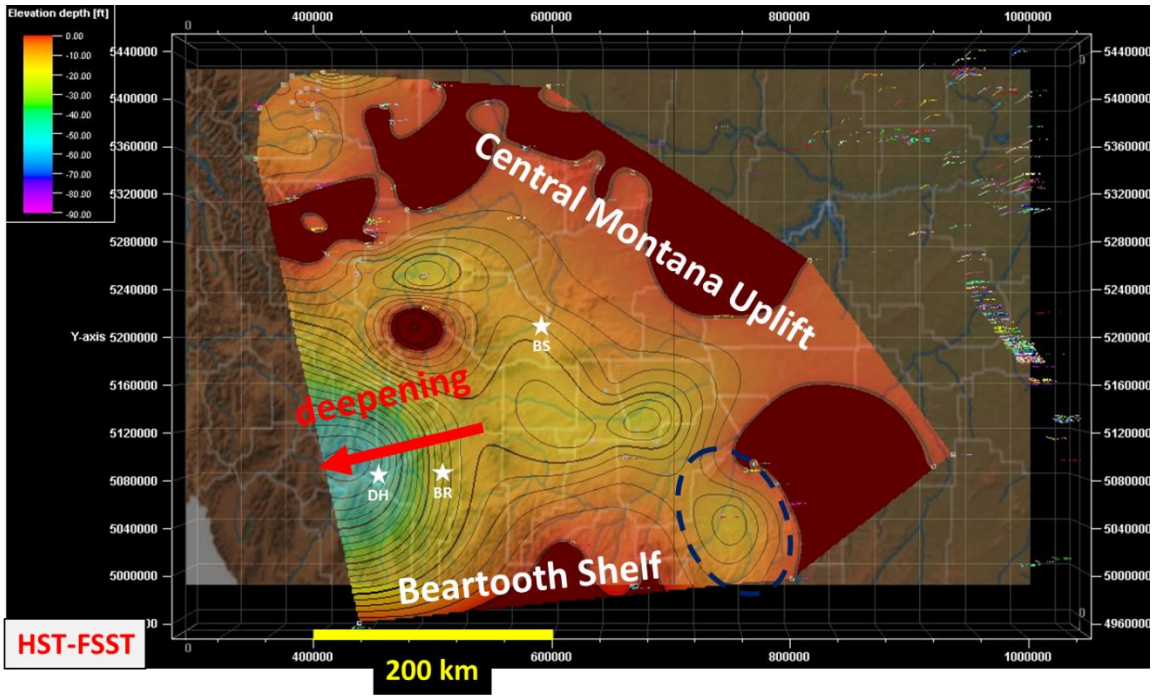
Elevation depth [ft]
0.00
-10.00
-20.00
-30.00
-40.00
-50.00
-60.00
-70.00
-80.00
-90.00
Central Montana Uplift
deepening
BS
DH
BR
Beartooth Shelf
HST-FSST
200 km
Y-axis

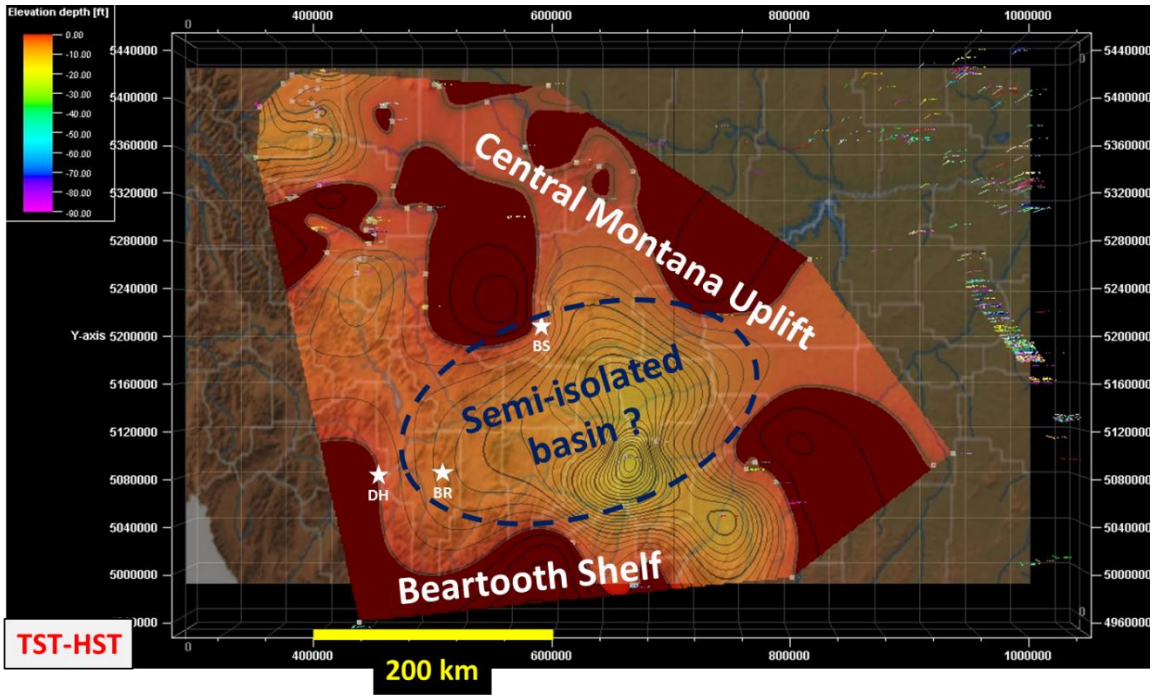

Fig. 24. Isopach maps for each systems tract including the TST in the lower member, the HST in the lower unit of the middle member, the TST in the middle unit of the middle member, the HST-FSST in the upper unit of the middle member, and the TST-HST in the upper member with annotations of major basin characteristics and paleogeographic features including the Central Montana Uplift and the Beartooth Shelf.

Mineral	Chemical Formula	Ref. Code
Quartz	Si O2	01-070-3755
Illite-2M1 (NR)	(K , H3 O) Al2 Si3 Al O10 (O H)2	00-026-0911
Potassium tecto-alumotrisilicate	K Al Si3 O8	01-084-1504
Fluorapatite, syn	Ca5 (P O4)3 F	00-015-0876
Iron persulfide	Fe S2	01-071-0053
Dolomite	Ca Mg (C O3)2	01-073-2361
Sodium tecto-alumotrisilicate	Na (Al Si3 O8)	01-078-1995
Clinochlore	(Mg2.96 Fe1.55 Fe.136 Al1.275) (Si2.622 Al1.376 O10) (O H)8	01-079-1270
Muscovite-2M1	K Al2 (Al Si3 O10) (O H)2	01-082-0576
Calcite	Ca (C O3)	01-086-2334
Calcium Aluminum closo-icosaoxodihydoxooctasilicate hydrate *	Ca1.2 Al4 (Si8 O20 (O H)2) O2.2 (H2 O)3.1	01-073-6746
Anhydrite	Ca (S O4)	01-086-2270
Kaolinite	Al4 (O H)8 (Si4 O10)	01-078-2110
Gypsum, syn	Ca S O4 ·2 H2 O	00-033-0311
Marcasite	Fe S2	00-037-0475
Siderite	Fe C O3	00-029-0696
Ankerite	Ca (Fe +2 , Mg) (C O3)2	00-041-0586

Table 1. Mineral subset used for XRD analysis.

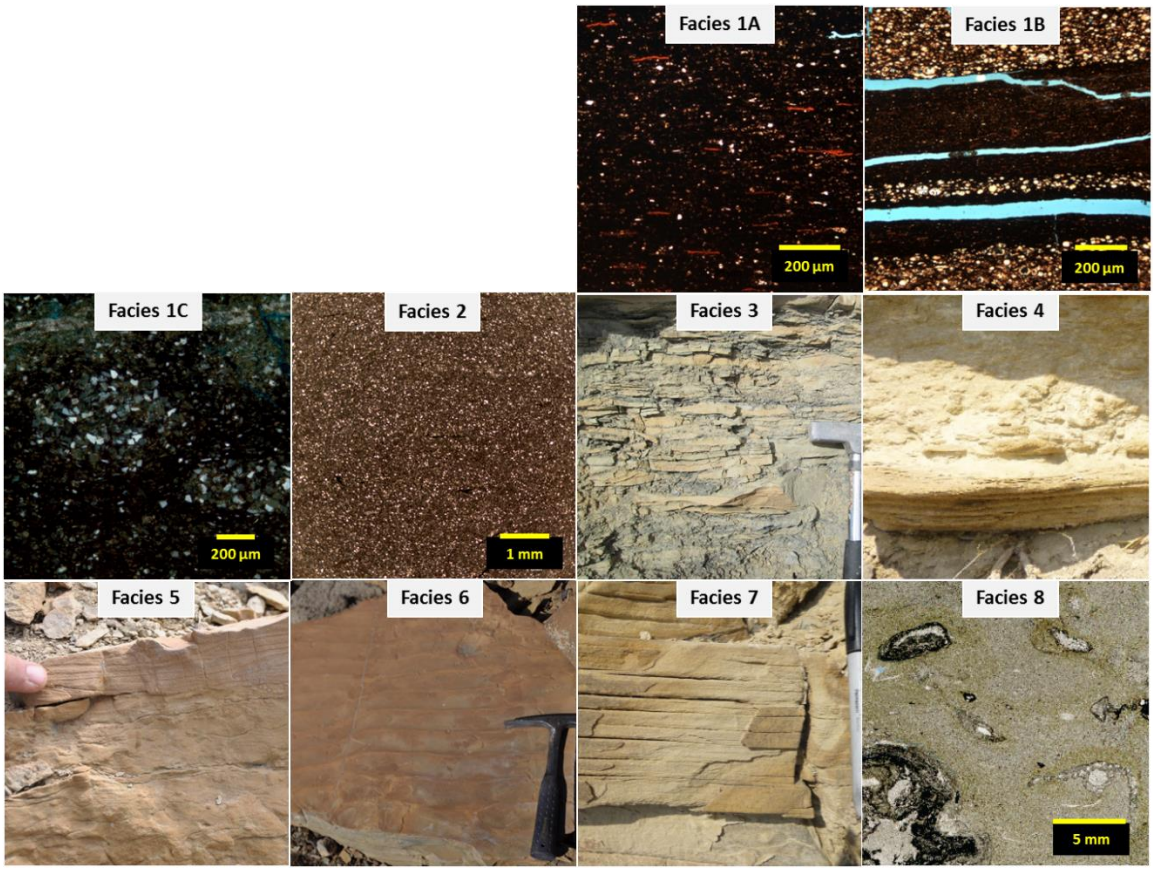

Table 2. Eight facies including three sub-facies of Facies 1 identified from the outcrops of the Sappington Formation: organic-rich mudstones with microfossils (F1A); organic-rich mudstones with pinch and swell lamination (F1B); bioturbated, organic-rich calcareous/dolomitic mudstones (F1C); bioturbated, calcareous/dolomitic muddy siltstone (F2); bioturbated, wavy-laminated silty dolostone with interbedded/interlaminated mudstone (F3); hummocky cross-stratified silty dolostone (F4); bioturbated, ripple-laminated, calcareous/dolomitic siltstone-silty dolostone (F5); ripple-laminated silty dolostone (F6); planar-bedded silty dolostone (F7); and oncolitic, fossil-bearing floatstone (F8).

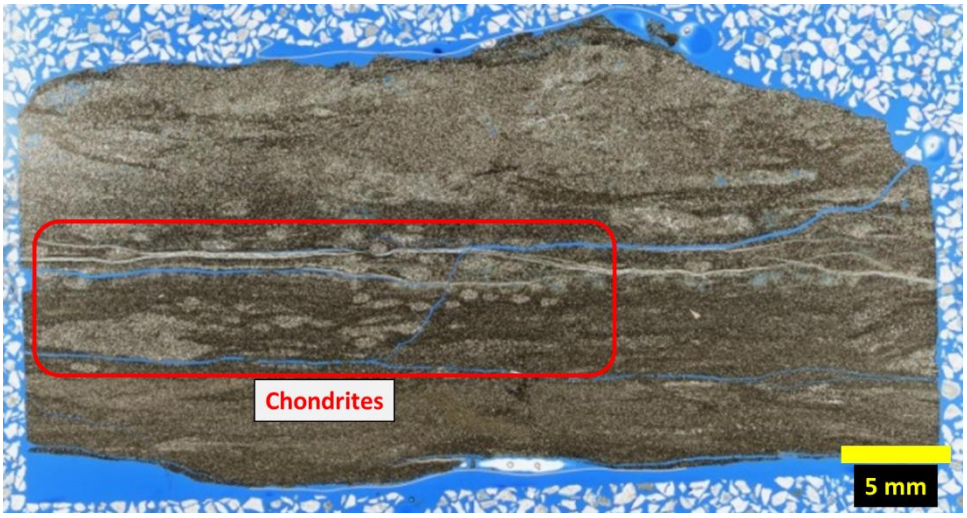
Chondrites
5 mm

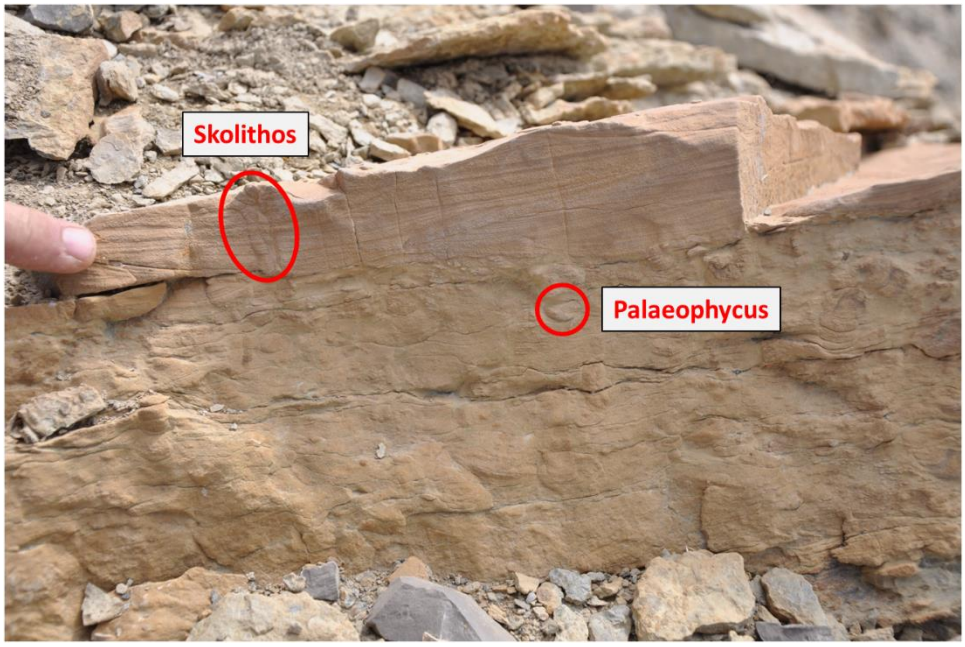
Skolithos
Palaeophycus

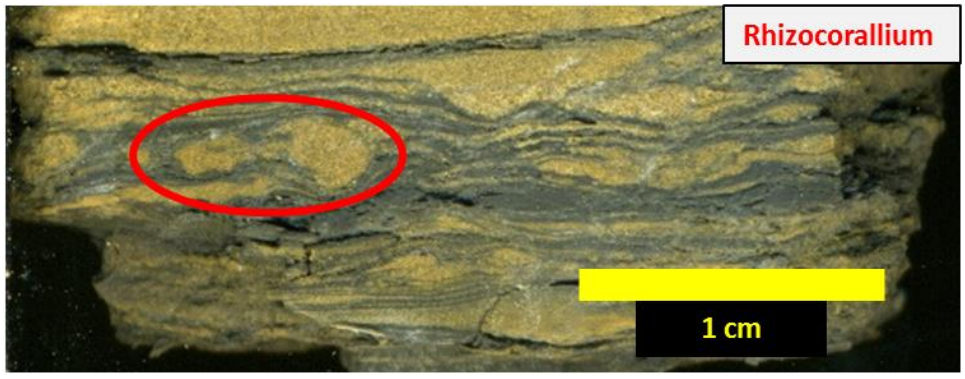
Rhizocorallium
1 cm

Table 3. Ichnofacies identified from the outcrops of the Sappington Formation including: *Chondrites*, *Palaeophycus*, *Planolites*, *Rhizocorallium*, *Teichichnus*, and *Thalassinoides*.